



Plate tectonics through Earth's history: constraints from the thermal evolution of Earth's upper mantle

Sarbajit Dash, E.V.S.S.K. Babu, Jérôme Ganne & Soumyajit Mukherjee

To cite this article: Sarbajit Dash, E.V.S.S.K. Babu, Jérôme Ganne & Soumyajit Mukherjee (2025) Plate tectonics through Earth's history: constraints from the thermal evolution of Earth's upper mantle, International Geology Review, 67:4, 500-533, DOI: [10.1080/00206814.2024.2394994](https://doi.org/10.1080/00206814.2024.2394994)

To link to this article: <https://doi.org/10.1080/00206814.2024.2394994>

 View supplementary material [↗](#)

 Published online: 02 Sep 2024.

 Submit your article to this journal [↗](#)

 Article views: 627

 View related articles [↗](#)

 View Crossmark data [↗](#)



Plate tectonics through Earth's history: constraints from the thermal evolution of Earth's upper mantle

Sarbajit Dash^{a,b}, E.V.S.S.K. Babu^{a,b}, Jérôme Ganne^c and Soumyajit Mukherjee^d

^aCSIR-National Geophysical Research Institute, Hyderabad, Uppal Road, India; ^bAcademy of Scientific and Innovative Research (AcSIR), Ghaziabad, India; ^cGET-OMP, Université de Toulouse, UPS, CNRS, IRD, CNES, Toulouse, France; ^dDepartment of Earth Sciences, Indian Institute of Technology Bombay, Mumbai, India

ABSTRACT

Temporal changes in Earth's tectonic style play a crucial role in understanding the planet's evolution. Modern-style tectonics is characterized by the formation of basaltic crust at divergent plate boundaries and its subsequent recycling at subduction zones, accompanied by wedge mantle formation and arc magmatism. It is commonly believed that the secular cooling of the mantle modified the tectonic style from stagnant lid or heat pipe on an early hotter Earth to horizontal tectonics during Meso-Neoproterozoic. However, various field, petrographic, and geochemical studies suggest that the onset of plate tectonics ranges from Hadean to Neoproterozoic. In this study, we re-evaluate the primary magma temperature (mantle potential temperature, T_p) of the upper ambient mantle, spanning from Eoarchean to Neoproterozoic. We used basalts from several Archean and Proterozoic greenstone belts worldwide, along with Proterozoic ophiolites, to (re) calculate the T_p using the FRACTIONATE-PT method. We observed a T_p range of 1444–1639°C during the Archean and 1414–1611°C during the Proterozoic. These findings indicate a strong correlation with previously estimated T_p values obtained from PRIMELT3 method. This further highlights strong internal consistency among different methods and supports models of a hot ambient mantle during the Archean and Proterozoic. We further reviewed numerical models regarding the effect of mantle temperature on the viability of early Earth plate tectonics. Such model results, composition of Archean continental crust, recent crustal growth models, and field evidence are consistent with the operation of plate tectonics on an early hotter Earth. The transition from a hotter mantle to a colder one from Eo-Neoproterozoic resulted in thinner oceanic lithosphere and a less depleted lithospheric mantle. Subduction of this thinner oceanic lithosphere led to modern-style tectonics. The intensity and style of plate tectonics on the early Earth differed from modern tectonics, which emerged during the Neoproterozoic.

ARTICLE HISTORY

Received 15 February 2024
Accepted 17 May 2024

KEYWORDS

Mantle potential temperature; modern-style plate tectonics; Hadean; ambient mantle

1. Introduction

Basalts and basaltic rocks constitute the most abundant igneous rocks on the planet. Since the compositions of basaltic magmas change with variations in mantle thermal conditions (Langmuir and Hanson 1980; Putirka 2005; Herzberg *et al.* 2007), examining these magmas enables effective constraint and tracking of a planet's thermal evolution. McKenzie and Bickle (1988) coined the term *mantle potential temperature* (T_p) to express the thermal state of the mantle. Later, many authors used basalt geochemistry to evaluate the temporal variation of T_p (Herzberg and O'Hara 2002; Putirka 2005, 2008; Herzberg *et al.* 2010; Ganne and Feng 2017). However, the calculation of T_p through geochemical modelling depends on factors such as extent of fractional crystallization of the primary magma before its

emplacement at crustal level (Herzberg *et al.* 2007, 2010; Herzberg and Asimow 2008; Ganne and Feng 2017). As volcanic rocks, e.g. basalts, are the direct fractionation products of mantle-derived primary melts, their compositions are the best candidates to track the thermal evolution of the mantle. The cumulate counterparts, i.e. gabbros, are the by-products of magmatic differentiation and thus more refractory than the volcanic ones (Wu *et al.* 2022).

T_p traditionally refers to the temperature of the mantle at surface if it ascends adiabatically without melting (McKenzie and Bickle 1988). The relations between the mantle peridotite solidus and adiabatic decompression melting are as follows: (i) The mantle peridotite remains solid below the solidus curve and undergoes partial melting only when it exceeds the solidus. (ii) The gentler

CONTACT Soumyajit Mukherjee  soumyajitm@gmail.com; smukherjee@iitb.ac.in  Department of Earth Sciences, Indian Institute of Technology Bombay, Powai, Mumbai, Maharashtra 400076, India

 Supplemental data for this article can be accessed online at <https://doi.org/10.1080/00206814.2024.2394994>

© 2024 Informa UK Limited, trading as Taylor & Francis Group

slope of the mantle adiabat than that of the solidus (i.e. $dT/dP_{\text{Adiabat}} < dT/dP_{\text{Solidus}}$) enables decompression melting. This is because the mantle rising adiabatically can intersect and surpass the solidus temperature. (iii) The adiabatically rising mantle with a higher potential temperature (e.g. plumes) intersects the solidus at greater depths than the rising mantle with a lower potential temperature (e.g. at ocean ridges).

T_p is dependent on (i) convective and conductive heat loss and the heat gain due to radioactive decay in the mantle, and (ii) gravitational heating at the core-mantle boundary (Korenaga 2008; Davies 2009; Ganne and Feng 2017). The decreasing abundance of radioactive elements and the segregation of the inner core from the outer core indicate that the T_p decreased from its initial value due to secular cooling (Verhoogen 1961; Davies 2015). The temporal variation of T_p is a complex and dynamic process that plays a crucial role in shaping the Earth's geologic history. For example, lithospheric differentiation driven by mantle melting develops a depleted residual mantle and a continental crust enriched in elements, e.g. K, Rb, U, Th, and light rare-earth elements (LREEs) (Capitanio *et al.* 2020; Giuliani *et al.* 2021). Further, the temporal evolution of Earth's tectonics has presumably evolved due to the secular cooling of the mantle (Palin *et al.* 2020).

Previous studies suggest that during Archean, relatively higher T_p led to greater degrees of mantle melting, as high as 40–50%, depending on the tectonic regime (Herzberg and Rudnick 2012). Studies argue that the mantle started to cool after the Archean (Korenaga 2008). In support of this, several authors documented signatures of modern-style plate tectonics during the Paleoproterozoic. Supplementary Table S1 summarizes such evidence, e.g. presence of ophiolites and retrograded eclogites (Vijaya Kumar *et al.* 2010; Ganne *et al.* 2012; Imayama *et al.* 2017; Weller and St-Onge 2017; François *et al.* 2018; Loose and Schenk 2018; Müller *et al.* 2018; Xu *et al.* 2018; Liu and Zhang 2019; de Oliveira Chaves and Porcher 2020; Pereira *et al.* 2021; Wang *et al.* 2021) from India, West Africa, North America, Republic of Congo during the Paleoproterozoic. Studies supporting early Earth plate tectonics commonly propose that the Archean was characterized by warm ductile subduction, later changing into cold subduction associated with rigid plate boundaries since the Neoproterozoic (Zheng and Zhao 2020).

Previous studies on the plausibility of Archean plate tectonics were based on two models. (i) With increasing T_p , the vigour of mantle convection increases, manifesting faster plate tectonics (Christensen 1985). In contrast, O'Neill *et al.* (2007) argued that elevated T_p could prohibit tectonic activity by reducing convective stress, effectively

leading to negligible tectonic movement. Introducing the concept of 'sluggish' plate tectonics, Korenaga (2006) suggested that high T_p would reduce plate velocities due to the development of a thick residual lithospheric mantle. (ii) At high T_p ~1700°C, komatiitic oceanic crust formed during the Archean (Nisbet and Fowler 1983). In this condition, the oceanic crust would be denser than the underlying mantle and could subduct easily below the asthenospheric mantle. When the T_p decreased to ~1500°C, the oceanic crust produced, would be lighter than the underlying mantle, and the nascent lithosphere might have cooled for a longer time before the density inversion. However, the komatiitic crust resulted from plume melting, and not the ambient mantle, which is believed to comprise the majority of the upper mantle. Moreover, the Archean was dominated by oceanic crust, formed through decompression melting of the ambient convecting mantle. The subductibility of this oceanic crust remains uncertain, as it hinges on parameters such as lithospheric thickness, buoyancy, density, and viscosity of the unmelted mantle (Korenaga 2006; Weller *et al.* 2019), all of which are influenced by the mantle's composition and thermal state.

Geoscientists have been debating the mechanism of plate tectonics, especially the subduction mechanism, during the Archean (van Hunen and Moyen 2012; Condie 2021; Duarte 2023). As the subduction process is related to the genesis of various ore deposits, e.g. porphyry Cu-Mo, volcanic massive sulphide (VMS), and large-scale gold and iron deposits (Bradley and Leach 2003; Sun *et al.* 2007, 2016; Wang *et al.* 2018), understanding paleo-subduction mechanisms can provide insights on such ancient mineralizations. The net influx of water into the deep mantle, early atmospheric carbon sequestration, regulation of geomagnetism, and origin and evolution of life have further been described in the light of tectonic evolution of the Earth (Korenaga 2011; Korenaga *et al.* 2017; Catling and Zahnle 2020; Fu *et al.* 2024). Therefore, backtracking the onset of plate tectonics becomes crucial.

In this study, we investigate the mantle potential temperature from non-arc basalts across the globe that range from Archean to Proterozoic and review the major petrological and geochemical changes that occurred since the Hadean. The objective is to determine the timeframe when plate tectonics or subduction-related tectonic were initiated by investigating the long-term thermal changes of the Earth's mantle.

2. Method

Based on the trace element and isotopic composition, three mantle sources have been identified for basalts

(Condie 2015): (i) the depleted mantle (DM), (ii) the enriched mantle (EM), and (iii) the hydrated mantle (HM). Further, komatiites, which possibly derive from a distinct hotter mantle plume, have been assigned to a separate source: the komatiitic mantle (KM) (Cawthorn 1975; Richard *et al.* 1996; Puchtel *et al.* 2022). The DM-derived basalts are sampled from the spreading centres or mid-oceanic ridges (Condie 2003, 2015). The EM-derived basalts can presently be found in hot spots or plume centres. However, during the Archean, basalts derived from EM did not have a plume source. Instead, they formed from an undifferentiated mantle resembling the primitive mantle (Condie *et al.* 2016). To summarize, during the Archean, both DM and EM basalts originated from a convecting upper ambient mantle, and after that, the EM basalts were obtained through mantle plumes. The HM-derived basalts represent water-saturated magmas that originate from arc-related tectonic settings.

Our study focuses on the secular thermal evolution of the convecting ambient mantle through the calculation of mantle potential temperature (T_p). The compiled dataset of basalt major oxide composition by Condie *et al.* (2016) from different Archean and Proterozoic greenstone belts and Proterozoic ophiolites has been used in this study (Supplementary Material, SM1). Specifically, we have utilized the Archean basalts derived from both the depleted mantle (DM) and enriched mantle (EM), as well as exclusively the DM-derived basalts from the Proterozoic, as those indicate convective upper ambient mantle thermal conditions.

Several previous authors (Herzberg *et al.* 2007, 2010; Ganne and Feng 2017) have employed the compositions of non-arc basalts to infer the thermal history of the Earth's upper mantle using the PRIMELT software package (PRIMELT2 (Herzberg and Asimow 2008) and PRIMELT3 (Herzberg and Asimow 2015)). In this study, we have used the programme FRACTIONATE-PT by Lee *et al.* (2009). Both the programmes calculate the primary magma composition for peridotite-derived melts that have experienced only olivine fractionation. However, PRIMELT calculates the primary magma composition for both accumulated fractional melting and batch melting model by adding or subtracting olivine to or from the basalt when there is a common melt fraction in MgO-FeO and Ol-An-Qz projection spaces for the fertile peridotite (see Figure 1 in Herzberg and Asimow (2015)). In contrast, FRACTIONATE-PT calculates the primary magma composition for batch melting by adding or subtracting olivine when it is in equilibrium with an assumed residual olivine composition. FRACTIONATE-PT is versatile in its applicability to both hydrous and anhydrous magmas. Nevertheless, its H₂O expression is

suitable for water-saturated arc basalts (IIT Bombay Repository R1). As the T_p estimations in our study are based on ambient mantle-derived basalts, we conducted all calculations assuming an anhydrous source (IIT Bombay Repository R1).

The unfiltered dataset consist of 1146 Archean and 68 Proterozoic basaltic samples. Figure 1 compiles sample locations on the world map (see SM1 for the final basaltic samples used to calculate T_p after the filtration process). The initial step in the filtration process entails discriminating samples that demonstrate mineral fractionation histories distinct from that of olivine. Highly evolved magmas are saturated with clinopyroxene (cpx) and plagioclase (plg), along with olivine. Back tracking the fractional crystallization of such magma is much more difficult. This is because the exact proportion of each fractionating mineral is not known. However, considering the most primitive magma composition will minimize the effect of cpx or plg fractionation (Lee *et al.* 2009). This explains why many workers choose olivine-based thermometers to calculate the T_p (Herzberg *et al.* 2007; Herzberg and Asimow 2008, 2015; Putirka 2008). Although Lee *et al.*'s thermobarometry is calibrated for input magma composition with MgO >8.5 wt%, cpx fractionates when MgO <9.2 wt% (Hao *et al.* 2021), and plg does when MgO <9.5 wt% (Leshner and Arndt 1995; Ganne and Feng 2017). For an accurate investigation, we considered basalts with a minimum 9.5 wt% of MgO. The SiO₂ content of the input basalts ranges from 43 to 52 wt%, according to the total alkali silica (TAS) classification (le Maitre 1984). Out of 1214 samples, 622 fall within this composition range. However, for the input basalts, FRACTIONATE-PT is calibrated for a total major oxide concentration of ≥ 97 wt%. Using this criterion, another 188 samples were filtered out.

Although it is widely believed that peridotites on partial melting produce basalts, pyroxenite can be another source (Lambart *et al.* 2016; Hole 2018). Notwithstanding, Lee *et al.* (2009) calibrated their thermobarometry for peridotite source melting. Peridotites constitute the bulk of the mantle with subordinate amounts of pyroxenites. Having a lower solidus than the peridotites, melting of pyroxenites under similar thermal conditions would result in a much higher degree of melting. Such melting will therefore yield higher temperatures than those obtained for peridotite melting. However, compositionally it is difficult to distinguish all pyroxenite-derived melts from those of peridotite-derived melts. And few pyroxenite-derived melts might equilibrate with Ol+Opx, a criterion required by the FRACTIONATE-PT calibration. Furthermore, FRACTIONATE-PT yields absolute temperatures and pressures for pyroxenite-sourced magmas that can be both too low and too high (e.g. Herzberg *et al.* 2023 and

references therein). Hence, considering basalts originating from a pyroxenite source can be misleading in this work.

We have used parameter, e.g. FC3MS [(FeO₇/CaO) - (3×MgO/SiO₂), all in wt%] (Yang and Zhou 2013) (Figures 2(a,b)) and FCKANTMS [$\ln(\text{FeO}/\text{CaO}) - 0.08 \times \ln(\text{K}_2\text{O}/\text{Al}_2\text{O}_3) - 0.052 \times \ln(\text{TiO}_2/\text{Na}_2\text{O}) - 0.036 \times \ln(\text{Na}_2\text{O}/\text{K}_2\text{O}) \times \ln(\text{Na}_2\text{O}/\text{TiO}_2) - 0.062 \times (\ln(\text{MgO}/\text{SiO}_2))^3 - 0.641 \times (\ln(\text{MgO}/\text{SiO}_2))^2 - 1.871 \times \ln(\text{MgO}/\text{SiO}_2) - 1.473$, all in wt %] (Yang *et al.* 2019) (Figure 2(c)) to distinguish samples of pyroxenite source melting. For peridotite-derived melts, Yang and Zhou (2013) showed that [FC3MS]_{max} = 0.65. However, FCKANTMS is a more robust parameter than FC3MS, and a combination of both parameters can exclude

most of the pyroxenite-sourced basalts. A comparison between (SiO₂/(CaO+Na₂O+TiO₂)) and FCKANTMS is shown in Figure 2(c), where the red and black line indicates experimentally constrained constant Mg# values of 0.6 and 0.7, respectively. Yang *et al.* (2019) suggested that any natural basalts resulting from peridotite melting with Mg# = 0.6–0.7 must fall within these two lines, while basalts with Mg# >0.7 should lie below it. Using these constraints, we sorted out 239 basaltic samples of pyroxenite origin.

However, cpx may crystallize from primary melts at crustal or mantle depths with elevated MgO content (Herzberg and Asimow 2008). The range of MgO vs. CaO for primary melts, which have not experienced any fractionation or accumulation of cpx was first

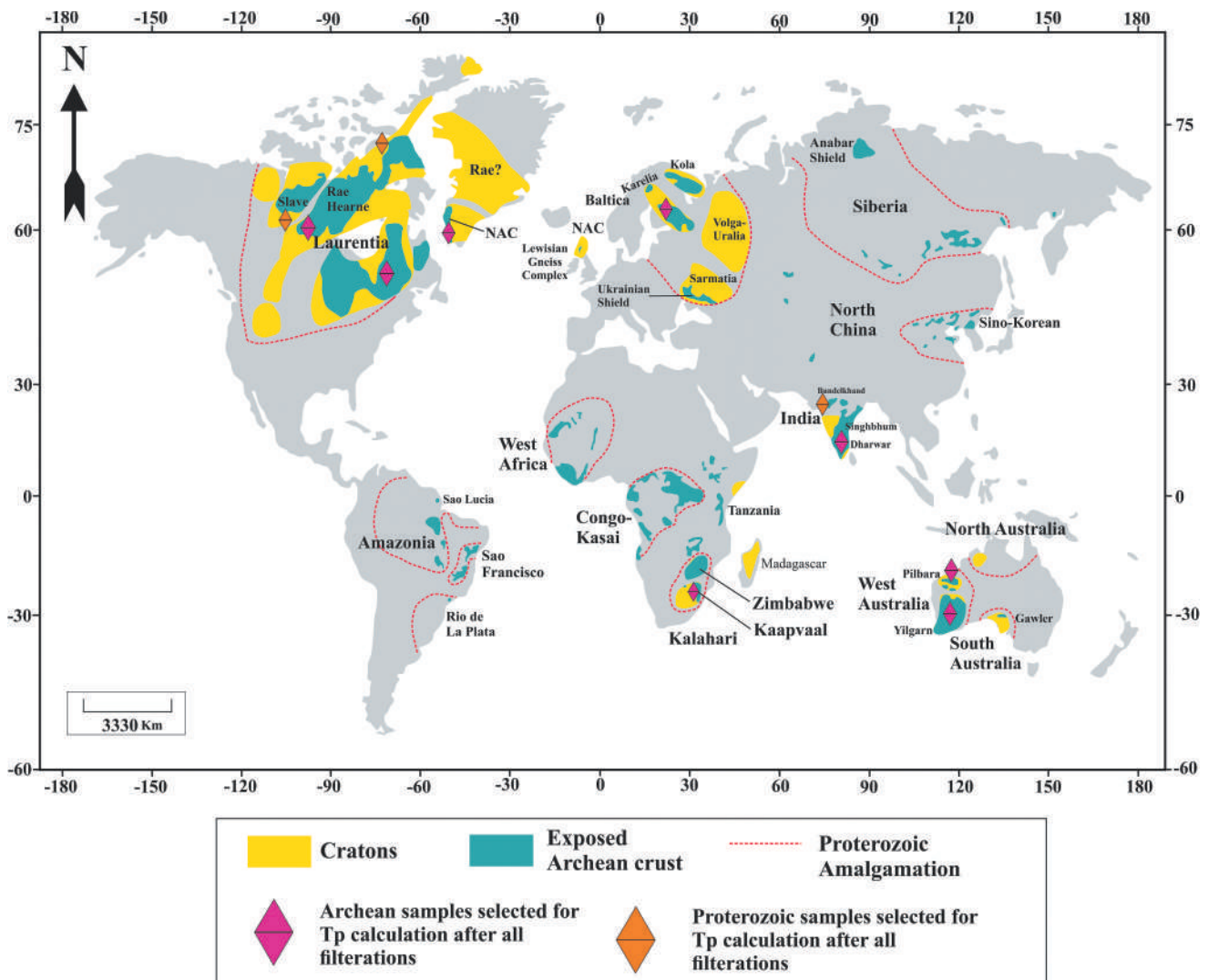


Figure 1. World-map (modified after Pearson and Wittig 2014) showing the sample locations of basalts used to calculate T_p in this work. The representative Archean basaltic compositions are from Greenland, Superior, and Wyoming craton (U.S.A. and Canada), Barberton craton (South Africa), Pilbara craton (Australia), Yilgarn craton (Australia), Baltic craton (Karelian Province, Finland), Dharwar craton (India). The representative proterozoic basaltic compositions are from Flin Flon and Cape Smith (Canada) and the Phulad ophiolite (India) (see IIT Bombay repository R2 for original basalt references).

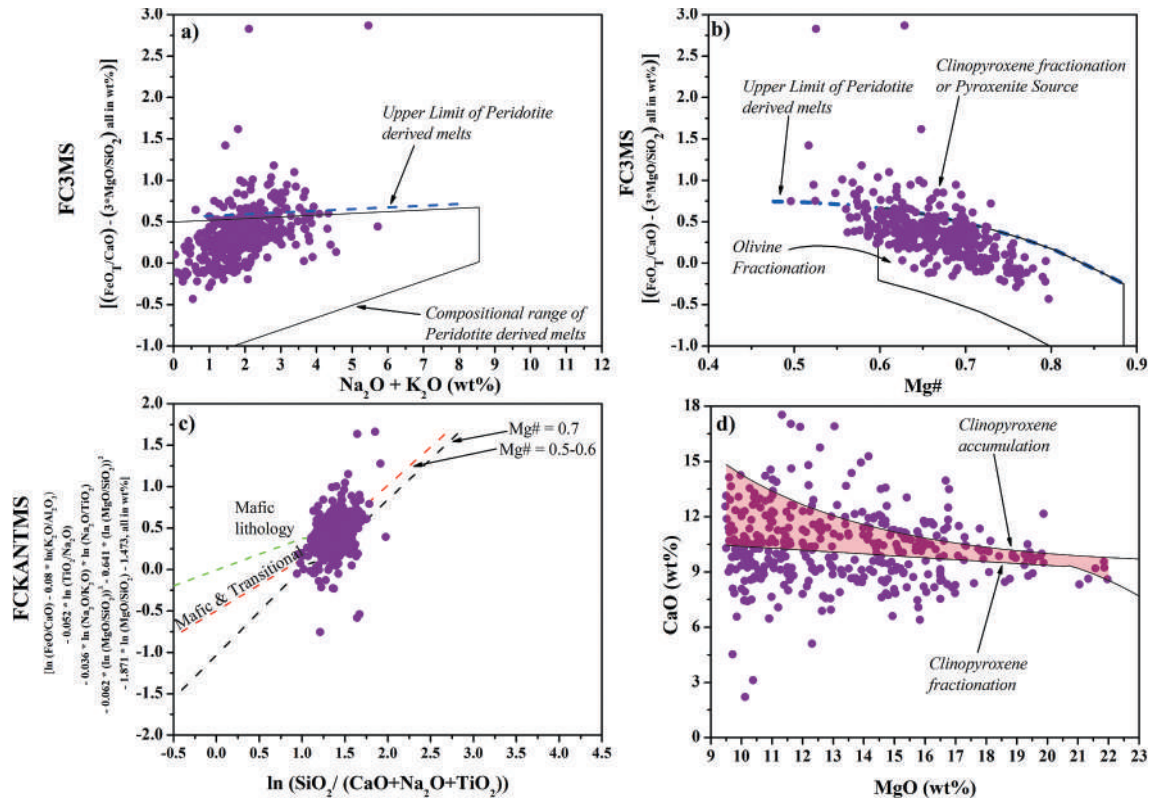


Figure 2. (a) $\text{Na}_2\text{O} + \text{K}_2\text{O}$ vs. FC3MS for the input basalt compositions. The parameter FC3MS is after Yang and Zhou (2013). (b) Mg# vs. FC3MS for the input basalt compositions (c) $\ln(\text{SiO}_2/(\text{CaO} + \text{Na}_2\text{O} + \text{TiO}_2))$ vs. FCKANTMS for input basalts (Yang *et al.* 2019). The red and black line indicate Mg# value of 0.5 - 0.6 and 0.7, respectively. The mafic transitional lithology indicates intermediate composition between peridotite and pyroxenite, whereas the mafic lithology indicates pyroxenites. (d) MgO vs. CaO of DM and EM-derived basalts. The shaded area indicates the range of primary magma compositions established based on the accumulated fractional melting model of a single fertile peridotite, KR-4003, which has not experienced clinopyroxene fractionation or accumulation. For the upper curve $\text{CaO} = 1.095 + 0.154 \times \text{MgO} + 116.58/\text{MgO}$. For lower curve $\text{CaO} = 11.436 - 0.104 \times \text{MgO}$, when MgO content is < 20.6% and $\text{CaO} = -23.209 + 3.643 \times \text{MgO} - 0.1 \times \text{MgO}^2$ when MgO content is > 20.6% (modified after Herzberg and Asimow 2008).

established experimentally by Walter (1998) and later modelled by Herzberg and Asimow (2008). Nevertheless, the narrow range of CaO established by the previous authors is based on the model accumulated fractional melts of a single fertile peridotite, KR-4003. In contrast, FRACTIONATE-PT has been calibrated using experimental melt compositions from various peridotite sources and is based on a batch melting approach for thermobarometry. Studies have shown that basalts produced through batch melting exhibit a broader range of CaO content (Herzberg 2006, 2011). Consequently, employing the MgO vs. CaO relationship (Figure 2(d)) would delineate the upper limit for clinopyroxene fractionation or accumulation. Using the MgO vs. CaO relation we filtered out 94 more samples. For the final calculation, we have 101 samples.

To calculate T_p , a certain assumption regarding the redox condition is necessary. An extreme redox condition can affect the measured temperature values. For example, T_p calculated in an oxidizing environment yields a lower value than that in a more reduced

condition (Ganne and Feng 2017). Hence, a neutral redox condition of $\text{Fe}^{+3}/\text{Fe}_{\text{Total}} = 0.1$ has been considered at the magma source by previous workers. We proceed here with the same consideration.

Unlike the fractional melting model, FRACTIONATE-PT does not simultaneously yield the T_p value and solve iteratively for the olivine Mg# due to its batch melting model of calculation. It rather requires the residual olivine Mg# (IIT Bombay Repository R1) to derive the primary magma composition from the input basalt, and subsequently determine the average pressure (P_g) and temperature (T_g). Conversely, T_p , calculated based on the accumulated fractional melting model, determines the Mg# of olivine to be crystallized from the primary melt at 1 atm pressure (Herzberg and Asimow 2015). With other conditions remaining the same, increasing the value of residual olivine Mg# elevates T_p and vice versa. For example, increasing olivine Mg# to 1 unit increases the T_p to ~50–100°C. Due to higher melting degrees, the residual olivine Mg# during the Archean was higher than those during the Proterozoic and

Phanerozoic (Herzberg and Rudnick 2012; see their Figures 3(d) and 4). As per the present work, a mean residual olivine Mg# value of 0.92 is assumed to calculate T_p (Herzberg and Rudnick 2012; Servali and Korenaga 2018) (IIT Bombay Repository R1). However, it is noteworthy that assuming a residual olivine Mg# of 0.92 might overestimate the T_p value for Proterozoic basalts by a few degrees. Alternatively, we consider a second scenario, assuming an olivine Mg# of 0.92 only to the Archean samples, and a value of 0.91 for the Proterozoic samples (IIT Bombay Repository R1).

The magma generation pressure (P_g) and temperature (T_g) for the input basalts calculated by FRACTIONATE-PT represent the average pressure-temperature (P-T) conditions and do not correspond to the potential temperature. This is because heat loss during adiabatic decompression melting reduces temperature relative to the solid mantle adiabat (Cawthorn 1975;

Putirka *et al.* 2007). However, considering only the heat loss due to adiabatic decompression will lead to apparent potential temperature (T_p^*). On other hand, calculation of the true potential temperature will require precise information regarding the degree of melting (F), rate of melt productivity (dF/dP)_{S (entropy)} (1–1.5% Kbar⁻¹ (Asimow *et al.* 1995, 1997; Behn and Grove 2015)) as was done by Putirka *et al.* (2007).

The apparent potential temperature (T_p^*) from the calculated P_g and T_g has been calculated by assuming an adiabatic gradient of 0.4°C km⁻¹ (0.4–0.5°C km⁻¹ for the upper mantle) (Katsura *et al.* 2010) and a depth (d) decrease of 31.5 km G Pa⁻¹ (Aulbach and Arndt 2019).

$$T_p^* = T_g - [(dT/dD) \times \text{Depth}(D)] \quad (1)$$

However, we simply use the term T_p to represent T_p^* in this study.

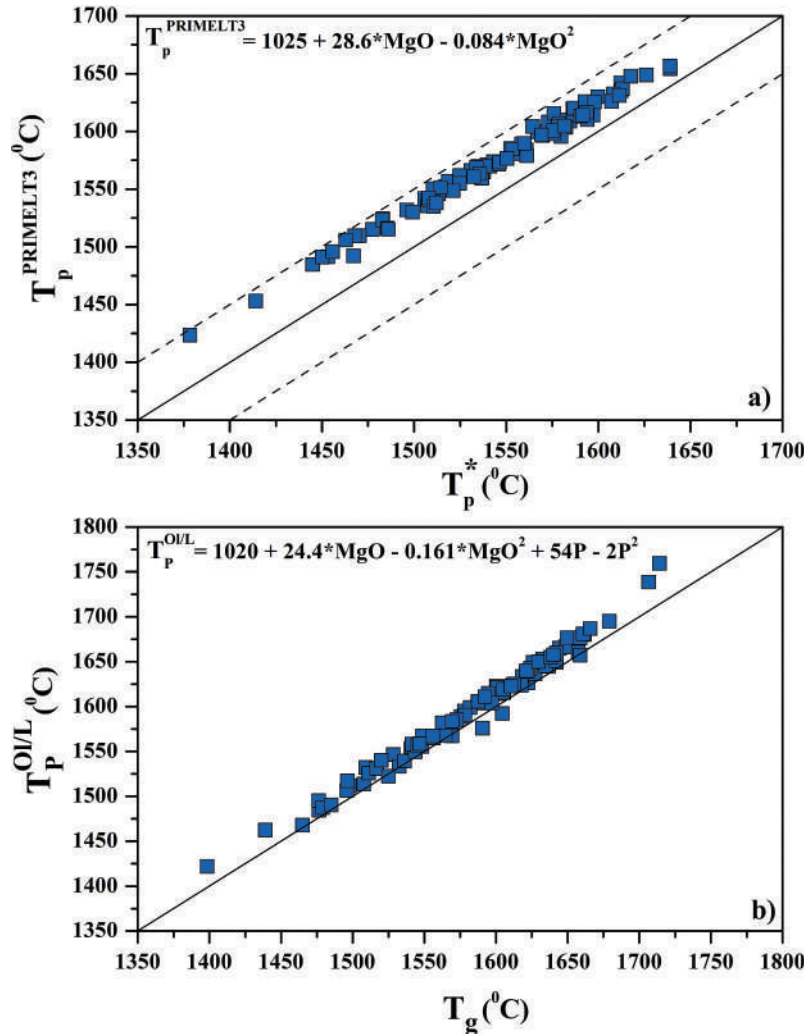


Figure 3. Comparison between (a) T_p^* vs. $T_p^{PRIMELT3}$ and (b) T_g vs. $T_p^{OI/L}$ observed from this study. $T_p^{PRIMELT3}$ is calculated using the primary magma MgO wt% from FRACTIONATE-PT. $T_p^{OI/L}$ is calculated using primary magma MgO wt% and average pressure (P_g) from FRACTIONATE-PT (see text for description). The dashed lines represent ± 50 .

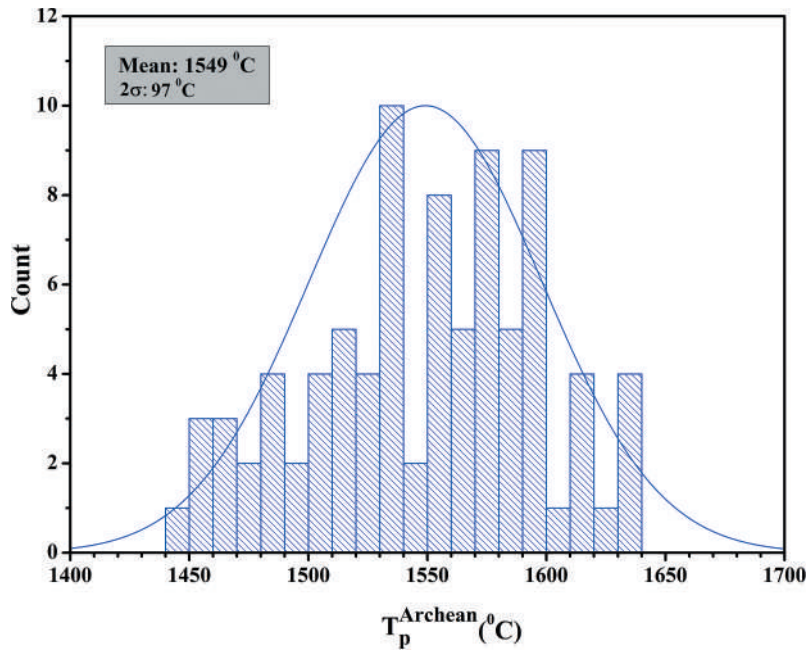


Figure 4. Summary of mantle potential temperature estimates during Archean from present study. All successful FRACTIONATE-PT solutions are given in supplementary material, SM1. Range of T_p during Archean is 1444–1639°C with a mean T_p of $1549 \pm 97^\circ\text{C}$ (2σ).

3. Accuracy and limitations in T_p estimations

As discussed in the previous section, the calculated T_p^* at any given residual olivine Mg# is lower than the actual T_p due to the consideration of a solid-state adiabatic decompression (dT/dD). To calculate T_p , one requires the initial pressure and temperature of melting; however, FRACTIONATE-PT calculates the average pressure and temperature. The only condition where $T_p^* = T_p$ is when melting begins at the solidus. Under all other conditions, $T_p^* < T_p$. However, studies show that the MgO content of primary magma remains almost constant during decompression (Herzberg and O'Hara 2002; Herzberg and Asimow 2008). Assuming that the adiabatic path follows the MgO isopleth during decompression, the PRIMELT algorithm (Herzberg and Asimow 2015) calculates T_p using the following equation:

$$T_p^{\text{PRIMELT3}}(^{\circ}\text{C}) = 1025 + 28.6 \times \text{MgO} - 0.084 \times \text{MgO}^2 \quad (2)$$

We have estimated the T_p^{PRIMELT3} value for our calculated primary magmas using equation 2, where MgO is the estimated primary magma MgO from FRACTIONATE-PT. A comparison between T_p^{PRIMELT3} and T_p^* is shown in Figure 3(a), where the ΔT_p ($T_p^{\text{PRIMELT3}} - T_p^*$) varies from 15°C to 45°C, with an average value of 29°C.

For a direct comparison, we have calculated the olivine liquidus temperature ($T_p^{\text{Ol/L}}$) at pressure P using the following equation from Herzberg and Asimow (2015).

$$T_p^{\text{Ol/L}}(^{\circ}\text{C}) = 1020 + 24.4 \times \text{MgO} - 0.161 \times \text{MgO}^2 + 54P - 2P^2 \quad (3)$$

Here MgO and P are the estimated primary magma MgO and average pressure (P_g) from FRACTIONATE-PT. We then compared the $T_p^{\text{Ol/L}}$ with T_g (Figure 3(b)). The ΔT ($T_p^{\text{Ol/L}} - T_g$) varies from -14°C to 45°C , with an average value of 12°C . Table R1T1 (IIT Bombay repository R1) presents a comparison of mantle potential temperature (T_p) values obtained through accumulated fractional melting and batch-melting model for non-arc basalts. The basalts were originally employed by Herzberg *et al.* (2010). The T_p values are re-calculated using their updated PRIMELT3 (Herzberg and Asimow 2015) algorithm and, concurrently, determined through the FRACTIONATE-PT method, incorporating an olivine Mg# of 0.92. The results are in good agreement and show strong internal consistency between the FRACTIONATE-PT and PRIMELT3 methods for calculating mantle potential temperature during the Precambrian. These findings support models of a hot ambient mantle in the Proterozoic and Archean.

4. Overall T_p trend during Archean

We observed an overall T_p range of 1444–1639°C during the Archean. The range of petrological T_p during the Precambrian is influenced by various factors, including

metamorphic alteration and mineralogical sorting, which are discussed later in this section. A single analysis showing significantly lower values of T_p^* (1378 °C) and $T_p^{PRIMELT3}$ (1423 °C) is excluded, as these values fall well below the lower outlier of T_p estimations and may be related to extensive metamorphic alteration during the Archean (Herzberg 2022b). The mean T_p value during Archean is $1549 \pm 97^\circ\text{C}$ (2σ) (Figure 4). The mean values of T_p from this study are $1569 \pm 13^\circ\text{C}$ (SE) ($n=11$) during the Eoarchean, $1564 \pm 18^\circ\text{C}$ ($n=7$) during the Paleoarchean, $1558 \pm 7^\circ\text{C}$ ($n=22$) during the Mesoarchean, and $1537 \pm 7^\circ\text{C}$ ($n=46$) during the Neoarchean. Our result is in excellent agreement with a T_p of $1550 \pm 48^\circ\text{C}$ (1σ), originally estimated by Herzberg *et al.* (2010) using PRIMELT2 from 14 samples of Archean age. This drops slightly to $1530 \pm 57^\circ\text{C}$ (1σ) using PRIMELT3 (Herzberg and Asimow 2015) on that same database.

While existing models of secular thermal evolution converge at a similar present-day T_p value, the

magnitudes differ significantly during the Archean. Supplementary Table S2 summarizes studies regarding the thermal evolution of the Earth, and a few major conclusions are presented below.

Many petrological as well as modelled T_p estimations (e.g. Abbott *et al.* 1994; Davies 2009; Ganne and Feng 2017; Keller and Schoene 2018) suggest a relatively colder Archean upper mantle. The authors argued that the upper mantle cooled from a maximum 1520–1400°C during 4000 Ma to the present-day value of 1350–1300°C (Figure 5). However, some of these T_p estimations (e.g. Keller and Schoene 2018) cannot be used to constrain the thermal evolution of the ambient convective mantle. This is partly because their T_p values pertain to continental arc basalts. These lower values explain the thermal evolution of a hydrous mantle rather than the anhydrous ambient mantle. Additionally, these basalts represent average compositions, reflecting fractionated lavas and not primary magmas.

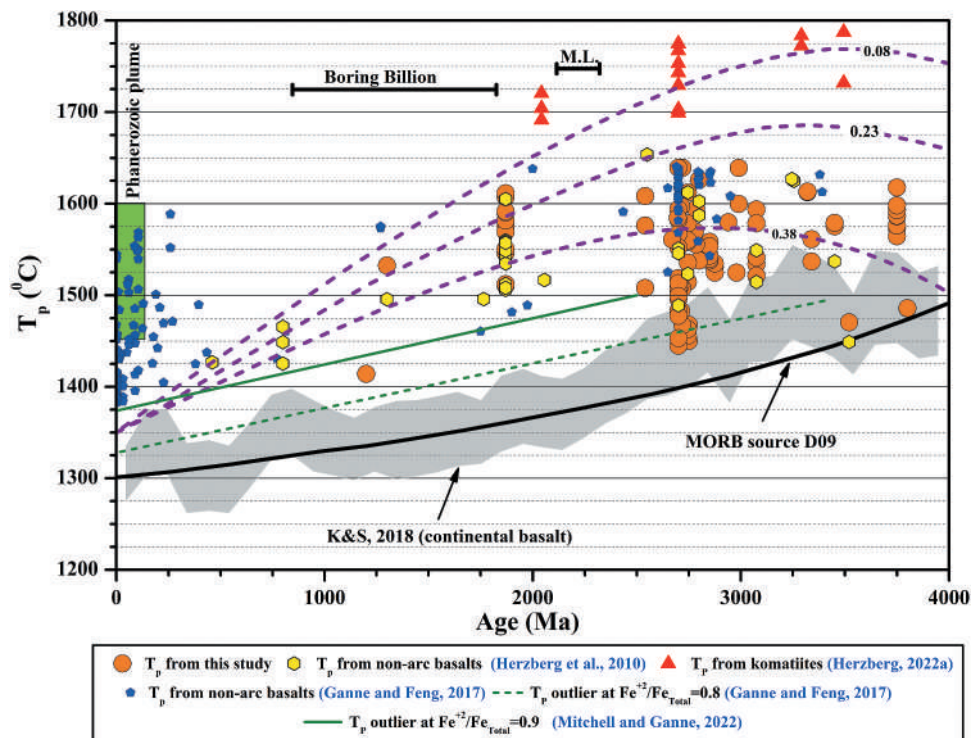


Figure 5. Variation in mantle potential temperature (T_p) with age. Orange circles represent T_p values calculated from basaltic magma generation temperature (T_g) and pressure (P_g) in the present study, using an olivine Mg# of 0.92. Redox conditions are considered as $\text{Fe}^{2+}/\text{Fe}_{\text{Total}} = 0.1$. The three Urey ratio values (0.08, 0.23 and 0.38) are from Korenaga (2008). The black curve illustrates the thermal evolution of the MORB source mantle from Davies (2009) (D09), based on parameterized convection models with conventional heat-flow scaling. Ambient mantle T_p from non-arc basalts from Herzberg *et al.* (2010) are shown in yellow hexagons. Blue pentagons represent T_p solutions at redox conditions of $\text{Fe}^{2+}/\text{Fe}_{\text{Total}} = 0.9$ for non-arc basalts from Ganne and Feng (2017). Ambient mantle T_p variations from Ganne and Feng (2017) are shown with green curves: dashed ($\text{Fe}^{2+}/\text{Fe}_{\text{Total}} = 0.8$). The solid green curve represents the T_p variation calculated by Mitchell and Ganne (2022) at redox condition of $\text{Fe}^{2+}/\text{Fe}_{\text{Total}} = 0.9$, based on the analysis of Ganne and Feng (2017) (detail in the text). T_p range for a pressure of 2.2 to 3.2 GPa based on the chemical composition of continental basalts, e.g. condition in the arc mantle wedge from Keller and Schoene (2018) (K&S, 2018) are shown (shaded region). For comparison, T_p values from Komatiites and Phanerozoic plume are shown (Herzberg 2022a). ML: magmatic lull from 2300 to 2200 Ma (Spencer *et al.* 2018). Boring billion from 1800 to 800 Ma (Roberts 2013).

Ganne and Feng (2017) used the PRIMELT3 programme (Herzberg and Asimow 2015) to calculate T_p from the non-arc basalts, assuming Fe^{+2}/Fe_{Total} of 0.8 and 0.9. Their individual T_p solutions for the more reduced condition, $Fe^{+2}/Fe_{Total} = 0.9$, are in good agreement with those obtained in this work and Herzberg *et al.* (2010). Primitive modern MORB that formed from ambient mantle melting also have $Fe^{+2}/Fe_{Total} = 0.9$ (Berry *et al.* 2018; Gaborieau *et al.* 2020; Bézou *et al.* 2021), but early Earth ambient mantle may have been more reducing (Hirschmann 2023). In case our assumed $Fe^{+2}/Fe_{Total} = 0.9$ in primary magma calculation is too low, our T_p results will also be slightly low as well; for example, it will be too low by $\sim 30^\circ\text{C}$ if $Fe^{+2}/Fe_{Total} = 0.95$. However, estimates made with more oxidizing conditions ($Fe^{+2}/Fe_{Total} = 0.8$) yields lower T_p values as in Ganne and Feng (2017). These authors further assumed that ambient mantle T_p was represented by their low T_p outlier solutions, not their averages. Moreover, outliers are insignificant because they could have been compromised by metamorphic alteration and/or long wavelength variations in ambient mantle T_p about a mean (Herzberg 2022b). The outlier T_p solution by Ganne and Feng (2017) at $Fe^{+2}/Fe_{Total} = 0.8$ suggests an ambient mantle $T_p = 1450\text{--}1520^\circ\text{C}$ during 2500–3800 Ma. Additionally, Mitchell and Ganne (2022) reported an outlier T_p solution for a more reduced condition of $Fe^{+2}/Fe_{Total} = 0.9$, based on the earlier work by Ganne and Feng (2017), which predicts an ambient mantle T_p of $\sim 1500^\circ\text{C}$ during 2700–2800 Ma. However, the ambient T_p variation obtained by Ganne and Feng (2017) and Mitchell and Ganne (2022) are cooler than the results presented here and in Herzberg *et al.* (2010).

Besides the petrological constraints, another parameter called the 'Urey ratio' is used to estimate mantle thermal evolution. The Urey ratio is a measure of mantle heat production due to internal heating relative to mantle heat flux. The thermal history proposed by Davies (2009) assumes a much higher value of convective Urey ratio – 0.84, while the present-day thermal budget fits to a much lower value of Urey ratio (~ 0.3) (Korenaga 2013). Considering a higher Urey ratio further suggests a minor role of secular cooling in Earth's evolution (Korenaga 2017). The petrological estimation by Abbott *et al.* (1994) shows similar results to that of Davies (2009). However, Abbott *et al.* (1994) constrained the olivine liquidus temperature from basalts and komatiites, not the mantle potential temperature.

Besides previous observations, a much hotter upper ambient mantle model was proposed by Herzberg *et al.* (2010). They used the tectonic setting as a proxy to select basaltic samples to calculate T_p using the PRIMELT software. They argued that the Earth warmed

up vigorously for the initial ~ 1500 My, and latter started to cool after ~ 3000 Ma. Most of the estimated T_p values by Herzberg and co-workers were $> 1500^\circ\text{C}$ during the Archean, reaching to a maximum of 1650°C . Komiya *et al.* (2002) also pointed out a hotter MORB source with $T_p \geq 1500^\circ\text{C}$ during the Paleoproterozoic (3500 Ma) from the Pilbara craton.

With hot and cold thermal models in consideration, a critical question comes up: which thermal model best fits with the Earth's evolution? As the mantle temperature is a function of internal heat production due to radiogenic heating, Korenaga (2008) estimated mantle temperature through time by backward modelling, considering a present-day T_p value of 1350°C and present-day convective heat production value of 8.5 ± 5.5 TW. They suggested that the secular cooling of the mantle corresponds to a present-day convective Urey ratio of 0.23 ± 0.15 . When compared, the petrological T_p expressions for Precambrian non-arc basalts from Herzberg *et al.* (2010) exhibited remarkable concordance with an Urey ratio of 0.38, with T_p values distributed within $\pm 100^\circ\text{C}$ around the Urey ratio curve of 0.38. In contrast, plume-derived magmas, such as komatiites, showed T_p values in excess of $150\text{--}200^\circ\text{C}$ than the ambient mantle (Figure 5).

At any given time during Precambrian, the variation in petrological T_p estimation depends on several factors. For example, Herzberg (2022a) showed that processes like metamorphic alteration and the addition of Fe-rich olivine can account for a $\pm 68^\circ\text{C}$ variation in T_p values for the Paleoproterozoic CSLIP basalts. Consequently, T_p values during Archean might be compromised depending on the degree of metamorphic alteration and/or mineralogical sorting. Additionally, Herzberg (2022b) pointed out that the long wavelength variations in T_p within the ambient mantle may have been $\pm 50^\circ\text{C}$, based on the estimates for present-day MORB-producing ambient mantle. Considering these factors as sources of error, the distribution of most T_p values within $\pm 100^\circ\text{C}$ around the curve for a Urey ratio of 0.38 can account for the total variability of ambient mantle temperature during the Precambrian. The remarkable correlation between the petrological (Herzberg *et al.* 2010) and geophysical findings (Korenaga 2008) has supported their combined thermal model, making it widely accepted in the geoscientific community.

The range of T_p values observed in this study supports a hotter Archean mantle hypothesis. Moreover, it aligns with the thermal evolution path proposed by Korenaga (2008) (Figure 5), where the T_p values are distributed within approximately $\pm 100^\circ\text{C}$ of an Urey ratio curve of 0.38. Our 'hotter Archean' hypothesis is further reinforced through the calculation of $T_p^{PRIMELT3}$

using the primary magma MgO wt% from this study, where the T_p^* is, on average, only 29°C less than the $T_p^{PRIMELT3}$ (Section 3). Notwithstanding, several authors contend that T_p values obtained from Archean non-arc basalts represent plume temperatures rather than those of the ambient mantle. This issue is further addressed in section 5.

5. Archean non-arc basalts: a dichotomy in genesis

Archean greenstone belts are characterized by widespread occurrences of basalts, having both arc and non-arc signatures and a minor amount of komatiites (<5 vol%) (de Wit and Ashwal 1997). The basalts are sometimes intercalated with komatiites but are typically observed as thick sequences of Archean tholeiites (Hallberg 1972). Archean non-arc basalts often occur as prodigious sequences of complex flows and define pillow structure. Some authors question the ambient mantle origin of non-arc basalts during the Archean and suggest that those formed due to melting of the colder plume head, whereas the komatiites were formed due to melting of the hotter plume axis (Campbell *et al.* 1989; Campbell and Griffiths 1990; Hauri *et al.* 1994). However, recent petrological constraints from many Phanerozoic plumes (e.g. Galapagos, Iceland) suggest the opposite; for example, basalts initially erupted from the plume head are hotter than the basalts erupted later from the plume axis (Thompson and Gibson 2000; Herzberg and Gazel 2009; Trela *et al.* 2015). There is a growing consensus that during the Archean, typical plume melting would result in Al-depleted and undepleted komatiites/ferrokatiites from the axial and head regions respectively, and that basalts can only be produced from the periphery region, where the plume temperature is equivalent to the ambient mantle temperature (Gibson 2002; Sproule *et al.* 2002; Sleep 2008). On the other hand, based on the plume head-tail structure, several Archean greenstones have been described to be formed in a hot spot setting, although the physical and thermal structure of the plume is debated (Supplementary Table S3).

There is currently no compelling evidence for the unique head-tail structure of plumes. For example, recent numerical modelling (Farnetani and Samuel 2005) suggests that the classical head-tail structure must not be true for all mantle plumes and that different plume geometries can be possible. The end member includes a poorly developed plume head with a 'spout' like structure. During Hadean and Archean, the core heat flux was higher than it is at present (Labrosse 2015; Korenaga 2017). However, predicting whether this

higher heat flux from the core would have resulted in larger plumes or more numerous plumes is challenging due to the largely unknown nature of the core-mantle boundary (CMB) during that period (Yamazaki and Karato 2001; Schott and Yuen 2004).

Geoscientists, advocating for the plume origin of granite-greenstone belts, often refer to the Paleo-Mesoarchean east Pilbara craton in Western Australia. The craton contains well-preserved, little deformed supracrustal belts. Based on stratigraphic relations and field evidence, it was previously suggested that the Paleo-Mesoarchean eastern Pilbara craton formed over a plume setting (Van Kranendonk *et al.* 2004, 2007; Smithies *et al.* 2005; Hickman 2012; Barnes *et al.* 2021). However, comprehensive studies by others (Kusky *et al.* 2018, 2021; Windley *et al.* 2021) challenge this view, indicating that the preserved stratigraphy in the eastern Pilbara craton matches more closely with an Oceanic Plate Stratigraphy (OPS) rather than a plume setting. Importantly, identifying features of sea-floor spreading in the greenstone belts can provide consensus on the nature of non-arc basalts. For example, the presence of sheeted dikes. The presence or absence of sheeted dike complexes is critically controlled by the relationship between spreading rate and magma supply (Robinson *et al.* 2008). These complexes develop when there is sufficient melt to fill the fractures created by spreading, a balance commonly observed at mid-ocean ridges (see reviews in Furnes and Dilek 2022; Kusky and Celâl Şengör 2023). Although rarely preserved (e.g. Kusky and Celâl Şengör 2023), few sheeted dike complexes have been identified in Archean greenstone belts, such as those in the 3800 Ma Isua greenstone belt (Greenland craton) (Furnes *et al.* 2009), the 3300 Ma Barberton Greenstone Belt (BGB, South Africa) (Grosch and Slama 2017) and the 2700 Ma Yellowknife volcanic belt (Slave craton, Canada) (Corcoran *et al.* 2004), indicating features of ocean spreading centres. It is important to note that non-arc basalts need not be associated with oceanic crust formed at spreading centres. Evidence from the CSLIP shows that they may form by ambient mantle melting in continental rift environments (Herzberg 2022a). This model may also work well for the Archean greenstone terranes of the eastern Yilgarn Craton (Barnes *et al.* 2021).

Previous T_p estimates show that non-arc basalts during Archean formed by ambient mantle melting, and that the komatiites represent mantle potential temperatures that are ~150–250°C greater than the then ambient mantle temperature (Nisbet *et al.* 1993; Herzberg 2022b). Herzberg and co-workers (Herzberg *et al.* 2010; Herzberg 2022b) calculated the potential temperature from basalts and then compared those values with the

modelled present-day secular cooling curve of the ambient mantle of Korenaga (2008). This corresponds to an Urey ratio of ~ 0.38 . The thermal evolution outlined by Korenaga is consistent with the present-day thermal budget of the Earth and hence a significant deviation from these values is equivalent to neglecting the established geophysical and geochemical constraints (Korenaga 2021). The strong fit between the petrological estimation and the modelled value led to the conclusion that the temperatures deduced from the Archean non-arc basalts were actually those of the convecting upper mantle and not the Archean plumes. Notwithstanding, based on trace element ratios, Brown *et al.* (2024) demonstrated the absence of present-day MORB-type crust during the Archean. They proposed that Archean non-arc basalts were derived through plume-crust interaction, as their composition is similar to present-day oceanic plateau basalts (OPB). However, given the higher ambient mantle T_p during Archean ($\sim 250^\circ\text{C}$ higher than today), others (Herzberg and Gazel 2009; Herzberg and Rudnick 2012) have shown that basalts derived from ambient mantle melting during Archean have similar composition to those of Phanerozoic plateau basalts. This is further evident from the secular thermal evolution of the ambient mantle and the plume. For example, the ambient mantle T_p during Archean ranges from 1450°C to 1650°C (this study; Korenaga 2008; Herzberg *et al.* 2010), which is comparable to the Phanerozoic plume temperature ($1450\text{--}1600^\circ\text{C}$) (Herzberg 2022b).

6. Early earth tectonics: inferred from various numerical modelling

The idea of a hotter Archean sparked interest among geoscientists, as researchers sought to rigorously assess the feasibility of plate tectonics on a warmer Earth through various numerical models. It is commonly believed that the characteristics of plate tectonics evolved due to the secular cooling of the mantle (O'Neill *et al.* 2007), with the recycling of oceanic crust via subduction occurring in a somewhat later phase of Earth's history (Palin *et al.* 2020). Although plate reconstruction modelling shows the presence of prominent subduction zones since the early Neoproterozoic (*review in* Chatterjee and Mukherjee (2022)), 'when did the plate tectonics begin?' is still debated (Condie and Kröner 2008; Van Kranendonk 2010; Korenaga 2013). Numerical models provide some indirect and intriguing results. However, it is important to note that the numerical models rely on various parameters, including ocean lithospheric thickness, density, plate velocity, slab length, as well as the viscosity of the convecting mantle.

These parameters are not understood accurately. A robust estimation of these parameters has remained contentious, and varying these parameters can yield different model results (Korenaga 2006). Results from several 2D and 3D thermomechanical models show the plausibility of both vertical tectonics and plate tectonics during the early Earth (Supplementary Table S4), which are briefly discussed below.

6.1. Vertical tectonics

Three mechanisms of vertical tectonics have been proposed: (i) sagduction, (ii) heat-pipe and (iii) stagnant-lid. Stagnant-lid considers a single lithospheric plate governed by intrusive type of magmatism (O'Neill *et al.* 2007). Heat-pipe, the most unstable type of stagnant-lid is characterized by surface volcanism, where magma traverses the lithosphere to the surface through vertical conduits (Stern *et al.* 2018). Sagduction, a less rigid mechanism than stagnant-lid convection, involves the foundering and partial melting of the base of a magmatically overthickened oceanic crust (Johnson *et al.* 2014).

The stagnant-lid hypothesis during early Earth is rooted in the idea that the mantle convected vigorously due to elevated internal temperatures resulting from higher internal heating (O'Neill *et al.* 2007; Beall *et al.* 2018; Bédard 2018). During the Hadean-early Archean, elevated internal temperatures plausibly reduced the convective stress, and could not exceed the lithospheric strength. Consequently, the lithosphere remained intact and did not promote plate tectonics. However, the assumption of a purely internally heated mantle in previous models has been questioned, given that the Earth's mantle likely exhibits mixed heating – heating from both within and below (Korenaga 2017; Lenardic *et al.* 2021). Moreover, a mixed-heated mantle does not exhibit lower convective stress, as convective stress depends on the magnitude of basal heating rather than internal temperature (Korenaga 2017). The core heat flux during Hadean and Archean was higher than at present, decreasing from approximately 40% at 4500 Ma to 25% at present (Korenaga 2017). The stagnant-lid mode further assumes a layered mantle convection during the Hadean-early Archean (e.g. Bédard 2018). However, thermodynamic experiments show whole-mantle convection and a more efficient plate subduction during early hotter Earth that better matches with the thermal evolution of the Earth (c.f., Agrusta *et al.* 2018).

Moore and Webb (2013) proposed a heat-pipe mechanism for the Hadean and early Archean Earth, inspired by its original proposal for Jupiter's satellite Io. However, their heat-pipe model produces a lower

geothermal gradient for the bulk lithosphere during Hadean and early Archean, which is considered as a major drawback of their model (Rozel *et al.* 2017; Roman and Arndt 2020; Korenaga 2021), and hence the model results cannot be applied to Earth-like planets.

'Sagduction,' a more widely accepted pre-plate tectonics mechanism, considers the destabilization and sinking of the base of a thick oceanic crust into the underlying hotter mantle. The central idea of sagduction comes from field observations, where the dome-and-keel structure of many Archean batholiths has been postulated to form from the down-sagging of the volcanic pile and subsequent upwelling of the granitic mass (Macgregor 1951; Sandiford *et al.* 2004; Hickman 2012). However, such a structure is not unique to Archean, and similar structures are found in many Phanerozoic and Proterozoic accretionary orogenic belts as well. In such cases, arc-related granitic domes rise through the older volcano-sedimentary sequence (*reviews in* Kusky *et al.* 2018; Windley *et al.* 2021). Given the analogous rock record and structural patterns observed in both modern accretionary orogens and Archean dome-and-keel provinces, the authors (Kusky *et al.* 2018, 2021; Windley *et al.* 2021) suggested that the later formed most likely within a mobile-lid setting rather than a stagnant-lid. Despite these debates, several workers performed numerical modelling of sagduction on a hotter Earth.

Studies show that the oceanic crust thickness is proportional to T_p (Sleep and Windley 1982; Van Thienen *et al.* 2004; Herzberg and Rudnick 2012). Melting and mantle depletion begins at ~45 km beneath the modern spreading ridges but initiate at 35 km deeper for every 100°C increase in mantle temperature (Vlaar *et al.* 1994). In other words, a colder mantle intersects the peridotite solidus at shallower depths. As a result, the oceanic crust produced at a colder T_p is significantly thinner. Various numerical models (Herzberg 2014; Johnson *et al.* 2014; Sizova *et al.* 2015; Rozel *et al.* 2017; Piccolo *et al.* 2019) show that at the base of a thick oceanic crust, the basalt converts to a garnet-rich dense lithology, most probably garnet amphibolite, which delaminates into the underlying mantle due to density inversion. The garnet amphibolite being hydrous produces TTG magma upon partial melting (Johnson *et al.* 2017).

However, the sagduction hypothesis has recently been re-evaluated and significant drawbacks have been pointed out. (i) First, all the models consider a homogeneous 40–45 km thick oceanic crust. In contrast, Archean oceanic crust is internally differentiated. With basalts at the top and gabbros forming the middle crust, the lower part of a thick Archean oceanic crust contains olivine ± pyroxene bearing ultramafic anhydrous cumulates (Roman and Arndt 2020). The in-situ transformation of these low-aluminium ultramafic

cumulates to a garnet-dominated lithology hence not feasible at the base of an oceanic crust. Recent experimental results further suggest that pressure in excess of 1.5 GPa (~54 km depth) is required for a hydrous basalt to stabilize plagioclase, amphibole, garnet and rutile to achieve the required Eoarchean TTG composition (Hastie *et al.* 2023). This equilibrium pressure is higher than those at the base of overthickened basaltic crust during Archean and may require subduction for their formation. (ii) Most models do not consider the true rheology of a garnet-dominated lithology, e.g. incorporating the viscosity of a garnet-dominated lithology yields a time period of 1–10 Ga for crustal delamination, making sagduction almost impossible (Mondal and Korenaga 2018). (iii) The volume of felsic crust produced by the sagduction model is much less than the recently proposed crustal production rate during Archean (Rosas and Korenaga 2018; Guo and Korenaga 2020). Moreover, the production of felsic crust requires both basalt and water at the site of melting. Sagduction model fails to explain the presence of both and therefore, crustal growth by sagduction is less likely during the early Earth.

Besides the mechanisms discussed above, where sagduction and crustal drips seem implausible for producing granitic masses, other mechanisms, such as intracrustal melting of Archean oceanic crust, might explain TTG formation on the early Earth. For example, the oceanic crust during the Archean might contain sills of melts that differentiated to form a thick middle and lower gabbroic crust, as seen in the present-day Iceland (MacLennan 2019; Baxter *et al.* 2023). Intracrustal melting of this gabbro under Archean geotherm can generate TTG melt, given that they are hydrous and have low Mg# to stabilize garnet, rutile and amphibole at a relatively low pressure (1 GPa ~36 km depth) (Smit *et al.* 2024). The TTG formation stage might be followed by crustal drip or delamination (e.g. Bédard 2006; Nebel *et al.* 2018; Smit *et al.* 2024). However, the Mg# in Archean gabbros ranges from 99 to 12, with a mean value of 53. Considering a low Mg# (e.g. ≤35) for the mafic source might lower the equilibrium pressure for garnet stability but would generate TTG with much lower Mg# than natural TTGs (e.g. Huang *et al.* 2020; c.f.; Johnson *et al.* 2017).

6.2. Plate tectonics

While vertical tectonics gained popularity amongst modellers, some authors attempted to model plate tectonics and subduction on an early hotter Earth (van Hunen and van den Berg 2008; van Hunen and Moyen 2012; Foley 2018; Weller *et al.* 2019; Perchuk *et al.* 2021, 2023). They proposed that subduction can happen under hotter mantle conditions for $T_p = 1550\text{--}1600^\circ\text{C}$,

but would experience frequent slab break-off due to the lower viscosity of the convective mantle. The lower viscosity of the mantle resulting from higher temperatures in the past would reduce oceanic lithosphere strength, leading to slab break-offs occurring approximately every 5–20 My (van Hunen and van den Berg 2008; van Hunen and Moyen 2012).

While temperature has a first-order control on mantle viscosity, the net water content also plays a significant role. For example, a hotter and drier mantle may have a viscosity similar to that of a colder wetter mantle (Hirth and Kohlstedt 1996; Crowley *et al.* 2011). The Archean convective mantle was drier and hotter than the present-day convective mantle (Korenaga *et al.* 2017). This challenges the notion that the early mantle invariably had a much lower viscosity than the present-day mantle. A quantitative estimation of the temperature-dependent viscosity profile of the convective mantle suggests ~12-fold increase in viscosity over the last 4000 Ma. However, when accounting for the effect of water, there is only a ~3-fold increase in viscosity over the same period (Crowley *et al.* 2011). Accounting for this viscosity effect in models can produce a different time period for slab break off during the Archean. A drier Archean mantle is consistent with the fact that, a substantial volume of ocean covered the surface during most of the Archean (Harrison 1999; Pope *et al.* 2012; Korenaga *et al.* 2017; Johnson and Wing 2020; Reimink *et al.* 2021).

Decompression melting at a high T_p produces a thick oceanic crust as well as a thick layer of dehydrated refractory lithospheric mantle (Bickle 1986; Korenaga 2006). When considering this effect of dehydration stiffening, the oceanic lithosphere as a whole may not necessarily exhibit lower strength at high T_p . For example, incorporating the effect of dehydration stiffening in numerical models revealed a substantial increase in the slab break-off time to 20 My (van Hunen and Moyen 2012), whereas neglecting this effect, indicates a significantly shorter break-off period of ~5 My (van Hunen and van den Berg 2008; van Hunen and Moyen 2012).

Oceanic crust produced at higher T_p are denser than that produced at lower T_p (Korenaga 2006; Weller *et al.* 2019). Consequently, one would anticipate a denser Archean oceanic crust than what is present today. Despite this, immediate subduction of the oceanic lithosphere during the Archean is not guaranteed. This is because the oceanic crust and the depleted lithospheric mantle produced at higher T_p still remain positively buoyant compared to the unmelted mantle (Korenaga 2006). Note that to initiate subduction, the oceanic lithosphere must acquire a net negative buoyancy. Two schools of thought exist, with various authors proposing different mechanisms for the oceanic lithosphere to

achieve negative buoyancy during Archean. The first mechanism involves the basalt-to-eclogite transition, where an external stimulus, such as plume-induced subduction, may be necessary (Gerya *et al.* 2015; Davaille *et al.* 2017; Baes *et al.* 2020; Tran *et al.* 2023). Once initiated, subduction can be sustained under a variety of scenarios. The second mechanism proposes a sluggish plate motion than the present, starting from the early Archean and potentially continuing into the Paleoproterozoic, allowing the lithosphere to attain a net negative buoyancy that facilitates subduction (Solomatov 1995; Korenaga 2003, 2006; Bradley 2008; Herzberg *et al.* 2010; Foley 2018, 2022). However, other studies, based on detailed mineral physics calculations, argue that net negative buoyancy is not a necessary requirement for subduction (Hynes 2005; Afonso *et al.* 2007). While grappling with these challenges, the task of bending and subducting a thick and stiff oceanic lithosphere during the Archean becomes complex. Notwithstanding, thermal cracking, encompassing the fracture and hydration of the stiff lithosphere in the presence of surface water, can introduce localized zones of weakness. This promotes bending and subduction of the lithospheric plate (Korenaga 2007, 2011).

Other mechanisms such as drip-like local subduction without involving a true plate boundary have been proposed for high T_p during the Hadean-early Archean (Foley 2018; Gunawardana *et al.* 2024). This later evolved into modern-style slab subduction during the Mesoarchean as the T_p declined. However, considering the effects of thermal cracking, core heating related high convective stress, and a wet and heterogeneous mantle, other researchers (e.g. Korenaga 2011; Miyazaki and Korenaga 2022) proposed a plate boundary-related subduction since the Hadean. The drier mantle and a sluggish plate motion discussed above mostly applies to the Archean. In contrast, the Hadean experienced a faster tempo of plate tectonics due to a wetter and hotter mantle, resulting in a much lower mantle viscosity (Moresi and Solomatov 1998; Turcotte and Schubert 2002). A vigorously convecting mantle with low viscosity can drive convecting instabilities that can erode and weakens the lithosphere (Huang *et al.* 2003; Korenaga and Jordan 2003). Consequently, subduction associated with frequent slab break-offs on a scale of a few million years might represent a potential tectonic scenario during the Hadean.

7. When did plate tectonics begin: constraints from geochemical, isotopic, mineralogic & petrologic evidence

While numerical modelling offers intriguing insights into the feasibility of plate tectonics on an early hotter Earth,

these studies are only indirect evidence. Direct evidence of plate tectonics is derived from petrological, mineralogical, geochemical, isotopic, and field studies. Several workers have contributed to estimating the time period of the onset of plate tectonics, suggesting a broad temporal spectrum extending from the Hadean to the Neoproterozoic. Referring to plate tectonics, while some authors assert the exclusive significance of subduction (Stern and Gerya 2018), others stress on the importance of the entire Wilson cycle (Shirey and Richardson 2011). Due to the nature of plate tectonics, which tends to erase the past evidence, caution must be exercised in interpreting the available data before establishing a timeline for the onset of plate tectonics. The existing evidence does not definitively establish a timeline for the same, and multiple working hypotheses should be considered (Harrison 2024). Therefore, rather than asking when plate tectonics began, a more pertinent question arises: is there any geological period devoid of discernible signatures of plate tectonics? (Kusky *et al.* 2018; Harrison 2024). See Supplementary Table S5 for a review of timing of onset of plate tectonics.

7.1. Proterozoic

Drawing upon numerous present-day subduction-zone indicators such as ophiolites, glaucophane-bearing blueschist facies rocks, and ultra-high pressure (UHP) rocks – several authors (Hamilton 1998, 2011; Stern 2005; Zheng and Zhao 2020; Chen *et al.* 2022) proposed that plate tectonics commenced during the Neoproterozoic. Others suggested a Mesoproterozoic (1400–1100 Ma) time for its onset based on the age of neutral buoyancy of oceanic lithosphere (Davies 1992) and widespread occurrences of kimberlites (Stern *et al.* 2016). However, Stern (2023) provided compelling evidence for plate tectonics including the presence of ophiolites, low T/P metamorphism including eclogites, seismic images of paleo-subduction zones, ore deposits, passive margin formation, etc., during the Orosirian period (2050–1800 Ma), Paleoproterozoic (see Supplementary Table S1 for other references). He further suggested that during the Proterozoic, the Earth shifted from a regime of plate tectonics to a single lid multiple times, with the single lid being associated with supercontinents.

Given their unstable nature, the ophiolites, blueschist facies, and the UHP rocks are susceptible to erosion, and the absence of these features from the geologic record probably reflects preservation issues (Harrison 2020). An illustrative contemporary example of this phenomenon is evident in the ongoing Himalayan orogeny, where approximately 70% of the exposed ophiolites, along with half of the accretionary complexes and nearly all

the UHP rocks, have been eroded (Yin and Harrison 2000). Nevertheless, the unequivocal examples of Paleoproterozoic ophiolites have been documented in various parts of the world (Supplementary Table S1), and the presence of such formations may extend further back in time, as evidenced by Neoproterozoic ophiolites from the North China craton associated with eclogite facies metagabbro (Ning *et al.* 2022) and Eoarchean Isua supracrustal belt in Greenland (Furnes *et al.* 2009). Following the 1972 Penrose field conference on ophiolites by Geological Society of America (GSA) (Anonymous 1972), several geologists have argued that to be classified as an ophiolite, the entire sequence, ranging from basal depleted harzburgites to the sheeted dike complex, must be preserved. However, preservation issues and dismemberment during ophiolite emplacement often result in scattered remnants. During Archean, higher T_p led to thicker oceanic crust, and a thickened crust during ophiolite emplacement could only effectively preserve the upper sections (Kusky and Celâl Şengör 2023; Zheng 2024), while the predominance of complete Penrose-type ophiolites since ~900 Ma indicates significant oceanic crust thinning due to secular cooling (Condie and Stern 2023).

Preserving UHP rocks poses a significant challenge, and observation of both oceanic and continental UHP rocks at surface is constrained by the exhumation process. Firstly, the exhumation of deeply subducted rocks is not a continuous process. Various factors, including the subduction geotherm and slab dip angle control crucially the exhumation of UHP rocks (Mukherjee and Mulchrone 2012). For example, a higher subduction geotherm and a shallower dip angle can exhume negligibly (Agard *et al.* 2009; Perchuk *et al.* 2023). Consequently, appearance of UHP rocks in the later rock-record might be an artefact of a steeper subduction angle and a colder mantle geotherm (Zheng and Zhao 2020) and not necessarily indicate the onset of plate tectonics. Recent developments in machine learning utilize the global litho-geochemical data to calculate the lithospheric thickness and correlate it with the secular change in metamorphic gradient (Zhang *et al.* 2023). These analyses reveal that low to intermediate T/P metamorphism has become widespread since the Neoproterozoic, whereas prior to this, subduction zone metamorphism was characterized by high to intermediate T/P conditions due to the warm and ductile nature of subduction (Brown and Johnson 2018; Brown *et al.* 2024).

Blueschist, a high-P and low-T metamorphic facies rock dominated by a Na-rich amphibole called glaucophane, is often cited in studies advocating the initiation of plate tectonics during the Neoproterozoic. Models explaining the absence of blueschist in older rock records include preservation bias, lack of

exhumation, or a hotter mantle (e.g. Pereira *et al.* 2021; Wu *et al.* 2024). An alternative model suggests that the absence of blueschist in ancient rock records is attributed to the high-MgO basaltic composition in the past. Petrological modelling indicates that high T_p in the past produced high-MgO basalts, leading to the destabilization of glaucophane during subduction (Palin and White 2016). However, with secular cooling, the production of low MgO basalts became prevalent, contributing to the widespread occurrences of glaucophane-bearing blueschists since the early Neoproterozoic (Wu *et al.* 2024).

Davies (1992) showed that Archean was characterized by rapid plate motion due to high mantle temperature. Based on this observation, he argued that the oceanic crust began to attain a neutral buoyancy since ~1400 Ma due to a gradual fall in plate velocity. However, this observation is contentious. High T_p during Archean would not necessarily indicate rapid plate motion, when the oceanic lithosphere was much thicker than the present. Further, the average age of the subducting slab was higher in the past (Korenaga 2006), suggesting a sluggish plate motion during Archean than the present (Section 6.2).

Stern *et al.* (2016) proposed that the 'build-up' of H_2O and CO_2 in the convecting mantle, resulting from the onset of modern-style deep subduction at ~1200 Ma, played a major role in initiating the frequent occurrence of subsequent kimberlite magmatism. Despite steeper subduction being a characteristic of the Proterozoic, its correlation with the distribution of kimberlite remains uncertain (e.g. Tappe *et al.* 2018). For example, the oldest known kimberlite is of late Mesoarchean age (2850 Ma) (de Wit *et al.* 2016). Recent petrologic and geochemical constraints suggest that the volatile-rich nature of kimberlite melt requires the incipient melting of the upper convecting mantle (Giuliani *et al.* 2023), a condition achievable in a relatively colder mantle. Tappe *et al.* (2018) proposed that secular cooling of the mantle has the dominant effect on the kimberlite magmatism and onset of plate tectonics cannot be inferred from the kimberlite distribution alone, although others (e.g. Liu *et al.* 2023) have acknowledged the importance of both thermo-tectonic changes for the occurrence of kimberlite throughout Earth's history.

7.2. Archean

7.2.1. Metamorphic T/P constraint

Paired metamorphic belts are parallel linear rock units that exhibit contrasting metamorphic P-T conditions. These belts are typically formed along convergent plate boundaries. Authors like Brown and Johnson

(2018) and Brown *et al.* (2024) proposed a widespread occurrence of two contrasting metamorphisms in terms of high and intermediate dT/dP in rock records since the beginning of the Neoproterozoic (Figure 6(a)). Although such metamorphism occurred during the Meso and Paleoproterozoic periods, they were local. They argued that the occurrence of dual thermal regimes, i.e. ultra-high temperature metamorphism (UHTM) with eclogite-high-pressure granulite (EHPG) metamorphism indicates the operation of modern plate tectonics at least since the Neoproterozoic. The paucity of such a metamorphic record in the older Meso-Paleoproterozoic rocks is attributed to preservation bias (Brown and Johnson 2018), emphasizing 'absence of evidence is not the evidence of absence.' For example, Nutman *et al.* (2020) recently documented Phanerozoic-like low and high T/P metamorphic conditions from the Eoproterozoic (3800 Ma) Itsaq Gneissic complex, Greenland. Olivine in these rocks is in equilibrium with antigorite and displays intergrowths of titanite-clinohumite replacing titanite-chondrodite, an apparent feature of decompression through a pressure ~3.0 GPa and 500–700°C.

7.2.2. Detrital zircons & orogenic records

Based on zircon U-Pb age data, Condie and others (Condie 2000; Puetz and Condie 2021) proposed that the peak age distribution of zircon corresponds to orogenic plutonism. Consequently, they suggested that local and global subduction commenced ~3000 Ma, reaching its peak around 2700 Ma. They further showed that subsequent periods of supercontinent (e.g. 1870, 600 Ma) assemblage (Figure 6(b)) are the major periods of crust formation. However, this inference has been debated.

First, the Archean rock record is susceptible to preservation challenges. For instance, the efficient recycling of Archean continental mass (Section 7.2.6) has preserved only a small fraction, ~8% of the actual mass produced during the Archean (Goodwin 1996). Second, since Zr is an incompatible element, its concentration in igneous rocks decreases with increasing age due to a higher degree of melting at higher T_p (Keller *et al.* 2017). This has two implications. First, similar mass added to the crust in the past would produce less zircon than at present. Second, older zircons might represent a greater volume of the crust due to the high degree of partial melting (Korenaga 2018b). Lastly, the zircon age peak coincides with the period of supercontinent assemblage and not the final stage of supercontinent amalgamation, and most of the crust was produced during the accretionary orogenic phase (Condie *et al.* 2017; Spencer *et al.* 2017). Based on the preserved field evidence and geochemical signatures, it is best to apply the recent

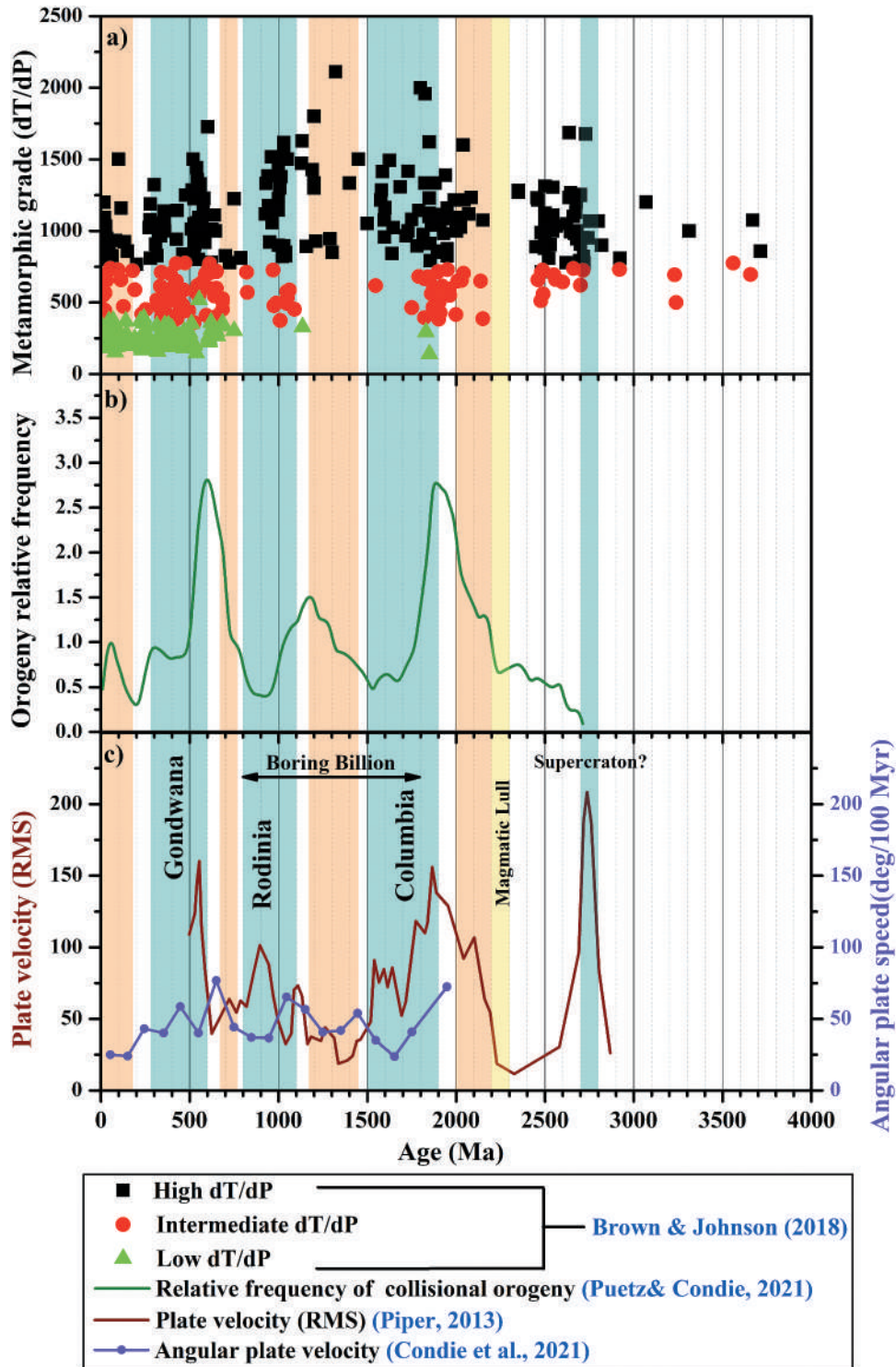


Figure 6. Indicators of continental tectonics: (a) metamorphic thermal gradient (dT/dP) grouped into three types are plotted against age. The three types of metamorphism shown are high dT/dP in black, intermediate dT/dP in red, and low dT/dP in green (Brown and Johnson 2018). The earliest record of paired metamorphism dates back to the Neoproterozoic, coinciding with the formation of first supercontinent (supercraton) around 2800–2700 Ma. First occurrence of low dT/dP metamorphism was during the Paleoproterozoic era, coinciding with the Columbia supercontinent period. (b) Relative frequency of collisional orogeny through time (Puetz and Condie 2021), starting from Neoproterozoic. High frequency of collisional orogeny are observed during the period of supercontinent formation, e.g. Columbia, Gondwana (shaded areas). (c) Continental plate velocity through time starting from Meso-Neoproterozoic boundary (Piper 2013), and continental angular speed since the last 2000 Ma (Condie et al. 2021). Supercontinent assembly, cyan; breakup, orange (modified after Condie et al. 2021). The Paleoproterozoic ‘Magmatic Lull’ (2300–2200 Ma) is characterized by tectono-magmatic shutdown (Spencer et al. 2018). The Mid-Proterozoic ‘Boring billion’ period (1800–800 Ma) (Roberts 2013) has also been shown, indicating a phase of tectonic stability where the Earth’s surface likely featured a single lithospheric lid (Stern 2023), leading to lower continental velocities, reduced frequency of continental orogeny, and a diminished record of metamorphism.

model of plate tectonics that accretionary orogen has been operating at least since ~4000 Ma (Windley 1993; Komiya *et al.* 1999; Nutman *et al.* 2002; Bédard *et al.* 2003; Shirey *et al.* 2008; Kusky *et al.* 2018; Windley *et al.* 2021; Kusky and Wang 2022), whereas the Wilson cycle started to operate since ~2700–2500 Ma (Section 8).

7.2.3. Palaeomagnetism and continental plate motion

Palaeomagnetic investigations show continental plate motion since the Neoproterozoic, with peak velocity coinciding with the period of supercontinent assemblage (Cawood *et al.* 2006, 2018; Piper 2013) (Figure 6(c)) and detrital zircon age distribution (Figure 6(b)). Based on this observation, the authors propose that a change from a stagnant lid to a mobile lid occurred during the Neoproterozoic, with peak continental velocity coinciding with enhanced subduction activity during the supercontinent assembly phase, although a recent study (Condie *et al.* 2021) indicates that the plate velocity has been nearly constant over the last 2000 Ma. However, the palaeomagnetic indicator of plate tectonics is debated, with the evidence most likely suggesting Wilson cycle-related plate tectonics over the accretionary model. This is because the Wilson cycle requires a huge and stable continental mass, which was most likely absent until the mid-Archean (Section 8). The older rocks have further undergone intense metamorphism, overprinting the primary geomagnetic features (Komiya *et al.* 2015). Nevertheless, few other studies have found modern plate-like motion in the Kaapvaal craton (Kröner 1991) and the Pilbara craton (Usui *et al.* 2020; Brenner *et al.* 2022) dating back to the Meso-Paleoproterozoic (3200–3470 Ma).

7.2.4. Eclogite xenoliths

Eclogites or eclogitic minerals can occur as discrete rocks or minerals, such as xenoliths or xenocrysts in kimberlites, or as inclusions within the continental lithospheric mantle (CLM) derived diamonds. Aulbach and Arndt (2019) identified the bi-mineralic eclogite xenoliths from the cratonic lithosphere as remnants of subducted oceanic crust, although a contrasting view suggests their formation via melt-rock reaction (e.g. Herzberg 2019; Emo and Kamber 2022). However, study (Shirey and Richardson 2011) suggests that the inclusions in the CLM-derived diamonds changed predominantly from peridotitic to eclogitic after 3000 Ma. Following the argument, others (e.g. Farquhar *et al.* 2002; Smit *et al.* 2019) analysed the sulphide inclusions in diamonds and showed mass-independent fractionation of sulphur, which can only happen at surface anoxic conditions.

Based on these observations, the authors suggested that subduction and plate tectonics started ~3000 Ma.

The scarcity of eclogite xenoliths or eclogitic inclusions in older (>3000 Ma) diamonds as well as the highly depleted nature of the Archean CLM led geoscientists to argue that the Archean CLM was produced *in-situ* by plume magmatism (Griffin *et al.* 2003; Griffin and O'Reilly 2007). However, recent petrological and geochemical observations support a shallower depth of origin for the CLM building blocks, similar to an Archean MOR setting, which later became continental through orogenic thickening or underthrusting (Bickle 1986; Kelemen *et al.* 1998; Gibson *et al.* 2008; Herzberg *et al.* 2010; Herzberg and Rudnick 2012; Pearson and Wittig 2014; Servali and Korenaga 2018). The mass imbalance arising from the absence of contemporaneous oceanic crust in the CLM can be explained by the viscous drainage of oceanic crust into the asthenosphere, which was incorporated early into the CLM at higher T_p (Wang *et al.* 2022). Those incorporated after a certain period are still preserved (Luo and Korenaga 2021; Wang *et al.* 2022). Therefore, the lack of older eclogites in the CLM does not necessarily indicate that plate tectonics was not operating before 3000 Ma.

7.2.5. Isotopic evidence

Short-lived radioactive isotopes have been studied to understand the nature of mantle convection and, consequently, the tectonic style. Given that the short-lived parent nuclides ceased to exist within the first few million years of Earth's formation, the changes observed in their daughter nuclide within the mantle are attributed to the efficiency of convective mixing. In other words, due to a more rapid decay rate, the early mantle plausibly contained elevated concentrations of these radiogenic daughter isotopes. However, since there were no parent nuclides to undergo decay and generate new daughter nuclides after a certain period, the effective mixing and homogenization of the mantle would have erased these early signs. Two such short-lived radioactive nuclides are ^{146}Sm and ^{182}Hf , which decay to ^{142}Nd and ^{182}W , respectively. Debaille *et al.* (2013) showed that the mantle had a consistently positive $\mu^{142}\text{Nd}$ value until 2700 Ma, gradually declining to negative values thereafter. Drawing from this observation, they proposed that Earth underwent a transition from a stagnant-lid to a mobile-lid during the Neoproterozoic. Their argument rests on the idea that if plate tectonics were active during early Earth, it would have eliminated the positive $\mu^{142}\text{Nd}$ signature in the mantle due to vigorous convective mixing. Supporting evidence can be found in the ^{182}Hf - ^{182}W systematics, which shows a decrease in $\mu^{182}\text{W}$ value from a range

of +20 to +12 during the Eoarchean to a modern mantle-like value of +8 to 0 around 3600 Ma. This shift signifies the initiation of convective mixing attributed to the onset of plate tectonics (Mei *et al.* 2020). However, the idea of inefficient mixing does not necessarily rule out the existence of plate tectonics, given the likelihood that plate tectonics operated at a slower pace during the Archean (Section 6.2). Furthermore, plate tectonics cannot homogenize the entire mantle equally, as early signatures of Nd-mantle heterogeneity persist in the modern-day mantle as well (Hyung and Jacobsen 2020). Variations in isotopic signatures can be explained by processes other than convective mixing. For example, the observed secular variation in $\mu^{142}\text{Nd}$ for the depleted MORB-source mantle can be explained by rapid crustal production rate and efficient recycling during the Hadean-Eoarchean (Rosas and Korenaga 2018). Unlike the ^{146}Sm - ^{142}Nd systematics, ^{182}Hf - ^{182}W is insensitive to silicate differentiation (Reimink *et al.* 2020) and processes such as core-mantle interaction and the mixing of CMB-derived material ($\mu^{182}\text{W} \sim -200$) with the ambient mantle can explain the observed shift in $\mu^{182}\text{W}$ magnitudes (Rizo *et al.* 2019; Reimink *et al.* 2020).

Hydrogen isotopes (δD) and other trace element ratios, e.g. $\text{H}_2\text{O}/\text{Ce}$, in melt inclusions of olivine from the Paleoarchean Barberton komatiites indicate a hydrous source for their origin (Sobolev *et al.* 2019). A comparable hydrous origin has been identified for Neoarchean komatiites in Zimbabwe and the Superior craton (Sobolev *et al.* 2016; Asafov *et al.* 2018). These findings support the notion of a long-term process of water recycling of global ocean and continuous mantle hydration attributed to the subduction process. Continuous recycling of water reduced the surface ocean volume towards the end of Mesoarchean, allowing continental land masses to emerge above sea level (Flament *et al.* 2008; Korenaga *et al.* 2017; Bada and Korenaga 2018; Bindeman *et al.* 2018; Reimink *et al.* 2021).

7.2.6. Secular compositional change of continental crust

Early continental crust is believed to have a more mafic composition ($\text{SiO}_2 \sim 60$ wt%, $\text{MgO} \sim 4.7$ wt%) and gradually transitioned to its present-day felsic composition ($\text{SiO}_2 \sim 66$ wt%, $\text{MgO} \sim 2.2$ wt%) (Taylor and McLennan 1985; Tang *et al.* 2016). The reconstructed MgO and SiO_2 concentrations of the upper continental crust (UCC), calculated from trace element ratios (e.g. Cr/U , Cu/Ag , Ni/Co , and Cr/Zn) in shales and glacial diamictites, reveal a significant shift (Tang *et al.* 2016; Smit and Mezger 2017; Chen *et al.* 2020). Specifically, the average MgO content decreased from ~ 15 wt% at 3200 Ma to ~ 4 wt% at 2600 Ma, while the average SiO_2 increased from ~ 53 wt%

at 3000 Ma to ~ 65 wt% at 2400 Ma. This translates to a UCC comprising ~ 50 – 90% basalt-komatiite and 10 – 40% granite before 3000 Ma (Windley *et al.* 2021). Dhuime *et al.* (2015), based on the Rb/Sr ratio of $\sim 13,000$ igneous rocks with Nd model ages spanning from Hadean to Phanerozoic, proposed that the juvenile crust had lower SiO_2 concentrations and was predominantly mafic before 3200–3000 Ma. These observations led to the hypothesis that plate tectonics commenced around 3000 Ma.

The trace element variation in the Archean and post-Archean shales, based on which the previous authors argued for an early mafic continental crust was further carefully investigated. First, a decline in the concentration of compatible elements, e.g. Cr and Ni, and major oxides, e.g. MgO , after 3000 Ma may be attributed to a reduction in the production of high- MgO -producing rocks in response to a decrease in potential temperature (Komiya 2007; Konhauser *et al.* 2009; Herzberg *et al.* 2010; Marty *et al.* 2019). Second, elements such as Cu, Zn, U, and Cr are redox sensitive and behave differently at different Eh-pH conditions. These variations in the post-Archean sediments might be attributed to the effect of oxygenation of ocean-atmospheric system due to the Great Oxidation Event (GOE) at ~ 2500 Ma (Keller and Harrison 2020). The reference model developed by Keller and Harrison (2020), where the mixture of mafic, intermediate, and felsic rock maintains a constant SiO_2 over time, can reproduce a similar Rb/Sr ratio for the continental crust as predicted by Dhuime *et al.* (2015) if the effect of secular cooling is considered. Similarly, the uniform Ti isotopic ($\delta^{49}\text{Ti}$) composition observed in shales (Greber *et al.* 2017) across ages (3500–0 Ma) suggests that the continental crust has been predominantly felsic at least since 3500 Ma. This observation has recently been confirmed by Zhang *et al.* (2023), who found limited Ti isotopic fractionation in Archean TTGs, a trend observed in modern calc-alkaline differentiation series. These results are consistent with the inverse mixing model of Ptáček *et al.* (2020) for terrigenous sediments, where it is argued that the UCC consisted of at least 50% felsic material at 3500 Ma, suggesting an early onset of plate tectonics.

Studies that argue for an onset of plate tectonics during 3000 Ma on the basis of UCC composition often cite the crustal growth rate of Dhuime *et al.* (2012). Based on the systematic variation in the hafnium and oxygen isotope of the detrital zircons, they showed that there is a marked decrease in crustal growth rate at 3000 Ma, which they demarcated as the period of onset of plate tectonics. However, the record of detrital zircon cannot quantify the total volume of crust recycled in the past, as net crustal growth reflects the running balance between the juvenile crust produced, internal overprinting, and crustal recycling (Harrison 2020; Condie 2021). And most

of the crustal growth models proposed till date misinterpret the present-day distribution of crust formation age as the net crustal growth (review in Korenaga (2018a)). The crustal growth model based on the mantle depletion history by Armstrong (1981) first predicted that continental crust, equivalent to 80% of present-day continental mass, existed by the end of Hadean (Figure 7). Given that the surface age distribution of Archean or older rocks comprises only 8% of the present-day continent (Goodwin 1996), Armstrong (1981) concluded a higher continental recycling rate in the past. However, Armstrong's model was overshadowed by alternative theories until recently, when an emerging consensus among contemporary models validated its significance. The estimated crustal growth rate, derived from both the secular Nd-isotopic variation of the depleted MORB-source mantle (Rosas and Korenaga 2018) and the mantle's argon degassing history (Guo and Korenaga 2020), aligns closely with Armstrong's crustal growth rate curve (Figure 7). This alignment suggests that the early Earth witnessed both rapid juvenile crust production and effective recycling of these crust. Such a high rate of crustal production during the early Earth indicates an active plate tectonic scenario.

Starting from 3000 Ma, the continental crust witnessed the appearance of sanukitoid, reaching its peak around 2700–2500 Ma (Martin *et al.* 2009; Laurent *et al.* 2014). This transition from predominantly TTG crust to a sanukitoid

one has been argued to demarcate the onset of modern-plate tectonics. It is widely accepted that sanukitoids are generated by the mixing of slab melt and sediment-driven melt metasomatized mantle wedge (Halla 2005; Laurent *et al.* 2011, 2014; Mikkola *et al.* 2011; Li *et al.* 2024). The high large ion lithophile element (LILE) budget and enriched radiogenic isotopes of sanukitoids signify continental input in their source (Martin *et al.* 2009). However, the absence of sanukitoid before 3000 Ma was mainly limited by two factors, e.g. the opening of mantle wedge and availability of terrigenous sediment. For example, flat subduction during early Earth (Abbott *et al.* 1994; Martin *et al.* 2005; Cawood *et al.* 2006; Perchuk *et al.* 2023) would leave a little space for the wedge mantle to form. Conversely, a relatively steep-dip subduction occurred in later periods due to secular cooling of the mantle that developed a prominent mantle wedge (Section 8). Terrigenous sediments were limited on the early Earth due to the limited exposure of continents above sea level. As stated in section 7.2.5, continents emerged above sea level during the Meso-Neoproterozoic period, which initiated subaerial weathering and supplied continental sediments to the ocean floor. The formation of a metasomatized wedge mantle during this period can describe the appearance of sanukitoids and large-scale orogenic, porphyric, and epithermal gold deposits (Frimmel 2018) and the emergence of S-type granites in

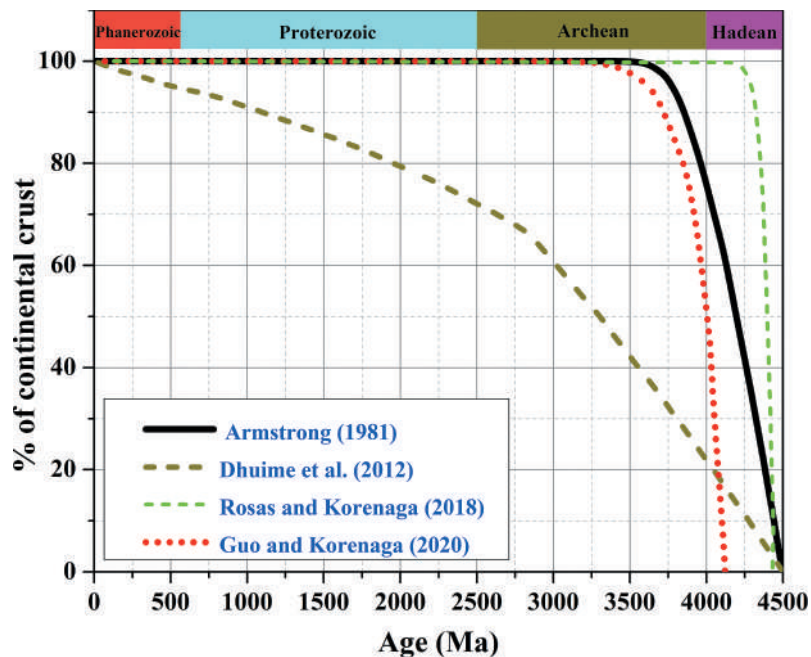


Figure 7. Crustal growth models. The dark-yellow curve represents the crustal growth model proposed by Dhuime *et al.* (2012), indicating a decrease in crustal growth rate around 3000 Ma. This decrease might be linked to the initiation of subduction-related activity. The higher crustal growth rates during the early earth are indicated by the black, green, and red curves (Armstrong 1981, Rosas and Korenaga 2018; Guo and Korenaga 2020) indicating an early earth plate tectonics.

a continent collision zone (Zhu *et al.* 2020). Further effects of large-scale continental emergence and subaerial weathering are reflected in the isotopic variation of seawater, such as the enrichment of radiogenic isotopes (Satkoski *et al.* 2017) and a decline in $\delta^{18}\text{O}$ values (Johnson and Wing 2020) during the Meso-Neoproterozoic.

7.3. Hadean

In the absence of preserved rocks older than 4000 Ma, most of the insights into the nature of the Hadean Earth are derived from the preserved zircons found in the Archean metasedimentary rock in the Yilgarn Craton, Western Australia. Notably, recent discoveries have expanded the presence of Hadean age zircons to 15 different sites globally (Harrison 2020). Various zircon geochemical techniques, including $\delta^{18}\text{O}$, Ti thermometry, inclusion mineralogy, and trace element chemistry, have been employed to assess the crustal composition and petrogenesis of the Jack Hills zircon source. The $\delta^{18}\text{O}$ values observed in the 4300 Ma Jack Hills zircons are higher than the pristine mantle value, suggesting that the zircons crystallized from magmas, incorporating supracrustal material that formed in the presence of surface water. This ultimately indicates the presence of a liquid hydrosphere during the Hadean (Mojzsis *et al.* 2001; Wilde *et al.* 2001). However, the operation of stagnant-lid appears to be inconsistent with the presence of a liquid hydrosphere during the Hadean (Mojzsis *et al.* 2001; Wilde *et al.* 2001).

The identification of silicic magmatism, constituting ~10% by volume in the present-day Iceland plume setting, sparked the development of the 'Icelandic rhyolite' model to elucidate the origin of the Jack Hills zircons (Valley *et al.* 2002). However, the crystallization temperature calculated from Ti concentrations in Jack Hills zircons (4200 Ma) is $680 \pm 25^\circ\text{C}$ (1σ), contrasting sharply with the higher average value of $780 \pm 50^\circ\text{C}$ (1σ) for Icelandic zircons (Harrison 2009). The lower crystallization temperature for the Jack Hills zircons suggests water-saturated conditions during their formation. This challenges the plume origin proposed in the 'Icelandic rhyolite' model. The markedly low crystallization temperature of Jack Hills zircons further distinguishes them from the impact-produced zircons, which exhibit a considerably higher average crystallization temperature (773°C) (Wielicki *et al.* 2012; Kenny *et al.* 2016). This interpretation gains additional support through thermobarometric calculations involving primary muscovite inclusions ($\text{Si}_{\text{apfu}} \sim 3.45$) from the 4200 Ma zircons. The geotherm value inferred from the inclusion study, measuring at 75 mW m^{-2} , is three to five times lower than the estimated heat flow during the Hadean. This finding suggests a low heat flow under-thrusting environment as the likely origin for these

zircons. Consequently, the Jack Hills zircons are interpreted to have formed in a subduction setting (Hopkins *et al.* 2008). Recent geochemical studies indicate a range of parent melt compositions for the Jack Hills zircons (3700–4400 Ma) ranging from an intermediate andesitic (Turner *et al.* 2020) to an I-type or a clay-rich S-type magma (Chowdhury *et al.* 2023). All these indicate a subduction zone origin.

While all the geochemical signatures point towards a subduction origin for the Jack Hills zircon, the possibility of continental crust produced in an oceanic island setting during the Hadean cannot be entirely dismissed (Reimink *et al.* 2014). For example, the high average crystallization temperature observed in the Hadean Zhejiang detrital zircon in Eastern China (Xing *et al.* 2014) may indicate a plume environment for its formation.

8. From proto-tectonics to modern-style tectonic evolution of the Earth: discussions & concluding remarks

The evolution of plate tectonics has primarily been discussed in the context of crustal evolution. Generation of felsic crust without subduction requires a suitable protolith composition to stabilize the necessary residual mineralogy in an overthickened crust (Section 6.1). Plate tectonics, supposedly active since the Hadean, plays critical roles beyond continental crust generation, including the regulation of the geodynamo (e.g. Fu *et al.* 2024; c.f.; Tarduno *et al.* 2023) and the rapid sequestration of early atmospheric CO_2 (Catling and Zahnle 2020). As per some definitions, 'plate tectonics' refers to the existence of a global network of interconnected plate boundaries, characterized by sustained and stable subduction. Several authors (e.g. Bédard 2006; O'Neill *et al.* 2007; Johnson *et al.* 2017; Nebel *et al.* 2018) have suggested that the early Earth was characterized by a stagnant-lid regime that transitioned to a mobile-lid during the Meso-Neoproterozoic Period. Contrarily, others (e.g. Korenaga 2021; Kusky *et al.* 2021; Windley *et al.* 2021) propose that the Earth is likely to enter a stagnant-lid mode in future since tectonic activity diminishes due to gradual cooling. However, the fundamental question remains: 'Was the Earth devoid of any mobile-lid activity during the Hadean or early Archean, even though the modern-day definition of plate tectonics does not fit this time-span?' Studies show that plate boundary formation during the Hadean and early Archean was facilitated by the presence of surface water and a higher rate of core heating in the past (Section 6.2). In the absence of these factors, a different tectonic condition, e.g. a plutonic squishy lid might represent an early Earth tectonic feature (Bédard 2006;

Lourenço and Rozel 2023). However, observational as well as theoretical evidence support the former.

There are numerous geological and geochemical indicators since the Hadean/early Archean that indicate operation of plate tectonics. Moreover, the preserved structural features of Archean can well be explained by compressional horizontal tectonics (Kusky *et al.* 2021; Cutts *et al.* 2024; Aldoud *et al.* 2024), eliminating the need for untestable models regarding the early Earth evolution. In the present-day tectonically active Earth, convergent margins occupy only ~2.4% of the Earth's total surface area (Kusky and Wang 2022). And whether globally connected or not, the Archean Earth might have similarly represented a mobile-lid planet.

After reviewing various numerical studies on the viability of plate tectonics on a hotter Earth, along with numerous investigations encompassing geochemical, isotopic, field and petrographic aspects, we now provide a concise overview of how plate tectonics evolved over time in tandem with the secular cooling of the mantle. The physical evidence for the mantle's thermal state, expressed in terms of mantle potential temperature (T_p) can be traced back to 3800 Ma (this study; Korenaga 2008; Herzberg *et al.* 2010; Ganne and Feng 2017; Herzberg 2022a). Theoretical calculations suggest a T_p value of ~1700°C at the end of putative magma ocean solidification (Abe 1997; Solomatov 2000) during the early Hadean (Figure 8); however, there is currently no direct physical evidence of the thermal state of the Hadean mantle. Theoretical studies argue initiation of proto-plate tectonics on a chemically stratified heterogeneous mantle formed by solidifying the magma ocean (e.g. Ernst (2017); Miyazaki and Korenaga (2022) and references therein). With most of the water in the mantle, the hotter Hadean mantle would facilitate a faster plate movement due to reduced viscosity of the mantle (Turcotte and Schubert 2002; Osei Tutu *et al.* 2018). The early onset of plate tectonics is consistent with the zircon geochemistry (Section 7.3), whereas the faster tempo of plate tectonics is reflected in a higher rate of crust generation rate (Section 7.2.6). Rapid plate movement would facilitate quick degassing (Li *et al.* 2016, Nakagawa 2023), forming a global ocean and a homogenous pyrolytic mantle towards the end of Hadean (Davies 2006; Miyazaki and Korenaga 2022). Formation of a global ocean is equivalent to a dry mantle during the early Archean.

Decompression melting of a pyrolytic mantle beneath mid-ocean ridges (MOR) would produce a thick crust and a thick melt-depleted lithospheric mantle at elevated T_p during the early Archean (Bickle 1986; Van Thienen *et al.* 2004; Korenaga 2006; Herzberg *et al.* 2010; Herzberg and Rudnick 2012). A thick oceanic lithospheric over a viscous mantle demarcates the onset of sluggish plate motion since the early Archean (Section 6.2). Sluggish tectonics

facilitates subduction of an older and thicker plate. Since a thicker plate is stiffer, subduction of such a plate would result in a wider curvature with a lower dip at shallower depths leading to flat subduction (Section 7.2.6).

The thermal evolution of Earth has further played a significant role in shaping continental tectonics temporally. Most of the felsic continental crust produced during the early Earth existed within a small relict oceanic arc setting, with only a minor portion produced in an oceanic island setting. The oldest continental mass, e.g. an Archean craton formed due to collision of such proto-arcs (e.g. Windley *et al.* 2021 and references therein). This idea is consistent with recent petrological estimations for the formation of cratonic mantle keels (Section 7.2.4). Highly depleted peridotites with low density, resulting from melting at high T_p , served as the building blocks of the cratonic lithospheric mantle, making mantle keels specifically unique to the Archean. However, peridotite xenoliths from Archean cratons indicate a formation age distribution between 3500 and 2500 Ma (Pearson *et al.* 2021). The absence of evidence of cratonic peridotite before 3500 Ma indicates that the early-formed cratons may have been destroyed.

Cratons form during orogenic thickening, and an initial grain-size reduction is a prerequisite for the orogenesis (Lee and Chin 2023). However, elevated T_p limits this factor, thereby hindering orogenic thickening during the Hadean or early Archean (England and Bickle 1984; Rey and Coltice 2008; Lee and Chin 2023). Even an overthickened lithospheric structure during the early Earth would be unstable because of high radiogenic heat production in the early-formed continental crust (Morgan 1985). An overthickened crust would eventually increase the total budget of heat-producing elements, resulting in further heating through the radioactive decay of elements such as U, Th and K. High radiogenic heating would elevate the Moho temperature to a threshold value of 800°C. Beyond this point, the total lithospheric structure becomes unstable, leading to the complete delamination of the lithospheric mantle along with the Moho (Morency and Doin 2004). Other observations suggest a lower stability of the CLM due to reduced viscosity of the convecting mantle during the Hadean (Section 6.2), while the stability of the CLM evolved through gradual hydration of the convecting mantle, driven by a net positive regassing during the Archean (Karato 2010; Korenaga 2013, 2018b). Lithospheric mantle is unlikely to be stabilized by hydrous flux melting, as this process would add water to the lithosphere and thus weaken it (Pearson and Wittig 2008). Interestingly, the Earth shifted from a state of net degassing to a state of regassing around 3500 Ma (Crowley *et al.* 2011), preserving the highly viscous nature of the continental

lithospheric mantle. Continuous collision of these stable proto-arcs led to the formation of cratons, which subsequently amalgamated to form the first supercontinent

during the Neoproterozoic, demarcating the initiation of the Wilson cycle (Figure 8). With this in mind, the rapid crustal recycling rate during the Hadean or early

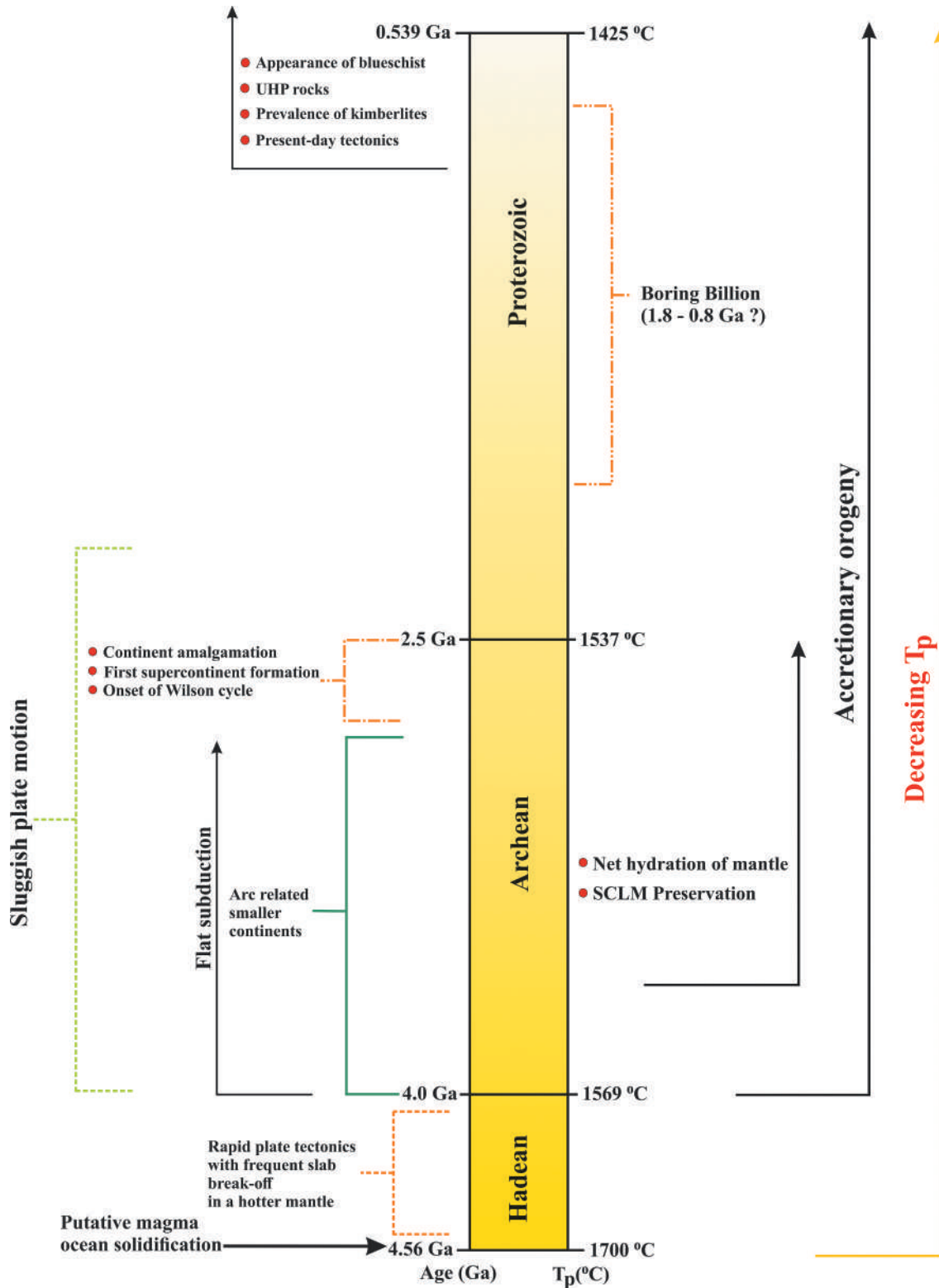


Figure 8. Schematic diagram illustrating major phases in tectonic evolution through Earth's history. T_p at the end of putative magma ocean phase is estimated to be ~1700°C (Abe 1997; Solomatov 2000). T_p decreased from an average value of 1569°C in the Eoarchean

Archean (Section 7.2.6) might be attributed to lithospheric mantle instability, where the continental crust was recycled via processes like arc subduction or subduction erosion (Yamamoto *et al.* 2009; Azuma *et al.* 2017).

Through continuous subduction and a net positive influx of water, the mantle efficiently cooled and underwent gradual hydration (Section 7.2.5). This process further led to the emergence of continents, initiating subaerial weathering and supplying terrigenous sediments to the ocean floor during the Meso-Neoproterozoic period (Section 7.2.6). Presence of oldest kimberlite of late Mesoarchean age (2850 Ma) (de Wit *et al.* 2016) supports the idea that a relatively colder ambient mantle was present locally during that period indicating rapid cooling of the mantle owing to subduction and positive water influx to mantle. With decreasing average T_p values from Eo-Neoproterozoic, decompression melting of a pyrolytic mantle resulted in a thinner oceanic lithosphere. Subduction of this thinner lithosphere facilitated a relatively steeper subduction geometry and laid the foundation for modern plate tectonics by developing a prominent wedge mantle and arc magmatism. With further secular cooling of the mantle, a contemporary tectonic style developed, giving rise to various present-day subduction zone features, e.g. blueschist facies, and UHP rocks since the Neoproterozoic (Section 7.1).

Some of the key observations from this study are listed below

- Unlike the colder Archean mantle theory, a hotter early Earth and its secular cooling can describe the geodynamical changes through Earth's history.
- T_p values observed from this study support a hotter Archean ambient mantle theory and is consistent with the present-day thermal budget of the Earth.
- Limited preserved evidence prior to 3000–3500 Ma indicate plate tectonics was operating deep in the time.
- The subduction geometry evolved temporally due to secular cooling of the mantle, with modern plate

tectonics initiating in the Neoproterozoic. A more typical present-day plate tectonics began during the Neoproterozoic.

Highlights

- (1) Our T_p estimation suggests a hot ambient mantle condition during Archean and Proterozoic.
- (2) The secular cooling of the mantle significantly influenced subduction geometry, with modern-style subduction beginning in the Neoproterozoic.
- (3) Preserved field, petrographic and geochemical evidences suggest that subduction-related tectonics have been active throughout Earth's history.

Abbreviations

CLM	Continental Lithospheric Mantle
CMB	Core-Mantle-Boundary
Cpx	Clinopyroxene
D	Depth
(dF/dP) _s	Melt productivity
DM	Depleted mantle
dT/dD	Adiabatic gradient with depth
EM	Enriched mantle
HM	Hydrated mantle
KM	Komatiitic mantle
Mg#	Magnesium number
MOR	Mid-oceanic ridge
MORB	Mid-oceanic ridge basalt
OPB	Oceanic Plateau Basalt
P_g	Magma generation pressure
Plg	Plagioclase
T_p	Potential temperature
T_p^*	Apparent potential temperature
T_g	Magma generation temperature
TTG	Tonalite Trondhjemite Granodiorite
GSA	Geological Society of America

Acknowledgments

We extend our sincere gratitude to Dr. Robert J. Stern for his editorial comments in several rounds, which enhanced the quality of our manuscript. Prof. Jun Korenaga has been an

to 1537°C in the neoproterozoic (this study). T_p (1425°C) at the Proterozoic-Phanerozoic boundary is from Herzberg and Asimow (2015). The Hadean was characterized by rapid plate tectonics with frequent slab break-offs due to a hotter and viscous mantle. At the Hadean-Archean boundary, there was a transition to sluggish plate movements and the occurrence of flat subduction involving a thick oceanic lithosphere (see text). The geological record of preserved continental rocks supports the operation of accretionary orogeny at least since Eoarchean (Windley *et al.* 2021), with felsic continental crust existing within a small relict oceanic arc setting. Subduction dynamics shifted from flat to relatively steep over time, accompanied by a gradual decrease in T_p values from the Eoarchean to the Neoproterozoic, leading to the development of a wedge mantle (see main text for detailed discussion). Around 3500 Ma, Earth transitioned from a state of net degassing to net regassing, contributing to the preservation of the subcontinental lithospheric mantle (SCLM). The continuous amalgamation of smaller felsic crustal units during the Meso-Neoproterozoic facilitated the formation of larger continents, which later formed the first supercontinent (supercontinent) around 2800–2700 Ma, marking the initiation of the Wilson cycle. Subsequent cooling led to the evolution of present-day plate tectonics during the Neoproterozoic, leading to the widespread occurrence of glaucophane bearing blueschists and other UHP rocks (Stern 2005).

invaluable mentor, offering extensive guidance and sharing his deep insights into the subject matter. Our thanks also go to Prof. Claude Herzberg for his clarifications, which significantly contributed to the refinement of our research. Insightful discussions with Professor Zong-Feng Yang, Timothy Kusky, Alan Hastie, Michael Brown, Owen Weller, Richard Palin, Alexei Perchuk, and Nicholas Greber improved the manuscript. We would like to extend our sincere apologies if, despite our best efforts, we have inadvertently overlooked any references related to the study of early Earth tectonics. SD acknowledges Senior Research Fellowship from Council of Scientific and Industrial Research (CSIR), India (Grant no: 31/023(0242)/2019-EMR-I). Research Development Grant (IIT Bombay) supported SM. This work is part of the PhD thesis of SD. We thank Prof. Claude Herzberg and two anonymous reviewers for their detailed comments in two rounds that helped to clarify several issues. The Director, CSIR-NGRI is thanked for giving permission to carry out this work. EVB and SD acknowledge the financial support from CSIR-NGRI (MLP-7016-28-EVB).

Disclosure statement

No potential conflict of interest was reported by the author(s).

Funding

The authors reported there is no funding associated with the work featured in this article.

References

- Abbott, D., Burgess, L., Longhi, J., and Smith, W.H.F., 1994, An empirical thermal history of the Earth's upper mantle: *Journal of Geophysical Research: Solid Earth*, v. 99, no. B7, p. 13835–13850. [10.1029/94JB00112](https://doi.org/10.1029/94JB00112).
- Abbott, D., Drury, R., and Smith, W.H.F., 1994, Flat to steep transition in subduction style: *Geology*, v. 22, no. 10, p. 937–940. [10.1130/0091-7613\(1994\)022<0937:FTSTIS>2.3.CO;2](https://doi.org/10.1130/0091-7613(1994)022<0937:FTSTIS>2.3.CO;2)
- Abe, Y., 1997, Thermal and chemical evolution of the terrestrial magma ocean: *Physics of the Earth and Planetary Interiors*, v. 100, no. 1–4, p. 27–39. [10.1016/S0031-9201\(96\)03229-3](https://doi.org/10.1016/S0031-9201(96)03229-3).
- Afonso, J.C., Ranalli, G., and Fernandez, M., 2007, Density structure and buoyancy of the oceanic lithosphere revisited: *Geophysical Research Letters*, v. 34, no. 10. [10.1029/2007GL029515](https://doi.org/10.1029/2007GL029515).
- Agard, P., Yamato, P., Jolivet, L., and Burov, E., 2009, Exhumation of oceanic blueschists and eclogites in subduction zones: Timing and mechanisms: *Earth-Science Reviews*, v. 92, no. 1–2, p. 53–79. [10.1016/j.earscirev.2008.11.002](https://doi.org/10.1016/j.earscirev.2008.11.002).
- Agrusta, R., van Hunen, J., and Goes, S., 2018, Strong plates enhance mantle mixing in early earth: *Nature Communications*, v. 9, no. 1, p. 2708. [10.1038/s41467-018-05194-5](https://doi.org/10.1038/s41467-018-05194-5)
- Aldoud, A., Kusky, T., and Wang, L., 2024, Is the mesoarchean mulgandinnah shear zone, Pilbara Craton, the world's oldest arc-slicing transform fault?: *Geology*. [10.1130/G52360.1](https://doi.org/10.1130/G52360.1)
- Anonymous, 1972, Penrose field conference on ophiolites: *Geotimes*, v. 17, p. 24–25
- Armstrong, R.L., 1981, Radiogenic isotopes: The case for crustal recycling on a near-steady-state no-continental-growth earth: *Philosophical Transactions of the Royal Society of London Series A: Mathematical & Physical Sciences*, v. 301, p. 443–472.
- Asafov, E.V., Sobolev, A.V., and Gurenko, A.A., 2018, Belingwe komatiites (2.7 Ga) originate from a plume with moderate water content, as inferred from inclusions in olivine: *Chemical Geology*, v. 478, p. 39–59. [10.1016/j.chemgeo.2017.11.002](https://doi.org/10.1016/j.chemgeo.2017.11.002)
- Asimow, P.D., Hirschmann, M.M., Ghiorso, M.S., and Stolper, E. M. (1995) Isentropic melting processes in the mantle.
- Asimow, P.D., Hirschmann, M.M., and Stolper, E.M., 1997, An analysis of variations in isentropic melt productivity: *Philosophical Transactions of the Royal Society of London Series A: Mathematical, Physical and Engineering Sciences*, v. 355, p. 255–281. [10.1098/rsta.1997.0009](https://doi.org/10.1098/rsta.1997.0009)
- Aulbach, S., and Arndt, N.T., 2019, Eclogites as palaeodynamic archives: Evidence for warm (not hot) and depleted (but heterogeneous) archaean ambient mantle: *Earth and Planetary Science Letters*, v. 505, p. 162–172. [10.1016/j.epsl.2018.10.025](https://doi.org/10.1016/j.epsl.2018.10.025)
- Azuma, S., Yamamoto, S., Ichikawa, H., and Maruyama, S., 2017, Why primordial continents were recycled to the deep: Role of subduction erosion: *Geoscience Frontiers*, v. 8, no. 2, p. 337–346. [10.1016/j.gsf.2016.08.001](https://doi.org/10.1016/j.gsf.2016.08.001)
- Bada, J.L., and Korenaga, J., 2018, Exposed areas above sea level on Earth > 3.5 gyr ago: Implications for prebiotic and primitive biotic chemistry: *Life*, v. 8, p. 55. [10.3390/life8040055](https://doi.org/10.3390/life8040055)
- Baes, M., Sobolev, S., Gerya, T., and Brune, S., 2020, Plume-induced subduction initiation: single-slab or multi-slab subduction?: *Geochemistry Geophysics Geosystems*, v. 21, no. 2, p. e2019GC008663. [10.1029/2019GC008663](https://doi.org/10.1029/2019GC008663)
- Barnes, S.J., Williams, M., Smithies, R.H., Hanski, E., and Lowrey, J.R., 2021, Trace element contents of mantle-derived magmas through time: *Journal of Petrology*, v. 62, no. 6, p. egab024. [10.1093/petrology/egab024](https://doi.org/10.1093/petrology/egab024)
- Baxter, R.J.M., MacLennan, J., Neave, D.A., and Thordarson, T., 2023, Depth of magma storage under Iceland controlled by magma fluxes: *Geochemistry Geophysics Geosystems*, v. 24, no. 7, p. e2022GC010811. [10.1029/2022GC010811](https://doi.org/10.1029/2022GC010811)
- Beall, A.P., Moresi, L., and Cooper, C.M., 2018, Formation of cratonic lithosphere during the initiation of plate tectonics: *Geology*, v. 46, no. 6, p. 487–490. [10.1130/G39943.1](https://doi.org/10.1130/G39943.1)
- Bédard, J.H., 2006, A catalytic delamination-driven model for coupled genesis of Archaean crust and sub-continental lithospheric mantle: *Geochimica et cosmochimica acta*, v. 70, no. 5, p. 1188–1214. [10.1016/j.gca.2005.11.008](https://doi.org/10.1016/j.gca.2005.11.008)
- Bédard, J.H., 2018, Stagnant lids and mantle overturns: Implications for Archaean tectonics, magmagenesis, crustal growth, mantle evolution, and the start of plate tectonics: *Geoscience Frontiers*, v. 9, no. 1, p. 19–49. [10.1016/j.gsf.2017.01.005](https://doi.org/10.1016/j.gsf.2017.01.005)
- Bédard, J.H., Brouillette, P., Madore, L., and Berclaz, A., 2003, Archaean cratonization and deformation in the northern superior province, Canada: an evaluation of plate tectonic versus vertical tectonic models: *Precambrian Research*, v. 127, no. 1–3, p. 61–87. [10.1016/S0301-9268\(03\)00181-5](https://doi.org/10.1016/S0301-9268(03)00181-5)
- Behn, M.D., and Grove, T.L., 2015, Melting systematics in mid-ocean Ridge basalts: Application of a plagioclase-spinel melting model to global variations in major element chemistry and crustal thickness: *Journal of Geophysical Research:*

- Solid Earth, v. 120, no. 7, p. 4863–4886. [10.1002/2015JB011885](https://doi.org/10.1002/2015JB011885)
- Berry, A.J., Stewart, G.A., and O'Neill, H.S.C., 2018, A re-assessment of the oxidation state of iron in MORB glasses: *Earth and Planetary Science Letters*, v. 483, p. 114–123. [10.1016/j.epsl.2017.11.032](https://doi.org/10.1016/j.epsl.2017.11.032)
- Bézos, A., Guivel, C., and La, C., 2021, Unraveling the confusion over the iron oxidation state in MORB glasses: *Geochimica et cosmochimica acta*, v. 293, p. 28–39. [10.1016/j.gca.2020.10.004](https://doi.org/10.1016/j.gca.2020.10.004)
- Bickle, M.J., 1986, Implications of melting for stabilisation of the lithosphere and heat loss in the Archaean: *Earth and Planetary Science Letters*, v. 80, no. 3–4, p. 314–324. [10.1016/0012-821X\(86\)90113-5](https://doi.org/10.1016/0012-821X(86)90113-5)
- Bindeman, I.N., Zakharov, D.O., Palandri, J., Greber, N.D., Dauphas, N., Retallack, G.J., Hofmann, A., Lackey, J.S., Bekker, A., 2018, Rapid emergence of subaerial landmasses and onset of a modern hydrologic cycle 2.5 billion years ago: *Nature*, v. 557, no. 7706, p. 545–548. [10.1038/s41586-018-0131-1](https://doi.org/10.1038/s41586-018-0131-1)
- Bradley, D.C., 2008, Passive margins through earth history: *Earth-Science Reviews*, v. 91, no. 1–4, p. 1–26. [10.1016/j.earscirev.2008.08.001](https://doi.org/10.1016/j.earscirev.2008.08.001)
- Bradley, D.C., and Leach, D.L., 2003, Tectonic controls of Mississippi valley-type lead–zinc mineralization in orogenic forelands: *Mineralium Deposita*, v. 38, p. 652–667. [10.1007/s00126-003-0355-2](https://doi.org/10.1007/s00126-003-0355-2)
- Brenner, A.R., Fu, R.R., and Kylander-Clark, A.R.C., 2022, Plate motion and a dipolar geomagnetic field at 3.25 Ga: *Proceedings of the National Academy of Sciences*, v. 119, p. e2210258119. [10.1073/pnas.2210258119](https://doi.org/10.1073/pnas.2210258119)
- Brown, M., and Johnson, T., 2018, Secular change in metamorphism and the onset of global plate tectonics: *American Mineralogist*, v. 103, no. 2, p. 181–196. [10.2138/am-2018-6166](https://doi.org/10.2138/am-2018-6166)
- Brown, M., Pearce, J.A., and Johnson, T.E., 2024, Is plate tectonics a post-Archaean phenomenon? A petrological perspective: *Journal of the Geological Society*, p. jgs2024–091. [10.1144/jgs2024-091](https://doi.org/10.1144/jgs2024-091)
- Campbell, I.H., and Griffiths, R.W., 1990, Implications of mantle plume structure for the evolution of flood basalts: *Earth and Planetary Science Letters*, v. 99, no. 1–2, p. 79–93. [10.1016/0012-821X\(90\)90072-6](https://doi.org/10.1016/0012-821X(90)90072-6)
- Campbell, I.H., Griffiths, R.W., and Hill, R.I., 1989, Melting in an Archaean mantle plume: Heads it's basalts, tails it's komatiites: *Nature*, v. 339, p. 697–699. [10.1038/339697a0](https://doi.org/10.1038/339697a0)
- Capitanio, F.A., Nebel, O., and Cawood, P.A., 2020, Thermochemical lithosphere differentiation and the origin of cratonic mantle: *Nature*, v. 588, no. 7836, p. 89–94. [10.1038/s41586-020-2976-3](https://doi.org/10.1038/s41586-020-2976-3)
- Catling, D.C., and Zahnle, K.J., 2020, The Archaean atmosphere: *Science Advances*, v. 6, no. 9, p. eaax1420. [10.1126/sciadv.aax1420](https://doi.org/10.1126/sciadv.aax1420)
- Cawood, P.A., Hawkesworth, C.J., Pisarevsky, S.A., Dhuime, B., Capitanio, F.A., Nebel, O., 2018, Geological archive of the onset of plate tectonics: *Philosophical Transactions of the Royal Society A: Mathematical, Physical and Engineering Sciences*, v. 376, no. 2132, p. 20170405. [10.1098/rsta.2017.0405](https://doi.org/10.1098/rsta.2017.0405)
- Cawood, P.A., Kroner, A., and Pisarevsky, S., 2006, Precambrian plate tectonics: Criteria and evidence: *GSA Today: A Publication of the Geological Society of America*, v. 16, no. 7, p. 4. [10.1130/GSAT01607.1](https://doi.org/10.1130/GSAT01607.1)
- Cawthorn, R.G., 1975, Degrees of melting in mantle diapirs and the origin of ultrabasic liquids: *Earth and Planetary Science Letters*, v. 27, no. 1, p. 113–120. [10.1016/0012-821X\(75\)90169-7](https://doi.org/10.1016/0012-821X(75)90169-7)
- Chatterjee, S., and Mukherjee, S., 2022, Overview on GPlates: Focus on plate reconstruction: *Turkish Journal of Earth Sciences*, v. 31, no. 2, p. 113–136. [10.55730/1300-0985.1758](https://doi.org/10.55730/1300-0985.1758)
- Chen, K., Rudnick, R.L., and Wang, Z., 2020, How mafic was the Archaean upper continental crust? Insights from Cu and Ag in ancient glacial diamictites: *Geochimica et cosmochimica acta*, v. 278, p. 16–29. [10.1016/j.gca.2019.08.002](https://doi.org/10.1016/j.gca.2019.08.002)
- Chen, Q., Liu, H., Johnson, T., Hartnady, M., Kirkland, C.L., Lu, Y., and Sun, W.-D., 2022, Intraplate continental basalts over the past billion years track cooling of the mantle and the onset of modern plate tectonics: *Earth and Planetary Science Letters*, v. 597, p. 117804. [10.1016/j.epsl.2022.117804](https://doi.org/10.1016/j.epsl.2022.117804)
- Chowdhury, W., Trail, D., Miller, M., and Savage, P., 2023, Eoarchean and hadean melts reveal arc-like trace element and isotopic signatures: *Nature Communications*, v. 14, no. 1, p. 1140. [10.1038/s41467-023-36538-5](https://doi.org/10.1038/s41467-023-36538-5)
- Christensen, U.R., 1985, Thermal evolution models for the earth: *Journal of Geophysical Research: Solid Earth*, v. 90, no. B4, p. 2995–3007. [10.1029/JB090iB04p02995](https://doi.org/10.1029/JB090iB04p02995)
- Condie, K., 2015, Changing tectonic settings through time: Indiscriminate use of geochemical discriminant diagrams: *Precambrian Research*, v. 266, p. 587–591. [10.1016/j.precamres.2015.05.004](https://doi.org/10.1016/j.precamres.2015.05.004)
- Condie, K.C., 2000, Episodic continental growth models: Afterthoughts and extensions: *Tectonophysics*, v. 322, no. 1–2, p. 153–162. [10.1016/S0040-1951\(00\)00061-5](https://doi.org/10.1016/S0040-1951(00)00061-5)
- Condie, K.C., 2003, Incompatible element ratios in oceanic basalts and komatiites: Tracking deep mantle sources and continental growth rates with time: *Geochemistry Geophysics Geosystems*, v. 4, no. 1, p. 1–28. [10.1029/2002GC000333](https://doi.org/10.1029/2002GC000333)
- Condie, K.C., 2021, *Earth as an evolving planetary system*. Elsevier Academic Press
- Condie, K.C., Arndt, N., Davaille, A., and Puetz, S.J., 2017, Zircon age peaks: Production or preservation of continental crust?: *Geosphere*, v. 13, no. 2, p. 227–234. [10.1130/GES01361.1](https://doi.org/10.1130/GES01361.1)
- Condie, K.C., Aster, R.C., and Van Hunen, J., 2016, A great thermal divergence in the mantle beginning 2.5 Ga: Geochemical constraints from greenstone basalts and komatiites: *Geoscience Frontiers*, v. 7, no. 4, p. 543–553. [10.1016/j.gsf.2016.01.006](https://doi.org/10.1016/j.gsf.2016.01.006)
- Condie, K.C., and Kröner, A., 2008, When did plate tectonics begin? Evidence from the geologic record, in Condie K.C., and Pease V., eds., *When did plate tectonics begin on planet earth*. Geological society of America special papers, v. 440, p. 281–294.
- Condie, K.C., Pisarevsky, S.A., and Puetz, S.J., 2021, Lips, orogens and supercontinents: The ongoing saga: *Gondwana Research*, v. 96, p. 105–121. [10.1016/j.gr.2021.05.002](https://doi.org/10.1016/j.gr.2021.05.002)
- Condie, K.C., and Stern, R.J., 2023, Ophiolites: Identification and tectonic significance in space and time: *Geoscience Frontiers*, v. 14, no. 6, p. 101680. [10.1016/j.gsf.2023.101680](https://doi.org/10.1016/j.gsf.2023.101680)
- Corcoran, P.L., Mueller, W.U., and Kusky, T.M., 2004, Inferred ophiolites in the Archaean slave craton: *Developments in Precambrian Geology*, v. 13, p. 363–404
- Crowley, J.W., G erault, M., and O'Connell, R.J., 2011, On the relative influence of heat and water transport on planetary dynamics: *Earth and Planetary Science Letters*, v. 310, no. 3–4, p. 380–388. [10.1016/j.epsl.2011.08.035](https://doi.org/10.1016/j.epsl.2011.08.035)

- Cutts, K.A., Lana, C., Stevens, G., and Buick, I.S., 2024, In situ Pb–pb garnet geochronology as a tool for investigating poly-metamorphism: A case for Paleoproterozoic lateral tectonic thickening: *Geological Society*, v. 537, no. 1, p. 209–229. [10.1144/SP537-2022-339](https://doi.org/10.1144/SP537-2022-339)
- Davaille, A., Smrekar, S.E., and Tomlinson, S., 2017, Experimental and observational evidence for plume-induced subduction on Venus: *Nature Geoscience*, v. 10, no. 5, p. 349–355. [10.1038/ngeo2928](https://doi.org/10.1038/ngeo2928)
- Davies, C.J., 2015, Cooling history of Earth's core with high thermal conductivity: *Physics of the Earth and Planetary Interiors*, v. 247, p. 65–79. [10.1016/j.pepi.2015.03.007](https://doi.org/10.1016/j.pepi.2015.03.007)
- Davies, G.F., 1992, On the emergence of plate tectonics: *Geology*, v. 20, no. 11, p. 963–966. [10.1130/0091-7613\(1992\)020<0963:OTEOPT>2.3.CO;2](https://doi.org/10.1130/0091-7613(1992)020<0963:OTEOPT>2.3.CO;2)
- Davies, G.F., 2006, Gravitational depletion of the early Earth's upper mantle and the viability of early plate tectonics: *Earth and Planetary Science Letters*, v. 243, no. 3–4, p. 376–382. [10.1016/j.epsl.2006.01.053](https://doi.org/10.1016/j.epsl.2006.01.053)
- Davies, G.F., 2009, Effect of plate bending on the Urey ratio and the thermal evolution of the mantle: *Earth and Planetary Science Letters*, v. 287, no. 3–4, p. 513–518. [10.1016/j.epsl.2009.08.038](https://doi.org/10.1016/j.epsl.2009.08.038)
- Debaille, V., O'Neill, C., Brandon, A.D., Haenecour, P., Yin, Q.-Z., Mattielli, N., and Treiman, A.H., 2013, Stagnant-lid tectonics in early Earth revealed by 142Nd variations in late Archean rocks: *Earth and Planetary Science Letters*, v. 373, p. 83–92. [10.1016/j.epsl.2013.04.016](https://doi.org/10.1016/j.epsl.2013.04.016)
- de Oliveira Chaves, A., and Porcher, C.C., 2020, Petrology, geochemistry and Sm–Nd systematics of the Paleoproterozoic Itaguara retroeclogite from São Francisco/Congo Craton: One of the oldest records of the modern-style plate tectonics: *Gondwana Research*, v. 87, p. 224–237. [10.1016/j.gr.2020.06.014](https://doi.org/10.1016/j.gr.2020.06.014)
- de Wit, M., Bhebhe, Z., Davidson, J., Haggerty, S.E., Hundt, P., Jacob, J., Lynn, M., Marshall, T.R., Skinner, C., Smithson, K., Stiefenhofer, J., Robert, M., Revitt, A., Spaggiari, R.S., Ward, J., 2016, Overview of diamond resources in Africa: Episodes *Journal of International Geoscience*, v. 39, no. 2, p. 199–237. [10.18814/epiugs/2016/v39i2/95776](https://doi.org/10.18814/epiugs/2016/v39i2/95776)
- de Wit, M.J., and Ashwal, L.D., 1997, *Greenstone belts: USA*, Oxford University Press
- Dhuime, B., Hawkesworth, C.J., Cawood, P.A., and Storey, C.D., 2012, A change in the geodynamics of continental growth 3 billion years ago: *Science (1979)*, v. 335, no. 6074, p. 1334–1336. [10.1126/science.1216066](https://doi.org/10.1126/science.1216066)
- Dhuime, B., Wuestefeld, A., and Hawkesworth, C.J., 2015, Emergence of modern continental crust about 3 billion years ago: *Nature Geoscience*, v. 8, no. 7, p. 552–555. [10.1038/ngeo2466](https://doi.org/10.1038/ngeo2466)
- Duarte, J.C., 2023, *Dynamics of plate tectonics and mantle convection*. Berlin: Elsevier, p. 594.
- Emo, R.B., and Kamber, B.S., 2022, Linking granulites, intraplate magmatism, and bi-mineralic eclogites with a thermodynamic-petrological model of melt–solid interaction at the base of anorogenic lower continental crust: *Earth and Planetary Science Letters*, v. 594, p. 117742. [10.1016/j.epsl.2022.117742](https://doi.org/10.1016/j.epsl.2022.117742)
- England, P., and Bickle, M., 1984, Continental thermal and tectonic regimes during the Archean: *The Journal of Geology*, v. 92, no. 4, p. 353–367. [10.1086/628872](https://doi.org/10.1086/628872)
- Ernst, W.G., 2017, Earth's thermal evolution, mantle convection, and Hadean onset of plate tectonics: *Journal of Asian Earth Sciences*, v. 145, p. 334–348. [10.1016/j.jseae.2017.05.037](https://doi.org/10.1016/j.jseae.2017.05.037)
- Farnetani, C.G., and Samuel, H., 2005, Beyond the thermal plume paradigm: *Geophysical Research Letters*, v. 32, no. 7. [10.1029/2005GL022360](https://doi.org/10.1029/2005GL022360)
- Farquhar, J., Wing, B.A., and McKeegan, K.D., 2002, Mass-independent sulfur of inclusions in diamond and sulfur recycling on early earth: *Science (1979)*, v. 298, no. 5602, p. 2369–2372. [10.1126/science.1078617](https://doi.org/10.1126/science.1078617)
- Flament, N., Coltice, N., and Rey, P.F., 2008, A case for late-Archaean continental emergence from thermal evolution models and hypsometry: *Earth and Planetary Science Letters*, v. 275, no. 3–4, p. 326–336. [10.1016/j.epsl.2008.08.029](https://doi.org/10.1016/j.epsl.2008.08.029)
- Foley, B., 2022, Generation of Archean TTGs by slab melting during sluggish, drip-like subduction. EGU Vienna, 23–27 May. [10.5194/egusphere-egu22-10873](https://doi.org/10.5194/egusphere-egu22-10873)
- Foley, B.J., 2018, The dependence of planetary tectonics on mantle thermal state: Applications to early earth evolution: *Philosophical Transactions of the Royal Society A: Mathematical, Physical and Engineering Sciences*, v. 376, no. 2132, p. 20170409. [10.1098/rsta.2017.0409](https://doi.org/10.1098/rsta.2017.0409)
- François, C., Debaille, V., Paquette, J.-L., Baudet, D., and Javaux, E.J., 2018, The earliest evidence for modern-style plate tectonics recorded by HP–LT metamorphism in the paleoproterozoic of the Democratic Republic of the Congo: *Scientific Reports*, v. 8, no. 1, p. 1–10. [10.1038/s41598-018-33823-y](https://doi.org/10.1038/s41598-018-33823-y)
- Frimmel, H.E., 2018, Episodic concentration of gold to ore grade through Earth's history: *Earth-Science Reviews*, v. 180, p. 148–158. [10.1016/j.earscirev.2018.03.011](https://doi.org/10.1016/j.earscirev.2018.03.011)
- Fu, R.R., Drabon, N., and Weiss, B.P., 2024, Statistical reanalysis of Archean zircon paleointensities: No evidence for stagnant-lid tectonics: *Earth and Planetary Science Letters*, v. 634, p. 118679. [10.1016/j.epsl.2024.118679](https://doi.org/10.1016/j.epsl.2024.118679)
- Furnes, H., and Dilek, Y., 2022, Archean versus Phanerozoic oceanic crust formation and tectonics: Ophiolites through time: *Geosystems and Geoenvironment*, v. 1, no. 1, p. 100004. [10.1016/j.geogeo.2021.09.004](https://doi.org/10.1016/j.geogeo.2021.09.004)
- Furnes, H., Rosing, M., Dilek, Y., and de Wit, M., 2009, Isua supracrustal belt (Greenland)—A vestige of a 3.8 Ga suprasubduction zone ophiolite, and the implications for Archean geology: *Lithos*, v. 113, p. 115–132. [10.1016/j.lithos.2009.03.043](https://doi.org/10.1016/j.lithos.2009.03.043)
- Gaborieau, M., Laubier, M., Bolfan-Casanova, N., McCammon, C. A., Vantelon, D., Chumakov, A.I., Schiavi, F., Neuville, D.R., and Venugopal, S., 2020, Determination of Fe³⁺/ΣFe of olivine-hosted melt inclusions using Mössbauer and XANES spectroscopy: *Chemical Geology*, v. 547, p. 119646. [10.1016/j.chemgeo.2020.119646](https://doi.org/10.1016/j.chemgeo.2020.119646)
- Ganne, J., de, A.V., Weinberg, R.F., Vidal, O., Dubacq, B., Kagambega, N., Naba, S., Baratoux, L., Jessell, M., and Allibon, J., 2012, Modern-style plate subduction preserved in the Palaeoproterozoic West African craton: *Nature Geoscience*, v. 5, no. 1, p. 60–65. [10.1038/ngeo1321](https://doi.org/10.1038/ngeo1321)
- Ganne, J., and Feng, X., 2017, Primary magmas and mantle temperatures through time: *Geochemistry Geophysics Geosystems*, v. 18, no. 3, p. 872–888. [10.1002/2016GC006787](https://doi.org/10.1002/2016GC006787)
- Gerya, T.V., Stern, R.J., and Baes, M., 2015, Plate tectonics on the Earth triggered by plume-induced subduction initiation: *Nature*, v. 527, no. 7577, p. 221–225. [10.1038/nature15752](https://doi.org/10.1038/nature15752)
- Gibson, S.A., 2002, Major element heterogeneity in Archean to recent mantle plume starting-heads: *Earth and Planetary*

- Science Letters, v. 195, no. 1–2, p. 59–74. [10.1016/S0012-821X\(01\)00566-0](https://doi.org/10.1016/S0012-821X(01)00566-0)
- Gibson, S.A., Malarkey, J., and Day, J.A., 2008, Melt depletion and enrichment beneath the western Kaapvaal Craton: Evidence from finch peridotite xenoliths: *Journal of Petrology*, v. 49, no. 10, p. 1817–1852. [10.1093/petrology/egn048](https://doi.org/10.1093/petrology/egn048)
- Giuliani, A., Jackson, M.G., Fitzpayne, A., and Dalton, H., 2021, Remnants of early earth differentiation in the deepest mantle-derived lavas: *Proceedings of the National Academy of Sciences*, v. 118, no. 1, p. e2015211118. [10.1073/pnas.2015211118](https://doi.org/10.1073/pnas.2015211118)
- Giuliani, A., Schmidt, M.W., Torsvik, T.H., and Fedortchouk, Y., 2023, Genesis and evolution of kimberlites: *Nature Reviews Earth and Environment*, v. 4, no. 11, p. 738–753. [10.1038/s43017-023-00481-2](https://doi.org/10.1038/s43017-023-00481-2)
- Goodwin, A.M., 1996, *Principles of Precambrian geology*. London: Academic Press, p. 327.
- Greber, N.D., Dauphas, N., and Bekker, A., 2017, Titanium isotopic evidence for felsic crust and plate tectonics 3.5 billion years ago: *Science* (1979), v. 357, no. 6357, p. 1271–1274. [10.1126/science.aan8086](https://doi.org/10.1126/science.aan8086)
- Griffin, W.L., and O'Reilly, S.Y., 2007, Cratonic lithospheric mantle: Is anything subducted?: *Episodes Journal of International Geoscience*, v. 30, no. 1, p. 43–53. [10.18814/epiugs/2007/v30i1/006](https://doi.org/10.18814/epiugs/2007/v30i1/006)
- Griffin, W.L., O'Reilly, S.Y., Abe, N., Aulbach, S., Davies, R.M., Pearson, N.J., Doyle, B.J., and Kivi, K., 2003, The origin and evolution of Archean lithospheric mantle: *Precambrian Research*, v. 127, no. 1–3, p. 19–41. [10.1016/S0301-9268\(03\)00180-3](https://doi.org/10.1016/S0301-9268(03)00180-3)
- Grosch, E.G., and Slama, J., 2017, Evidence for 3.3-billion-year-old oceanic crust in the Barberton greenstone belt, South Africa: *Geology*, v. 45, p. 695–698. [10.1130/G39035.1](https://doi.org/10.1130/G39035.1)
- Gunawardana, P.M., Chowdhury, P., Morra, G., and Cawood, P. A., 2024, Correlating mantle cooling with tectonic transitions on early earth: *Geology*, v. 52, no. 4, p. 230–234. [10.1130/G51874.1](https://doi.org/10.1130/G51874.1)
- Guo, M., and Korenaga, J., 2020, Argon constraints on the early growth of felsic continental crust: *Science Advances*, v. 6, no. 21, p. eaaz6234. [10.1126/sciadv.aaz6234](https://doi.org/10.1126/sciadv.aaz6234)
- Halla, J., 2005, Late Archean high-mg granitoids (sanukitoids) in the southern Karelian domain, eastern Finland: Pb and Nd isotopic constraints on crust–mantle interactions: *Lithos*, v. 79, no. 1–2, p. 161–178. [10.1016/j.lithos.2004.05.007](https://doi.org/10.1016/j.lithos.2004.05.007)
- Hallberg, J.A., 1972, Geochemistry of Archean volcanic belts in the Eastern Goldfields region of Western Australia: *Journal of Petrology*, v. 13, no. 1, p. 45–56. [10.1093/petrology/13.1.45](https://doi.org/10.1093/petrology/13.1.45)
- Hamilton, W.B., 1998, Archean magmatism and deformation were not products of plate tectonics: *Precambrian Research*, v. 91, no. 1–2, p. 143–179. [10.1016/S0301-9268\(98\)00042-4](https://doi.org/10.1016/S0301-9268(98)00042-4)
- Hamilton, W.B., 2011, Plate tectonics began in neoproterozoic time, and plumes from deep mantle have never operated: *Lithos*, v. 123, no. 1–4, p. 1–20. [10.1016/j.lithos.2010.12.007](https://doi.org/10.1016/j.lithos.2010.12.007)
- Hao, H., Campbell, I.H., Arculus, R.J., and Perfit, M.R., 2021, Using precious metal probes to quantify mid-ocean Ridge magmatic processes: *Earth and Planetary Science Letters*, v. 553, p. 116603. [10.1016/j.epsl.2020.116603](https://doi.org/10.1016/j.epsl.2020.116603)
- Harrison, C.G.A., 1999, Constraints on ocean volume change since the archaean: *Geophysical Research Letters*, v. 26, no. 13, p. 1913–1916. [10.1029/1999GL900425](https://doi.org/10.1029/1999GL900425)
- Harrison, T.M., 2009, The Hadean crust: Evidence from > 4 Ga zircons: *Annual Review of Earth and Planetary Sciences*, v. 37, no. 1, p. 479–505. [10.1146/annurev.earth.031208.100151](https://doi.org/10.1146/annurev.earth.031208.100151)
- Harrison, T.M., 2020, *Hadean earth*. Springer, ebook, p. 291. [10.1007/978-3-030-46687-9](https://doi.org/10.1007/978-3-030-46687-9)
- Harrison, T.M., 2024, We don't know when plate tectonics began: *Journal of the Geological Society*, v. 181, no. 4, p. jgs2023–212. [10.1144/jgs2023-212](https://doi.org/10.1144/jgs2023-212)
- Hastie, A.R., Law, S., Bromiley, G.D., Fitton, J.G., Harley, S.L., and Muir, D.D., 2023, Deep formation of Earth's earliest continental crust consistent with subduction: *Nature Geoscience*, v. 16, no. 9, p. 816–821. [10.1038/s41561-023-01249-5](https://doi.org/10.1038/s41561-023-01249-5)
- Hauri, E.H., Whitehead, J.A., and Hart, S.R., 1994, Fluid dynamic and geochemical aspects of entrainment in mantle plumes: *Journal of Geophysical Research: Solid Earth*, v. 99, no. B12, p. 24275–24300. [10.1029/94JB01257](https://doi.org/10.1029/94JB01257)
- Herzberg, C., 2006, Petrology and thermal structure of the Hawaiian plume from Mauna Kea volcano: *Nature*, v. 444, no. 7119, p. 605–609. [10.1038/nature05254](https://doi.org/10.1038/nature05254)
- Herzberg, C., 2011, Identification of source lithology in the Hawaiian and Canary Islands: Implications for origins: *Journal of Petrology*, v. 52, no. 1, p. 113–146. [10.1093/petrology/egq075](https://doi.org/10.1093/petrology/egq075)
- Herzberg, C., 2014, Archaean drips: *Nature Geoscience*, v. 7, no. 1, p. 7–8. [10.1038/ngeo2033](https://doi.org/10.1038/ngeo2033)
- Herzberg, C., 2019, Origin of high-mg biminerally eclogite xenoliths in kimberlite: A comment on a paper by Aulbach and Arndt (2019): *Earth and Planetary Science Letters*, v. 510, p. 231–233. [10.1016/j.epsl.2019.01.014](https://doi.org/10.1016/j.epsl.2019.01.014)
- Herzberg, C., 2022a, Thermal history of the earth: Reply to “less is not always more: A more inclusive data-filtering approach to secular mantle cooling” by Ross N. Mitchell and Jérôme Ganne: *Precambrian Research*, v. 381, p. 10–1016. [10.1016/j.precamres.2022.106844](https://doi.org/10.1016/j.precamres.2022.106844)
- Herzberg, C., 2022b, Understanding the paleoproterozoic circum-superior large igneous province constrains the thermal properties of Earth's mantle through time: *Precambrian Research*, v. 375, p. 106671. [10.1016/j.precamres.2022.106671](https://doi.org/10.1016/j.precamres.2022.106671)
- Herzberg, C., and Asimow, P.D., 2008, Petrology of some oceanic island basalts: PRIMELT2.XLS software for primary magma calculation: *Geochemistry Geophysics Geosystems*, v. 9, no. 9. [10.1029/2008GC002057](https://doi.org/10.1029/2008GC002057)
- Herzberg, C., and Asimow, P.D., 2015, PRIMELT3 MEGA.XLSM software for primary magma calculation: Peridotite primary magma MgO contents from the liquidus to the solidus: *Geochemistry Geophysics Geosystems*, v. 16, no. 2, p. 563–578. [10.1002/2014GC005631](https://doi.org/10.1002/2014GC005631)
- Herzberg, C., Asimow, P.D., Arndt, N., Niu, Y., Leshner, C.M., Fitton, J.G., Cheadle, M.J., and Saunders, A.D., 2007, Temperatures in ambient mantle and plumes: Constraints from basalts, picrites, and komatiites: *Geochemistry Geophysics Geosystems*, v. 8, no. 2. [10.1029/2006GC001390](https://doi.org/10.1029/2006GC001390)
- Herzberg, C., Condie, K., and Korenaga, J., 2010, Thermal history of the Earth and its petrological expression: *Earth and Planetary Science Letters*, v. 292, no. 1–2, p. 79–88. [10.1016/j.epsl.2010.01.022](https://doi.org/10.1016/j.epsl.2010.01.022)
- Herzberg, C., and Gazel, E., 2009, Petrological evidence for secular cooling in mantle plumes: *Nature*, v. 458, no. 7238, p. 619–622. [10.1038/nature07857](https://doi.org/10.1038/nature07857)

- Herzberg, C., and O'Hara, M.J., 2002, Plume-associated ultramafic magmas of Phanerozoic age: *Journal of Petrology*, v. 43, no. 10, p. 1857–1883. [10.1093/petrology/43.10.1857](https://doi.org/10.1093/petrology/43.10.1857)
- Herzberg, C., and Rudnick, R., 2012, Formation of cratonic lithosphere: An integrated thermal and petrological model: *Lithos*, v. 149, p. 4–15. [10.1016/j.lithos.2012.01.010](https://doi.org/10.1016/j.lithos.2012.01.010)
- Herzberg, C.T., Asimow, P.D., and Hernández-Montenegro, J.D., 2023, The meaning of pressure for primary magmas: New insights from PRIMELT3-P: *Geochemistry Geophysics Geosystems*, v. 24, no. 1, p. e2022GC010657. [10.1029/2022GC010657](https://doi.org/10.1029/2022GC010657)
- Hickman, A.H., 2012, Review of the Pilbara Craton and Fortescue Basin, Western Australia: Crustal evolution providing environments for early life: *The Island Arc*, v. 21, no. 1, p. 1–31. [10.1111/j.1440-1738.2011.00783.x](https://doi.org/10.1111/j.1440-1738.2011.00783.x)
- Hirschmann, M.M., 2023, The deep earth oxygen cycle: Mass balance considerations on the origin and evolution of mantle and surface oxidative reservoirs: *Earth and Planetary Science Letters*, v. 619, p. 118311. [10.1016/j.epsl.2023.118311](https://doi.org/10.1016/j.epsl.2023.118311)
- Hirth, G., and Kohlstedt, D.L., 1996, Water in the oceanic upper mantle: Implications for rheology, melt extraction and the evolution of the lithosphere: *Earth and Planetary Science Letters*, v. 144, no. 1–2, p. 93–108. [10.1016/0012-821X\(96\)00154-9](https://doi.org/10.1016/0012-821X(96)00154-9)
- Hole, M.J., 2018, Mineralogical and geochemical evidence for polybaric fractional crystallization of continental flood basalts and implications for identification of peridotite and pyroxenite source lithologies: *Earth-Science Reviews*, v. 176, p. 51–67. [10.1016/j.earscirev.2017.09.014](https://doi.org/10.1016/j.earscirev.2017.09.014)
- Hopkins, M., Harrison, T.M., and Manning, C.E., 2008, Low heat flow inferred from > 4 gyr zircons suggests hadean plate boundary interactions: *Nature*, v. 456, no. 7221, p. 493–496. [10.1038/nature07465](https://doi.org/10.1038/nature07465)
- Huang, G., Palin, R., Wang, D., and Guo, J., 2020, Open-system fractional melting of Archean basalts: Implications for tonalite–trondhjemite–granodiorite (TTG) magma genesis: *Contributions to Mineralogy and Petrology*, v. 175, no. 11, p. 1–25. [10.1007/s00410-020-01742-9](https://doi.org/10.1007/s00410-020-01742-9)
- Huang, J., Zhong, S., and van Hunen, J., 2003, Controls on sublithospheric small-scale convection: *Journal of Geophysical Research: Solid Earth*, v. 108, no. B8. [10.1029/2003JB002456](https://doi.org/10.1029/2003JB002456)
- Hynes, A., 2005, Buoyancy of the oceanic lithosphere and subduction initiation: *International Geology Review*, v. 47, no. 9, p. 938–951. [10.2747/0020-6814.47.9.938](https://doi.org/10.2747/0020-6814.47.9.938)
- Hyung, E., and Jacobsen, S.B., 2020, The ¹⁴²Nd/¹⁴⁴Nd variations in mantle-derived rocks provide constraints on the stirring rate of the mantle from the hadean to the present: *Proceedings of the National Academy of Sciences*, v. 117, no. 26, p. 14738–14744. [10.1073/pnas.2006950117](https://doi.org/10.1073/pnas.2006950117)
- Imayama, T., Oh, C.-W., Baltybaev, S.K., Park, C.-S., Yi, K., Jung, H., 2017, Paleoproterozoic high-pressure metamorphic history of the Salma eclogite on the Kola Peninsula, Russia: *Lithosphere*, v. 9, no. 6, p. 855–873. [10.1130/L657.1](https://doi.org/10.1130/L657.1)
- Johnson, B.W., and Wing, B.A., 2020, Limited archaean continental emergence reflected in an early archaean ¹⁸O-enriched ocean: *Nature Geoscience*, v. 13, no. 3, p. 243–248. [10.1038/s41561-020-0538-9](https://doi.org/10.1038/s41561-020-0538-9)
- Johnson, T.E., Brown, M., Gardiner, N.J., Kirkland, C.L., Smithies, R.H., 2017, Earth's first stable continents did not form by subduction: *Nature*, v. 543, no. 7644, p. 239–242. [10.1038/nature21383](https://doi.org/10.1038/nature21383)
- Johnson, T.E., Brown, M., Kaus, B.J.P., and VanTongeren, J.A., 2014, Delamination and recycling of Archaean crust caused by gravitational instabilities: *Nature Geoscience*, v. 7, no. 1, p. 47–52. [10.1038/ngeo2019](https://doi.org/10.1038/ngeo2019)
- Karato, S., 2010, Rheology of the deep upper mantle and its implications for the preservation of the continental roots: A review: *Tectonophysics*, v. 481, no. 1–4, p. 82–98. [10.1016/j.tecto.2009.04.011](https://doi.org/10.1016/j.tecto.2009.04.011)
- Katsura, T., Yoneda, A., Yamazaki, D., Yoshino, T., Ito, E., et al, 2010, Adiabatic temperature profile in the mantle: Physics of the Earth and Planetary Interiors, v. 183, no. 1–2, p. 212–218. [10.1016/j.pepi.2010.07.001](https://doi.org/10.1016/j.pepi.2010.07.001)
- Kelemen, P.B., Hart, S.R., and Bernstein, S., 1998, Silica enrichment in the continental upper mantle via melt/rock reaction: *Earth and Planetary Science Letters*, v. 164, no. 1–2, p. 387–406. [10.1016/S0012-821X\(98\)00233-7](https://doi.org/10.1016/S0012-821X(98)00233-7)
- Keller, B., and Schoene, B., 2018, Plate tectonics and continental basaltic geochemistry throughout earth history: *Earth and Planetary Science Letters*, v. 481, p. 290–304. [10.1016/j.epsl.2017.10.031](https://doi.org/10.1016/j.epsl.2017.10.031)
- Keller, C.B., Boehnke, P., and Schoene, B., 2017, Temporal variation in relative zircon abundance throughout Earth history: *Geochemical Perspectives Letters*, p. 179–189. [10.7185/geochemlet.1721](https://doi.org/10.7185/geochemlet.1721)
- Keller, C.B., and Harrison, T.M., 2020, Constraining crustal silica on ancient earth: *Proceedings of the National Academy of Sciences*, v. 117, no. 35, p. 21101–21107. [10.1073/pnas.2009431117](https://doi.org/10.1073/pnas.2009431117)
- Kenny, G.G., Whitehouse, M.J., and Kamber, B.S., 2016, Differentiated impact melt sheets may be a potential source of hadean detrital zircon: *Geology*, v. 44, no. 6, p. 435–438. [10.1130/G37898.1](https://doi.org/10.1130/G37898.1)
- Komiya, T., 2007, Material circulation through time: Chemical differentiation within the mantle and secular variation of temperature and composition of the mantle, in Yuen, D.A., Maruyama, S., Karato S.I., and Windley, B.F., eds., *Superplumes: Beyond plate tectonics*, Springer, p. 187–234.
- Komiya, T., Maruyama, S., Hirata, T., and Yurimoto, H., 2002, Petrology and geochemistry of MORB and OIB in the Mid-Archaean North Pole Region, Pilbara Craton, Western Australia: Implications for the composition and temperature of the upper mantle at 3.5 Ga: *International Geology Review*, v. 44, no. 11, p. 988–1016. [10.2747/0020-6814.44.11.988](https://doi.org/10.2747/0020-6814.44.11.988)
- Komiya, T., Maruyama, S., Masuda, T., Nohda, S., Hayashi, M., and Okamoto, K., 1999, Plate tectonics at 3.8–3.7 Ga: Field evidence from the isua accretionary complex, southern West Greenland: *The Journal of Geology*, v. 107, no. 5, p. 515–554. [10.1086/314371](https://doi.org/10.1086/314371)
- Komiya, T., Yamamoto, S., and Aoki, S., 2015, Geology of the Eoarchean, >3.95Ga, nulliak supracrustal rocks in the saglek block, northern Labrador, Canada: The oldest geological evidence for plate tectonics: *Tectonophysics*, v. 662, p. 40–66. [10.1016/j.tecto.2015.05.003](https://doi.org/10.1016/j.tecto.2015.05.003)
- Konhauser, K.O., Pecoits, E., and Lalonde, S.V., 2009, Oceanic nickel depletion and a methanogen famine before the great oxidation event: *Nature*, v. 458, no. 7239, p. 750–753. [10.1038/nature07858](https://doi.org/10.1038/nature07858)
- Korenaga, J., 2003, Energetics of mantle convection and the fate of fossil heat: *Geophysical Research Letters*, v. 30, no. 8. [10.1029/2003GL016982](https://doi.org/10.1029/2003GL016982)

- Korenaga, J., 2006, Archean geodynamics and the thermal evolution of earth: Geophysical Monograph-American Geophysical Union, v. 164, p. 7
- Korenaga, J., 2007, Thermal cracking and the deep hydration of oceanic lithosphere: A key to the generation of plate tectonics?: *Journal of Geophysical Research: Solid Earth*, v. 112, no. B5. [10.1029/2006JB004502](https://doi.org/10.1029/2006JB004502)
- Korenaga, J., 2008, Urey ratio and the structure and evolution of Earth's mantle: *Reviews of Geophysics*, v. 46, p. 1–32. [10.1029/2007RG000241](https://doi.org/10.1029/2007RG000241)
- Korenaga, J., 2011, Thermal evolution with a hydrating mantle and the initiation of plate tectonics in the early earth: *Journal of Geophysical Research*, v. 116, no. B12. [10.1029/2011JB008410](https://doi.org/10.1029/2011JB008410)
- Korenaga, J., 2013, Initiation and evolution of plate tectonics on earth: Theories and observations: *Annual Review of Earth and Planetary Sciences*, v. 41, no. 1, p. 117–151. [10.1146/annurev-earth-050212-124208](https://doi.org/10.1146/annurev-earth-050212-124208)
- Korenaga, J., 2017, Pitfalls in modeling mantle convection with internal heat production: *Journal of Geophysical Research: Solid Earth*, v. 122, no. 5, p. 4064–4085. [10.1002/2016JB013850](https://doi.org/10.1002/2016JB013850)
- Korenaga, J., 2018a, Crustal evolution and mantle dynamics through earth history: *Philosophical Transactions of the Royal Society A: Mathematical, Physical and Engineering Sciences*, v. 376, no. 2132, p. 20170408. [10.1098/rsta.2017.0408](https://doi.org/10.1098/rsta.2017.0408)
- Korenaga, J., 2018b, Estimating the formation age distribution of continental crust by unmixing zircon ages: *Earth and Planetary Science Letters*, v. 482, p. 388–395. [10.1016/j.epsl.2017.11.039](https://doi.org/10.1016/j.epsl.2017.11.039)
- Korenaga, J., 2021, Hadean geodynamics and the nature of early continental crust: *Precambrian Research*, v. 359, p. 106178. [10.1016/j.precamres.2021.106178](https://doi.org/10.1016/j.precamres.2021.106178)
- Korenaga, J., and Jordan, T.H., 2003, Physics of multiscale convection in Earth's mantle: Onset of sublithospheric convection: *Journal of Geophysical Research: Solid Earth*, v. 108, no. B7. [10.1029/2002JB001760](https://doi.org/10.1029/2002JB001760)
- Korenaga, J., Planavsky, N.J., and Evans, D.A.D., 2017, Global water cycle and the coevolution of the Earth's interior and surface environment: *Philosophical Transactions of the Royal Society A: Mathematical, Physical and Engineering Sciences*, v. 375, no. 2094, p. 20150393. [10.1098/rsta.2015.0393](https://doi.org/10.1098/rsta.2015.0393)
- Kröner, A., 1991, Tectonic evolution in the Archean and proterozoic: *Tectonophysics*, v. 187, no. 4, p. 393–410. [10.1016/0040-1951\(91\)90478-B](https://doi.org/10.1016/0040-1951(91)90478-B)
- Kusky, T.M., and Celâl Şengör, A.M., 2023, Comparative orotomorphism of the Archean superior and Phanerozoic alitid orogenic systems: *National Science Review*, v. 10, no. 2, p. nwac235. [10.1093/nsr/nwac235](https://doi.org/10.1093/nsr/nwac235)
- Kusky, T.M., Windley, B.F., and Polat, A., 2018, Geological evidence for the operation of plate tectonics throughout the Archean: Records from Archean paleo-plate boundaries: *Journal of Earth Science*, v. 29, no. 6, p. 1291–1303. [10.1007/s12583-018-0999-6](https://doi.org/10.1007/s12583-018-0999-6)
- Kusky, T., and Wang, L., 2022, Growth of continental crust in intra-oceanic and continental-margin arc systems: Analogs for Archean systems: *Science China Earth Sciences*, v. 65, no. 9, p. 1615–1645. [10.1007/s11430-021-9964-1](https://doi.org/10.1007/s11430-021-9964-1)
- Kusky, T., Windley, B.F., Polat, A., Wang, L., Ning, W., and Zhong, Y., 2021, Archean dome-and-basin style structures form during growth and death of intraoceanic and continental margin arcs in accretionary orogens: *Earth-Science Reviews*, v. 220, p. 103725. [10.1016/j.earscrev.2021.103725](https://doi.org/10.1016/j.earscrev.2021.103725)
- Labrosse, S., 2015, Thermal evolution of the core with a high thermal conductivity: *Physics of the Earth and Planetary Interiors*, v. 247, p. 36–55. [10.1016/j.pepi.2015.02.002](https://doi.org/10.1016/j.pepi.2015.02.002)
- Lambart, S., Baker, M.B., and Stolper, E.M., 2016, The role of pyroxenite in basalt genesis: Melt-px, a melting parameterization for mantle pyroxenites between 0.9 and 5 GPa: *Journal of Geophysical Research: Solid Earth*, v. 121, no. 8, p. 5708–5735. [10.1002/2015JB012762](https://doi.org/10.1002/2015JB012762)
- Langmuir, C.H., and Hanson, G.N., 1980, An evaluation of major element heterogeneity in the mantle sources of basalts: *Philosophical Transactions of the Royal Society of London Series A: Mathematical & Physical Sciences*, v. 297, p. 383–407
- Laurent, O., Martin, H., Doucelance, R., Moyen, J.-F., Paquette, J.-L., 2011, Geochemistry and petrogenesis of high-K “sanukitoids” from the Bulai pluton, Central Limpopo Belt, South Africa: Implications for geodynamic changes at the Archean–Proterozoic boundary: *Lithos*, v. 123, no. 1–4, p. 73–91. [10.1016/j.lithos.2010.12.009](https://doi.org/10.1016/j.lithos.2010.12.009)
- Laurent, O., Martin, H., Moyen, J.F., and Doucelance, R., 2014, The diversity and evolution of late-Archean granitoids: Evidence for the onset of “modern-style” plate tectonics between 3.0 and 2.5Ga: *Lithos*, v. 205, p. 208–235. [10.1016/j.lithos.2014.06.012](https://doi.org/10.1016/j.lithos.2014.06.012)
- Lee, C.-T., and Chin, E.J., 2023, Cratonization and a journey of healing: From weakness to strength: *Earth and Planetary Science Letters*, v. 624, p. 118439. [10.1016/j.epsl.2023.118439](https://doi.org/10.1016/j.epsl.2023.118439)
- Lee, C.-T., Luffi, P., Plank, T., Dalton, H., and Leeman, W.P., 2009, Constraints on the depths and temperatures of basaltic magma generation on Earth and other terrestrial planets using new thermobarometers for mafic magmas: *Earth and Planetary Science Letters*, v. 279, no. 1–2, p. 20–33. [10.1016/j.epsl.2008.12.020](https://doi.org/10.1016/j.epsl.2008.12.020)
- le Maitre, R.W., 1984, A proposal by the IUGS subcommission on the systematics of igneous rocks for a chemical classification of volcanic rocks based on the total alkali silica (TAS) diagram: (on behalf of the IUGS subcommission on the systematics of igneous rocks): *Australian Journal of Earth Sciences*, v. 31, no. 2, p. 243–255. [10.1080/08120098408729295](https://doi.org/10.1080/08120098408729295)
- Lenardic, A., Seales, J., Moore, W., and Weller, M., 2021, Convective and tectonic plate velocities in a mixed heating mantle: *Geochemistry Geophysics Geosystems*, v. 22, no. 2, p. e2020GC009278. [10.1029/2020GC009278](https://doi.org/10.1029/2020GC009278)
- Leshner, C.M., and Arndt, N.T., 1995, REE and Nd isotope geochemistry, petrogenesis and volcanic evolution of contaminated komatiites at Kambalda, Western Australia: *Lithos*, v. 34, no. 1–3, p. 127–157. [10.1016/0024-4937\(95\)90017-9](https://doi.org/10.1016/0024-4937(95)90017-9)
- Li, J., Liu, S.-A., and Ma, H., 2024, Pervasive Neoproterozoic melting of subducted sediments generating sanukitoid and associated magmatism in the North China Craton, with implications for the operation of plate tectonics: *GSA Bulletin*, no.136, p. 3121–3136. [10.1130/B37279.1](https://doi.org/10.1130/B37279.1)
- Li, M., Black, B., Zhong, S., Manga, M., Rudolph, M.L., Olson, P., 2016, Quantifying melt production and degassing rate at mid-ocean ridges from global mantle convection models with plate motion history: *Geochemistry Geophysics*

- Geosystems, v. 17, no. 7, p. 2884–2904. [10.1002/2016GC006439](https://doi.org/10.1002/2016GC006439)
- Liu, H., and Zhang, H.-F., 2019, Paleoproterozoic ophiolite remnants in the northern margin of the North China Craton: Evidence from the Chicheng peridotite massif: *Lithos*, v. 344–345, p. 311–323. [10.1016/j.lithos.2019.06.025](https://doi.org/10.1016/j.lithos.2019.06.025)
- Liu, S.-L., Ma, L., Zou, X., Fang, L., Qin, B., Melnik, A.E., Kirscher, U., Yang, K.-F., Fan, H.-R., Mitchell, R.N., 2023, Trends and rhythms in carbonatites and kimberlites reflect thermo-tectonic evolution of earth: *Geology*, v. 51, no. 1, p. 101–105. [10.1130/G50775.1](https://doi.org/10.1130/G50775.1)
- Loose, D., and Schenk, V., 2018, 2.09 Ga old eclogites in the eburnian-Transamazonian orogen of southern Cameroon: Significance for palaeoproterozoic plate tectonics: *Precambrian Research*, v. 304, p. 1–11. [10.1016/j.precamres.2017.10.018](https://doi.org/10.1016/j.precamres.2017.10.018)
- Lourenço, D.L., and Rozel, A.B., 2023, The past and the future of plate tectonics and other tectonic regimes, in Duarte, J. C., ed., *Dynamics of plate tectonics and mantle convection*, Elsevier, p. 181–196
- Luo, Y., and Korenaga, J., 2021, Efficiency of eclogite removal from continental lithosphere and its implications for cratonic diamonds: *Geology*, v. 49, no. 4, p. 438–441. [10.1130/G48204.1](https://doi.org/10.1130/G48204.1)
- Macgregor, A.M., 1951, Some milestones in the Precambrian of Southern Rhodesia. in *Proceedings of the Geological Society of South Africa*, v. 54, p. 27–71.
- MacLennan, J., 2019, Mafic tiers and transient mushes: Evidence from Iceland: *Philosophical Transactions of the Royal Society A: Mathematical, Physical and Engineering Sciences*, v. 377, no. 2139, p. 20180021. [10.1098/rsta.2018.0021](https://doi.org/10.1098/rsta.2018.0021)
- Martin, H., Moyen, J.-F., and Rapp, R., 2009, The sanukitoid series: Magmatism at the Archaean–Proterozoic transition: *Earth and Environmental Science Transactions of the Royal Society of Edinburgh*, v. 100, no. 1–2, p. 15–33. [10.1017/S1755691009016120](https://doi.org/10.1017/S1755691009016120)
- Martin, H., Smithies, R.H., Rapp, R., Moyen, J.-F., Champion, D., 2005, An overview of adakite, tonalite–trondhjemite–granodiorite (TTG), and sanukitoid: Relationships and some implications for crustal evolution: *Lithos*, v. 79, no. 1–2, p. 1–24. [10.1016/j.lithos.2004.04.048](https://doi.org/10.1016/j.lithos.2004.04.048)
- Marty, B., Bekaert, D.V., Broadley, M.W., and Jaupart, C., 2019, Geochemical evidence for high volatile fluxes from the mantle at the end of the Archaean: *Nature*, v. 575, no. 7783, p. 485–488. [10.1038/s41586-019-1745-7](https://doi.org/10.1038/s41586-019-1745-7)
- Mckenzie, D., and Bickle, M.J., 1988, The volume and composition of melt generated by extension of the lithosphere: *Journal of Petrology*, v. 29, no. 3, p. 625–679. [10.1093/ptrology/29.3.625](https://doi.org/10.1093/ptrology/29.3.625)
- Mei, Q.-F., Yang, J.-H., Wang, Y.-F., Wang, H., and Peng, P., 2020, Tungsten isotopic constraints on homogenization of the Archaean silicate earth: Implications for the transition of tectonic regimes: *Geochimica et cosmochimica acta*, v. 278, p. 51–64. [10.1016/j.gca.2019.07.050](https://doi.org/10.1016/j.gca.2019.07.050)
- Mikkola, P., Huhma, H., Heilimo, E., and Whitehouse, M., 2011, Archaean crustal evolution of the Suomussalmi district as part of the kianta complex, Karelia: Constraints from geochemistry and isotopes of granitoids: *Lithos*, v. 125, no. 1–2, p. 287–307. [10.1016/j.lithos.2011.02.012](https://doi.org/10.1016/j.lithos.2011.02.012)
- Mitchell, R.N., and Ganne, J., 2022, Less is not always more: A more inclusive data-filtering approach to secular mantle cooling: *Precambrian Research*, v. 379, p. 106787. [10.1016/j.precamres.2022.106787](https://doi.org/10.1016/j.precamres.2022.106787)
- Miyazaki, Y., and Korenaga, J., 2022, A wet heterogeneous mantle creates a habitable world in the hadean: *Nature*, v. 603, no. 7899, p. 86–90. [10.1038/s41586-021-04371-9](https://doi.org/10.1038/s41586-021-04371-9)
- Mojszsis, S.J., Harrison, T.M., and Pidgeon, R.T., 2001, Oxygen-isotope evidence from ancient zircons for liquid water at the Earth's surface 4,300 myr ago: *Nature*, v. 409, no. 6817, p. 178–181. [10.1038/35051557](https://doi.org/10.1038/35051557)
- Mondal, P., and Korenaga, J., 2018, A propagator matrix method for the Rayleigh–Taylor instability of multiple layers: A case study on crustal delamination in the early earth: *Geophysical Journal International*, v. 212, no. 3, p. 1890–1901. [10.1093/gji/ggx513](https://doi.org/10.1093/gji/ggx513)
- Moore, W.B., and Webb, A.A.G., 2013, Heat-pipe earth: *Nature*, v. 501, no. 7468, p. 501–505. [10.1038/nature12473](https://doi.org/10.1038/nature12473)
- Morency, C., and Doin, M., 2004, Numerical simulations of the mantle lithosphere delamination: *Journal of Geophysical Research: Solid Earth*, v. 109, no. B3. [10.1029/2003JB002414](https://doi.org/10.1029/2003JB002414)
- Moresi, L., and Solomatov, V., 1998, Mantle convection with a brittle lithosphere: Thoughts on the global tectonic styles of the Earth and Venus: *Geophysical Journal International*, v. 133, no. 3, p. 669–682. [10.1046/j.1365-246X.1998.00521.x](https://doi.org/10.1046/j.1365-246X.1998.00521.x)
- Morgan, P., 1985, Crustal radiogenic heat production and the selective survival of ancient continental crust: *Journal of Geophysical Research: Solid Earth*, v. 90, no. S02, p. C561–C570. [10.1029/JB090iS02p0C561](https://doi.org/10.1029/JB090iS02p0C561)
- Mukherjee, S., and Mulchrone, K.F., 2012, Estimating the viscosity and prandtl number of the tso morari crystalline gneiss dome, Indian western Himalaya: *International Journal of Earth Sciences*, v. 101, no. 7, p. 1929–1947. [10.1007/s00531-012-0758-3](https://doi.org/10.1007/s00531-012-0758-3)
- Müller, S., Dziggel, A., Kolb, J., and Sindern, S., 2018, Mineral textural evolution and pt-path of relict eclogite-facies rocks in the paleoproterozoic nagssugtoqidian orogen, South-East Greenland: *Lithos*, v. 296–299, p. 212–232. [10.1016/j.lithos.2017.11.008](https://doi.org/10.1016/j.lithos.2017.11.008)
- Nakagawa, T., 2023, Numerical modeling on global-scale mantle water cycle and its impact on the sea-level change: *Earth and Planetary Science Letters*, v. 619, p. 118312. [10.1016/j.epsl.2023.118312](https://doi.org/10.1016/j.epsl.2023.118312)
- Nebel, O., Capitanio, F.A., Moyen, J.-F., Weinberg, R.F., Clos, F., Nebel-Jacobsen, Y.J., Cawood, P.A., 2018, When crust comes of age: On the chemical evolution of Archaean, felsic continental crust by crustal drip tectonics: *Philosophical Transactions of the Royal Society A: Mathematical, Physical and Engineering Sciences*, v. 376, no. 2132, p. 20180103. [10.1098/rsta.2018.0103](https://doi.org/10.1098/rsta.2018.0103)
- Ning, W., Kusky, T., Wang, L., and Huang, B., 2022, Archean eclogite-facies oceanic crust indicates modern-style plate tectonics: *Proceedings of the National Academy of Sciences*, v. 119, no. 15, p. e2117529119. [10.1073/pnas.2117529119](https://doi.org/10.1073/pnas.2117529119)
- Nisbet, E.G., Cheadle, M.J., Arndt, N.T., and Bickle, M.J., 1993, Constraining the potential temperature of the Archaean mantle: A review of the evidence from komatiites: *Lithos*, v. 30, no. 3–4, p. 291–307. [10.1016/0024-4937\(93\)90042-B](https://doi.org/10.1016/0024-4937(93)90042-B)
- Nisbet, E.G., and Fowler, C.M.R., 1983, Model for Archean plate tectonics: *Geology*, v. 11, no. 7, p. 376–379. [10.1130/0091-7613\(1983\)11<376:MFAPT>2.0.CO;2](https://doi.org/10.1130/0091-7613(1983)11<376:MFAPT>2.0.CO;2)
- Nutman, A.P., Bennett, V.C., Friend, C.R.L., and Yi, K., 2020, Eoarchean contrasting ultra-high-pressure to low-pressure

- metamorphisms ($< 250 \rightarrow 1000^\circ \text{ C/GPa}$) explained by tectonic plate convergence in deep time: *Precambrian Research*, v. 344, p. 105770. [10.1016/j.precamres.2020.105770](https://doi.org/10.1016/j.precamres.2020.105770)
- Nutman, A.P., Friend, C.R.L., and Bennett, V.C., 2002, Evidence for 3650–3600 ma assembly of the northern end of the itsaq gneiss complex, Greenland: Implication for early Archaean tectonics: *Tectonics*, v. 21, no. 1, p. 1–5. [10.1029/2000TC001203](https://doi.org/10.1029/2000TC001203)
- O'Neill, C., Lenardic, A., Moresi, L., Torsvik, T.H., and Lee, C.-T.A., 2007, Episodic Precambrian subduction: Earth and Planetary Science Letters, v. 262, no. 3–4, p. 552–562. [10.1016/j.epsl.2007.04.056](https://doi.org/10.1016/j.epsl.2007.04.056)
- Osei Tutu, A., Sobolev, S.V., and Steinberger, B., 2018, Evaluating the influence of plate boundary friction and mantle viscosity on plate velocities: *Geochemistry Geophysics Geosystems*, v. 19, no. 3, p. 642–666. [10.1002/2017GC007112](https://doi.org/10.1002/2017GC007112)
- Palin, R.M., Santosh, M., Cao, W., Li, S.-S., Hernández-Urbe, D., and Parsons, A., 2020, Secular change and the onset of plate tectonics on earth: *Earth-Science Reviews*, v. 207, p. 103172. [10.1016/j.earscirev.2020.103172](https://doi.org/10.1016/j.earscirev.2020.103172)
- Palin, R.M., and White, R.W., 2016, Emergence of blueschists on Earth linked to secular changes in oceanic crust composition: *Nature Geoscience*, v. 9, no. 1, p. 60–64. [10.1038/ngeo2605](https://doi.org/10.1038/ngeo2605)
- Pearson, D.G., Scott, J.M., Liu, J., Schaeffer, A., Wang, L.H., van Hunen, J., Szilas, K., Chacko, T., Kelemen, P.B., 2021, Deep continental roots and cratons: *Nature*, v. 596, no. 7871, p. 199–210. [10.1038/s41586-021-03600-5](https://doi.org/10.1038/s41586-021-03600-5)
- Pearson, D.G., and Wittig, N., 2008, Formation of Archaean continental lithosphere and its diamonds: The root of the problem: *Journal of the Geological Society*, v. 165, no. 5, p. 895–914. [10.1144/0016-76492008-003](https://doi.org/10.1144/0016-76492008-003)
- Pearson, D.G., and Wittig, N., 2014, The formation and evolution of cratonic mantle lithosphere: evidence from mantle xenoliths. *in* Carlson, R.W., ed., *Treatise on Geochemistry*. Elsevier, Amsterdam, p. 255–292.
- Perchuk, A.L., Gerya, T.V., Zakharov, V.S., and Griffin, W.L., 2021, Depletion of the upper mantle by convergent tectonics in the early earth: *Scientific Reports*, v. 11, no. 1, p. 1–12. [10.1038/s41598-021-00837-y](https://doi.org/10.1038/s41598-021-00837-y)
- Perchuk, A.L., Zakharov, V.S., Gerya, T.V., and Griffin, W.L., 2023, Flat subduction in the early earth: The key role of discrete eclogitization kinetics: *Gondwana Research*, v. 119, p. 186–203. [10.1016/j.gr.2023.03.015](https://doi.org/10.1016/j.gr.2023.03.015)
- Pereira, I., Storey, C.D., Darling, J.R., Moreira, H., Strachan, R.A., and Cawood, P.A., 2021, Detrital rutile tracks the first appearance of subduction zone low T/P paired metamorphism in the palaeoproterozoic: *Earth and Planetary Science Letters*, v. 570, p. 117069. [10.1016/j.epsl.2021.117069](https://doi.org/10.1016/j.epsl.2021.117069)
- Piccolo, A., Palin, R.M., Kaus, B.J.P., and White, R.W., 2019, Generation of Earth's early continents from a relatively cool Archean mantle: *Geochemistry Geophysics Geosystems*, v. 20, p. 1679–1697. [10.1029/2018GC008079](https://doi.org/10.1029/2018GC008079)
- Piper, J.D.A., 2013, Continental velocity through Precambrian times: The link to magmatism, crustal accretion and episodes of global cooling: *Geoscience Frontiers*, v. 4, no. 1, p. 7–36. [10.1016/j.gsf.2012.05.008](https://doi.org/10.1016/j.gsf.2012.05.008)
- Pope, E.C., Bird, D.K., and Rosing, M.T., 2012, Isotope composition and volume of Earth's early oceans: *Proceedings of the National Academy of Sciences*, v. 109, no. 12, p. 4371–4376. [10.1073/pnas.1115705109](https://doi.org/10.1073/pnas.1115705109)
- Ptáček, M.P., Dauphas, N., and Greber, N.D., 2020, Chemical evolution of the continental crust from a data-driven inversion of terrigenous sediment compositions: *Earth and Planetary Science Letters*, v. 539, p. 116090. [10.1016/j.epsl.2020.116090](https://doi.org/10.1016/j.epsl.2020.116090)
- Puchtel, I.S., Blichert-Toft, J., Horan, M.F., Touboul, M., and Walker, R.J., 2022, The komatiite testimony to ancient mantle heterogeneity: *Chemical Geology*, v. 594, p. 120776. [10.1016/j.chemgeo.2022.120776](https://doi.org/10.1016/j.chemgeo.2022.120776)
- Puetz, S.J., and Condie, K.C., 2021, Applying popperian falsifiability to geodynamic hypotheses: Empirical testing of the episodic crustal/zircon production hypothesis and selective preservation hypothesis: *International Geology Review*, v. 63, no. 15, p. 1920–1950. [10.1080/00206814.2020.1818143](https://doi.org/10.1080/00206814.2020.1818143)
- Putirka, K., 2008, Excess temperatures at ocean islands: Implications for mantle layering and convection: *Geology*, v. 36, no. 4, p. 283–286. [10.1130/G24615A.1](https://doi.org/10.1130/G24615A.1)
- Putirka, K.D., 2005, Mantle potential temperatures at Hawaii, Iceland, and the mid-ocean ridge system, as inferred from olivine phenocrysts: Evidence for thermally driven mantle plumes: *Geochemistry Geophysics Geosystems*, v. 6, no. 5. [10.1029/2005GC000915](https://doi.org/10.1029/2005GC000915)
- Putirka, K.D., Perfit, M., Ryerson, F.J., and Jackson, M.G., 2007, Ambient and excess mantle temperatures, olivine thermometry, and active vs. passive upwelling: *Chemical Geology*, v. 241, no. 3–4, p. 177–206. [10.1016/j.chemgeo.2007.01.014](https://doi.org/10.1016/j.chemgeo.2007.01.014)
- Reimink, J.R., Chacko, T., Stern, R.A., and Heaman, L.M., 2014, Earth's earliest evolved crust generated in an Iceland-like setting: *Nature Geoscience*, v. 7, no. 7, p. 529–533. [10.1038/ngeo2170](https://doi.org/10.1038/ngeo2170)
- Reimink, J.R., Davies, J.H.F.L., and Ielpi, A., 2021, Global zircon analysis records a gradual rise of continental crust throughout the Neoproterozoic: *Earth and Planetary Science Letters*, v. 554, p. 116654. [10.1016/j.epsl.2020.116654](https://doi.org/10.1016/j.epsl.2020.116654)
- Reimink, J.R., Mundl-Petermeier, A., Carlson, R.W., Shirey, S.B., Walker, R.J., Pearson, D.G., 2020, Tungsten isotope composition of Archean crustal reservoirs and implications for terrestrial $\mu^{182}\text{W}$ evolution: *Geochemistry Geophysics Geosystems*, v. 21, no. 7, p. e2020GC009155. [10.1029/2020GC009155](https://doi.org/10.1029/2020GC009155)
- Rey, P.F., and Coltice, N., 2008, Neoproterozoic lithospheric strengthening and the coupling of Earth's geochemical reservoirs: *Geology*, v. 36, p. 635–638. [10.1130/G25031A.1](https://doi.org/10.1130/G25031A.1)
- Richard, D., Marty, B., Chaussidon, M., and Arndt, N., 1996, Helium isotopic evidence for a lower mantle component in depleted Archean komatiite: *Science* (1979), v. 273, no. 5271, p. 93–95. [10.1126/science.273.5271.93](https://doi.org/10.1126/science.273.5271.93)
- Rizo, H., Andrault, D., Bennett, N.R., Humayun, M., Brandon, A., Vlastelic, I., Moine, B., Poirier, A., Bouhifd, M.A., and Murphy, D. T., 2019, ^{182}W evidence for core-mantle interaction in the source of mantle plumes: *Geochemical Perspectives Letters*, v. 11, p. 6–11. [10.7185/geochemlet.1917](https://doi.org/10.7185/geochemlet.1917)
- Roberts, N.M.W., 2013, The boring billion?—lid tectonics, continental growth and environmental change associated with the Columbia supercontinent: *Geoscience Frontiers*, v. 4, no. 6, p. 681–691. [10.1016/j.gsf.2013.05.004](https://doi.org/10.1016/j.gsf.2013.05.004)
- Robinson, P.T., Malpas, J., Dilek, Y., and Zhou, M.F., 2008, The significance of sheeted dike complexes in ophiolites: *GSA*

- Today: A Publication of the Geological Society of America, v. 18, no. 11, p. 4–10. [10.1130/GSATG22A.1](https://doi.org/10.1130/GSATG22A.1)
- Roman, A., and Arndt, N., 2020, Differentiated Archean oceanic crust: Its thermal structure, mechanical stability and a test of the sagduction hypothesis: *Geochimica et cosmochimica acta*, v. 278, p. 65–77. [10.1016/j.gca.2019.07.009](https://doi.org/10.1016/j.gca.2019.07.009)
- Rosas, J.C., and Korenaga, J., 2018, Rapid crustal growth and efficient crustal recycling in the early earth: Implications for hadean and Archean geodynamics: *Earth and Planetary Science Letters*, v. 494, p. 42–49. [10.1016/j.epsl.2018.04.051](https://doi.org/10.1016/j.epsl.2018.04.051)
- Rozel, A.B., Golabek, G.J., Jain, C., Tackley, P.J., Gerya, T., 2017, Continental crust formation on early Earth controlled by intrusive magmatism: *Nature*, v. 545, no. 7654, p. 332–335. [10.1038/nature22042](https://doi.org/10.1038/nature22042)
- Sandiford, M., Van Kranendonk, M.J., and Bodorkos, S., 2004, Conductive incubation and the origin of dome-and-keel structure in Archean granite-greenstone terrains: A model based on the eastern Pilbara Craton, Western Australia: *Tectonics*, v. 23, no. 1. [10.1029/2002TC001452](https://doi.org/10.1029/2002TC001452)
- Satkoski, A.M., Fralick, P., Beard, B.L., and Johnson, C.M., 2017, Initiation of modern-style plate tectonics recorded in Mesoarchean marine chemical sediments: *Geochimica et cosmochimica acta*, v. 209, p. 216–232. [10.1016/j.gca.2017.04.024](https://doi.org/10.1016/j.gca.2017.04.024)
- Schott, B., and Yuen, D.A., 2004, Influences of dissipation and rheology on mantle plumes coming from the D"-layer: *Physics of the Earth and Planetary Interiors*, v. 146, no. 1–2, p. 139–145. [10.1016/j.pepi.2003.07.026](https://doi.org/10.1016/j.pepi.2003.07.026)
- Servali, A., and Korenaga, J., 2018, Oceanic origin of continental mantle lithosphere: *Geology*, v. 46, no. 12, p. 1047–1050. [10.1130/G45180.1](https://doi.org/10.1130/G45180.1)
- Shirey, B.S., and Richardson, H.S., 2011, Start of the Wilson cycle at 3 Ga shown by diamonds from Subcontinental Mantle: *Science* (1979), v. 333, no. 6041, p. 434–436. [10.1126/science.1206275](https://doi.org/10.1126/science.1206275)
- Shirey, S.B., Kamber, B.S., and Whitehouse, M.J., 2008, A review of the isotopic and trace element evidence for mantle and crustal processes in the hadean and Archean: Implications for the onset of plate tectonic subduction: *When Did Plate Tectonics Begin on Planet Earth?* v. 440, p. 1
- Sizova, E., Gerya, T., Stüwe, K., and Brown, M., 2015, Generation of felsic crust in the Archean: A geodynamic modeling perspective: *Precambrian Research*, v. 271, p. 198–224. [10.1016/j.precamres.2015.10.005](https://doi.org/10.1016/j.precamres.2015.10.005)
- Sleep, N.H., 2008, Channeling at the base of the lithosphere during the lateral flow of plume material beneath flow line hot spots: *Geochemistry Geophysics Geosystems*, v. 9, no. 8. [10.1029/2008GC002090](https://doi.org/10.1029/2008GC002090)
- Sleep, N.H., and Windley, B.F., 1982, Archean plate tectonics: Constraints and inferences: *The Journal of Geology*, v. 90, no. 4, p. 363–379. [10.1086/628691](https://doi.org/10.1086/628691)
- Smit, K.V., Shirey, S.B., Hauri, E.H., and Stern, R.A., 2019, Sulfur isotopes in diamonds reveal differences in continent construction: *Science* (1979), v. 364, no. 6438, p. 383–385. [10.1126/science.aaw9548](https://doi.org/10.1126/science.aaw9548)
- Smit, M.A., and Mezger, K., 2017, Earth's early O₂ cycle suppressed by primitive continents: *Nature Geoscience*, v. 10, no. 10, p. 788–792. [10.1038/ngeo3030](https://doi.org/10.1038/ngeo3030)
- Smit, M.A., Musiyachenko, K.A., and Goumans, J., 2024, Archean continental crust formed from mafic cumulates: *Nature Communications*, v. 15, no. 1, p. 692. [10.1038/s41467-024-44849-4](https://doi.org/10.1038/s41467-024-44849-4)
- Smithies, R.H., Van Kranendonk, M.J., and Champion, D.C., 2005, It started with a plume—early Archean basaltic proto-continental crust: *Earth and Planetary Science Letters*, v. 238, no. 3–4, p. 284–297. [10.1016/j.epsl.2005.07.023](https://doi.org/10.1016/j.epsl.2005.07.023)
- Sobolev, A.V., Asafov, E.V., and Gurenko, A.A., 2016, Komatiites reveal a hydrous Archean deep-mantle reservoir: *Nature*, v. 531, no. 7596, p. 628–632. [10.1038/nature17152](https://doi.org/10.1038/nature17152)
- Sobolev, A.V., Asafov, E.V., and Gurenko, A.A., 2019, Deep hydrous mantle reservoir provides evidence for crustal recycling before 3.3 billion years ago: *Nature*, v. 571, p. 555–559
- Solomatov, V.S., 1995, Scaling of temperature- and stress-dependent viscosity convection: *Physics of Fluids*, v. 7, no. 2, p. 266–274. [10.1063/1.868624](https://doi.org/10.1063/1.868624)
- Solomatov, V.S., 2000, Fluid dynamics of a terrestrial magma ocean: *Origin of the Earth and Moon*, v. 1, p. 323–338
- Spencer, C.J., Murphy, J.B., Kirkland, C.L., Liu, Y., and Mitchell, R. N., 2018, A palaeoproterozoic tectono-magmatic lull as a potential trigger for the supercontinent cycle: *Nature Geoscience*, v. 11, no. 2, p. 97–101. [10.1038/s41561-017-0051-y](https://doi.org/10.1038/s41561-017-0051-y)
- Spencer, C.J., Roberts, N.M.W., and Santosh, M., 2017, Growth, destruction, and preservation of Earth's continental crust: *Earth-Science Reviews*, v. 172, p. 87–106. [10.1016/j.earscirev.2017.07.013](https://doi.org/10.1016/j.earscirev.2017.07.013)
- Sproule, R.A., Leshner, C.M., Ayer, J.A., Thurston, P.C., Herzberg, C.T., 2002, Spatial and temporal variations in the geochemistry of komatiites and komatiitic basalts in the abitibi greenstone belt: *Precambrian Research*, v. 115, no. 1–4, p. 153–186. [10.1016/S0301-9268\(02\)00009-8](https://doi.org/10.1016/S0301-9268(02)00009-8)
- Stern, R.J., 2005, Evidence from ophiolites, blueschists, and ultrahigh-pressure metamorphic terranes that the modern episode of subduction tectonics began in neoproterozoic time: *Geology*, v. 33, no. 7, p. 557–560. [10.1130/G21365.1](https://doi.org/10.1130/G21365.1)
- Stern, R.J., 2023, The Orosirian (1800–2050 ma) plate tectonic episode: Key for reconstructing the Proterozoic tectonic record: *Geoscience Frontiers*, v. 14, no. 3, p. 101553. [10.1016/j.gsf.2023.101553](https://doi.org/10.1016/j.gsf.2023.101553)
- Stern, R.J., and Gerya, T., 2018, Subduction initiation in nature and models: A review: *Tectonophysics*, v. 746, p. 173–198. [10.1016/j.tecto.2017.10.014](https://doi.org/10.1016/j.tecto.2017.10.014)
- Stern, R.J., Gerya, T., and Tackley, P.J., 2018, Stagnant lid tectonics: Perspectives from silicate planets, dwarf planets, large moons, and large asteroids: *Geoscience Frontiers*, v. 9, no. 1, p. 103–119. [10.1016/j.gsf.2017.06.004](https://doi.org/10.1016/j.gsf.2017.06.004)
- Stern, R.J., Leybourne, M.I., and Tsujimori, T., 2016, Kimberlites and the start of plate tectonics: *Geology*, v. 44, no. 10, p. 799–802. [10.1130/G38024.1](https://doi.org/10.1130/G38024.1)
- Sun, W., Ding, X., Hu, Y.-H., and Li, X.-H., 2007, The golden transformation of the Cretaceous plate subduction in the west Pacific: *Earth and Planetary Science Letters*, v. 262, no. 3–4, p. 533–542. [10.1016/j.epsl.2007.08.021](https://doi.org/10.1016/j.epsl.2007.08.021)
- Sun, W., Li, C., Hao, X., Ling, M.-X., Ireland, T., Ding, X., Fan, W.-M., 2016, Oceanic anoxic events, subduction style and molybdenum mineralization: *Solid Earth Sciences*, v. 1, no. 2, p. 64–73. [10.1016/j.sesci.2015.11.001](https://doi.org/10.1016/j.sesci.2015.11.001)
- Tang, M., Chen, K., and Rudnick, R.L., 2016, Archean upper crust transition from mafic to felsic marks the onset of plate tectonics: *Science* (1979), v. 351, no. 6271, p. 372–375. [10.1126/science.aad5513](https://doi.org/10.1126/science.aad5513)
- Tappe, S., Smart, K., Torsvik, T., Massuyeau, M., and de Wit, M., 2018, Geodynamics of kimberlites on a cooling earth: Clues to plate tectonic evolution and deep volatile cycles: *Earth*

- and Planetary Science Letters, v. 484, p. 1–14. [10.1016/j.epsl.2017.12.013](https://doi.org/10.1016/j.epsl.2017.12.013)
- Tarduno, J.A., Cottrell, R.D., Bono, R.K., Rayner, N., Davis, W.J., Zhou, T., Nimmo, F., Hofmann, A., Jodder, J., Ibañez-Mejia, M., Watkeys, M.K., Oda, H., Mitra, G., 2023, Hadaean to palaeoarchean stagnant-lid tectonics revealed by zircon magnetism: *Nature*, v. 618, no. 7965, p. 531–536. [10.1038/s41586-023-06024-5](https://doi.org/10.1038/s41586-023-06024-5)
- Taylor, S.R., and McLennan, S.M. (1985) The continental crust: Its composition and evolution
- Thompson, R.N., and Gibson, S.A., 2000, Transient high temperatures in mantle plume heads inferred from magnesian olivines in Phanerozoic picrites: *Nature*, v. 407, no. 6803, p. 502–506. [10.1038/35035058](https://doi.org/10.1038/35035058)
- Tran, T.-D., Wang, K.-L., Kovach, V., Kotov, A., Velikoslavinsky, S., Popov, N., Dril, S., Chu, Z.-Y., Lee, D.-C., Kuo, L.-W., Iizuka, Y., and Lee, H.-Y., 2023, Plate tectonics in action in the Mesoarchean: Implication from the Olondo greenstone belt on the Aldan shield of Siberian Craton: *Earth and Planetary Science Letters*, v. 603, p. 117975. [10.1016/j.epsl.2022.117975](https://doi.org/10.1016/j.epsl.2022.117975)
- Trela, J., Vidito, C., Gazel, E., Herzberg, C., Class, C., Whalen, W., Jicha, B., Bizimis, M., and Alvarado, G.E., 2015, Recycled crust in the Galapagos plume source at 70 ma: Implications for plume evolution: *Earth and Planetary Science Letters*, v. 425, p. 268–277. [10.1016/j.epsl.2015.05.036](https://doi.org/10.1016/j.epsl.2015.05.036)
- Turcotte, D.L., and Schubert, G., 2002, *Geodynamics* (second edition). Cambridge: Cambridge University Press, p. 456.
- Turner, S., Wilde, S., Wörner, G., Schaefer, B., Lai, Y.-J., 2020, An andesitic source for Jack Hills zircon supports onset of plate tectonics in the hadean: *Nature Communications*, v. 11, no. 1, p. 1–5. [10.1038/s41467-020-14857-1](https://doi.org/10.1038/s41467-020-14857-1)
- Usui, Y., Saitoh, M., Tani, K., Nishizawa, M., Shibuya, T., Kato, C., Okumura, T., Kashiwabara, T., 2020, Identification of paleomagnetic remanence carriers in ca. 3.47 Ga dacite from the duffer formation, the Pilbara Craton: *Physics of the Earth and Planetary Interiors*, v. 299, p. 106411. [10.1016/j.pepi.2019.106411](https://doi.org/10.1016/j.pepi.2019.106411)
- Valley, J.W., Peck, W.H., King, E.M., and Wilde, S.A., 2002, A cool early earth: *Geology*, v. 30, no. 4, p. 351–354. [10.1130/0091-7613\(2002\)030<0351:ACEE>2.0.CO;2](https://doi.org/10.1130/0091-7613(2002)030<0351:ACEE>2.0.CO;2)
- van Hunen, J., and Moyn, J.-F., 2012, Archean subduction: Fact or fiction?: *Annual Review of Earth and Planetary Sciences*, v. 40, no. 1, p. 195–219. [10.1146/annurev-earth-042711-105255](https://doi.org/10.1146/annurev-earth-042711-105255)
- van Hunen, J., and van den Berg, A.P., 2008, Plate tectonics on the early earth: Limitations imposed by strength and buoyancy of subducted lithosphere: *Lithos*, v. 103, no. 1–2, p. 217–235. [10.1016/j.lithos.2007.09.016](https://doi.org/10.1016/j.lithos.2007.09.016)
- Van Kranendonk, M.J., 2010, Two types of Archean continental crust: Plume and plate tectonics on early earth: *The American Journal of Science*, v. 310, no. 10, p. 1187–1209. [10.2475/10.2010.01](https://doi.org/10.2475/10.2010.01)
- Van Kranendonk, M.J., Collins, W.J., Hickman, A., and Pawley, M. J., 2004, Critical tests of vertical vs. horizontal tectonic models for the Archean East Pilbara granite–greenstone terrane, Pilbara craton, western Australia: *Precambrian Research*, v. 131, no. 3–4, p. 173–211. [10.1016/j.precamres.2003.12.015](https://doi.org/10.1016/j.precamres.2003.12.015)
- Van Kranendonk, M.J., Hugh Smithies, R., Hickman, A.H., and Champion, D.C., 2007, Review: Secular tectonic evolution of Archean continental crust: Interplay between horizontal and vertical processes in the formation of the Pilbara Craton, Australia: *Terra Nova*, v. 19, no. 1, p. 1–38. [10.1111/j.1365-3121.2006.00723.x](https://doi.org/10.1111/j.1365-3121.2006.00723.x)
- Van Thienen, P., Vlaar, N.J., and Van den Berg, A.P., 2004, Plate tectonics on the terrestrial planets: *Physics of the Earth and Planetary Interiors*, v. 142, no. 1–2, p. 61–74. [10.1016/j.pepi.2003.12.008](https://doi.org/10.1016/j.pepi.2003.12.008)
- Verhoogen, J., 1961, Heat balance of the Earth's core: *Geophysical Journal International*, v. 4, no. s0, p. 276–281. [10.1111/j.1365-246X.1961.tb06819.x](https://doi.org/10.1111/j.1365-246X.1961.tb06819.x)
- Vijaya Kumar, K., Ernst, W.G., Leelanandam, C., Wooden, J.L., Grove, M.J., 2010, First paleoproterozoic ophiolite from Gondwana: Geochronologic–geochemical documentation of ancient oceanic crust from Kandra, SE India: *Tectonophysics*, v. 487, no. 1–4, p. 22–32. [10.1016/j.tecto.2010.03.005](https://doi.org/10.1016/j.tecto.2010.03.005)
- Vlaar, N.J., Van Keken, P.E., and Van den Berg, A.P., 1994, Cooling of the Earth in the Archaean: Consequences of pressure-release melting in a hotter mantle: *Earth and Planetary Science Letters*, v. 121, no. 1–2, p. 1–18. [10.1016/0012-821X\(94\)90028-0](https://doi.org/10.1016/0012-821X(94)90028-0)
- Walter, M.J., 1998, Melting of garnet peridotite and the origin of komatiite and depleted lithosphere: *Journal of Petrology*, v. 39, no. 1, p. 29–60. [10.1093/ptro/39.1.29](https://doi.org/10.1093/ptro/39.1.29)
- Wang, J.-M., Lanari, P., Wu, F.-Y., Zhang, J.-J., Khanal, G.P., and Yang, L., 2021, First evidence of eclogites overprinted by ultrahigh temperature metamorphism in Everest East, Himalaya: Implications for collisional tectonics on early earth: *Earth and Planetary Science Letters*, v. 558, p. 116760. [10.1016/j.epsl.2021.116760](https://doi.org/10.1016/j.epsl.2021.116760)
- Wang, X.-S., Zhang, X., Gao, J., Li, J.-L., Jiang, T., and Xue, S.-C., 2018, A slab break-off model for the submarine volcanic-hosted iron mineralization in the Chinese Western Tianshan: Insights from Paleozoic subduction-related to post-collisional magmatism: *Ore Geology Reviews*, v. 92, p. 144–160. [10.1016/j.oregeorev.2017.11.015](https://doi.org/10.1016/j.oregeorev.2017.11.015)
- Wang, Z., Kusky, T.M., and Wang, L., 2022, Long-lasting viscous drainage of eclogites from the cratonic lithospheric mantle after Archean subduction stacking: *Geology*, v. 50, no. 5, p. 583–587. [10.1130/G49793.1](https://doi.org/10.1130/G49793.1)
- Weller, O.M., Copley, A., Miller, W.G.R., Palin, R.M., and Dyck, B., 2019, The relationship between mantle potential temperature and oceanic lithosphere buoyancy: *Earth and Planetary Science Letters*, v. 518, p. 86–99. [10.1016/j.epsl.2019.05.005](https://doi.org/10.1016/j.epsl.2019.05.005)
- Weller, O.M., and St-Onge, M.R., 2017, Record of modern-style plate tectonics in the palaeoproterozoic trans-Hudson orogen: *Nature Geoscience*, v. 10, no. 4, p. 305–311. [10.1038/ngeo2904](https://doi.org/10.1038/ngeo2904)
- Wielicki, M.M., Harrison, T.M., and Schmitt, A.K., 2012, Geochemical signatures and magmatic stability of terrestrial impact produced zircon: *Earth and Planetary Science Letters*, v. 321–322, p. 20–31. [10.1016/j.epsl.2012.01.009](https://doi.org/10.1016/j.epsl.2012.01.009)
- Wilde, S.A., Valley, J.W., Peck, W.H., and Graham, C.M., 2001, Evidence from detrital zircons for the existence of continental crust and oceans on the earth 4.4 gyr ago: *Nature*, v. 409, no. 6817, p. 175–178. [10.1038/35051550](https://doi.org/10.1038/35051550)
- Windley, B.F., 1993, Uniformitarianism today: Plate tectonics is the key to the past: *Journal of the Geological Society*, v. 150, no. 1, p. 7–19. [10.1144/gsjgs.150.1.0007](https://doi.org/10.1144/gsjgs.150.1.0007)
- Windley, B.F., Kusky, T., and Polat, A., 2021, Onset of plate tectonics by the Eoarchean: *Precambrian Research*, v. 352, p. 105980. [10.1016/j.precamres.2020.105980](https://doi.org/10.1016/j.precamres.2020.105980)

- Wu, L.-G., Chen, Y., Palin, R.M., Li, Q.-L., Zhao, L., Li, Y.-B., Li, C.-F., Li, Y.-L., and Li, X.-H., 2024, Reinitiation of modern-style plate tectonics in the early neoproterozoic: Evidence from a~ 930 ma blueschist-facies terrane in South China: Precambrian Research, v. 401, p. 107276. [10.1016/j.precamres.2023.107276](https://doi.org/10.1016/j.precamres.2023.107276).
- Wu, Y., Guo, F., Wang, X., and Liao, J., 2022, Discovery of Ultra-depleted melt inclusion in late cretaceous intracontinental basaltic andesites in South China: Implications for recycling of lower oceanic crust, Journal of Geophysical Research: Solid Earth, v. 127, no. 12, p. e2022JB025324. [10.1029/2022JB025324](https://doi.org/10.1029/2022JB025324).
- Xing, G.-F., Wang, X.-L., Wan, Y., Chen, Z.-H., Jiang, Y., Kitajima, K., Ushikubo, T., and Gojon, P., 2014, Diversity in early crustal evolution: 4100 ma zircons in the cathaysia block of southern China: Scientific Reports, v. 4, no. 1, p. 5143. [10.1038/srep05143](https://doi.org/10.1038/srep05143).
- Xu, C., Kynický, J., Song, W., Tao, R., Lü, Z., Li, Y., Yang, Y., Pohanka, M., Galiova, M.V., Zhang, L., and Fei, Y., 2018, Cold deep subduction recorded by remnants of a paleoproterozoic carbonated slab: Nature Communications, v. 9, no. 1, p. 2790. [10.1038/s41467-018-05140-5](https://doi.org/10.1038/s41467-018-05140-5).
- Yamamoto, S., Senshu, H., Rino, S., Omori, S., Maruyama, S., 2009, Granite subduction: Arc subduction, tectonic erosion and sediment subduction: Gondwana Research, v. 15, no. 3–4, p. 443–453. [10.1016/j.gr.2008.12.009](https://doi.org/10.1016/j.gr.2008.12.009).
- Yamazaki, D., and Karato, S.-I., 2001, Some mineral physics constraints on the rheology and geothermal structure of Earth's lower mantle: American Mineralogist, v. 86, no. 4, p. 385–391. [10.2138/am-2001-0401](https://doi.org/10.2138/am-2001-0401).
- Yang, Z.-F., and Zhou, J.-H., 2013, Can we identify source lithology of basalt?: Scientific Reports, v. 3, no. 1, p. 1–7. [10.1038/srep01856](https://doi.org/10.1038/srep01856).
- Yang, Z., Li, J., Jiang, Q., Xu, F., Guo, S.-Y., Li, Y., and Zhang, J., 2019, Using major element logratios to recognize compositional patterns of basalt: Implications for source lithological and compositional heterogeneities: Journal of Geophysical Research: Solid Earth, v. 124, no. 4, p. 3458–3490. [10.1029/2018JB016145](https://doi.org/10.1029/2018JB016145).
- Yin, A., and Harrison, T.M., 2000, Geologic evolution of the Himalayan-Tibetan orogen: Annual Review of Earth and Planetary Sciences, v. 28, no. 1, p. 211–280. [10.1146/annurev.earth.28.1.211](https://doi.org/10.1146/annurev.earth.28.1.211).
- Zhang, Z.-J., Chen, G.-X., Kusky, T., Yang, J., and Cheng, Q.-M., 2023, Lithospheric thickness records tectonic evolution by controlling metamorphic conditions: Science Advances, v. 9, no. 50, p. eadi2134. [10.1126/sciadv.adi2134](https://doi.org/10.1126/sciadv.adi2134).
- Zhang, Z.J., Dauphas, N., Johnson, A.C., Aarons, S.M., Bennett, V. C., Nutman, A.P., MacLennan, S., and Schoene, B., 2023, Titanium and iron isotopic records of granitoid crust production in diverse Archean cratons: Earth and Planetary Science Letters, v. 620, p. 118342. [10.1016/j.epsl.2023.118342](https://doi.org/10.1016/j.epsl.2023.118342).
- Zheng, Y., 2024, Plate tectonics in the Archean: Observations versus interpretations: Science China Earth Sciences, v. 67, no. 1, p. 1–30. [10.1007/s11430-023-1210-5](https://doi.org/10.1007/s11430-023-1210-5).
- Zheng, Y.-F., and Zhao, G., 2020, Two styles of plate tectonics in Earth's history: Science Bulletin, v. 65, no. 4, p. 329–334. [10.1016/j.scib.2018.12.029](https://doi.org/10.1016/j.scib.2018.12.029).
- Zhu, Z., Campbell, I.H., Allen, C.M., and Burnham, A.D., 2020, S-type granites: Their origin and distribution through time as determined from detrital zircons: Earth and Planetary Science Letters, v. 536, p. 116140. [10.1016/j.epsl.2020.116140](https://doi.org/10.1016/j.epsl.2020.116140).